Conformal Shape Representation

by

Matt Feiszli

B. A., Yale University, 1996

Submitted in partial fulfillment of the

requirements for the degree of Doctor of Philosophy

in the Division of Applied Mathematics at Brown University

Providence, Rhode Island

May 2008

This dissertation by Matt Feiszli is accepted in its present form by the Division of Applied Mathematics as satisfying the dissertation requirement for the degree of Doctor of Philosophy.

Date ____________ ______________________________

David Mumford, Director

Recommended to the Graduate Council

Date ____________ ______________________________

Jeffrey F. Brock, Reader

Date ____________ ______________________________

Stuart Geman, Reader

Approved by the Graduate Council

Date ____________ ______________________________

Sheila Bonde, Dean of the Graduate School

Vitæ

Matt Feiszli was born March 15th, 1974 in Mansfield, Ohio. He graduated from Yale University *cum laude* in 1996, with degrees in Computer Science and Psychology.

Acknowledgements

First and foremost, I wish to thank my thesis advisor, David Mumford; David, your brilliance, broad-mindedness, and humanity are uncommon taken alone, and truly wonderful to find in one individual. Working with you was a transformational experience; I do not think it would have been possible to do a thesis like this anywhere else.

I am extremely grateful to Stu Geman for his insight, suggestions, assistance, and support. His talents for mathematics and his gift for exposition were a tremendous influence on me here.

I am also very appreciative of Jeff Brock for his help, patience, and tutoring as I moved into the world of hyperbolic geometry and Teichmüller theory.

Thank you to Alan Yuille for everything I learned working with you; in particular I learned how I wanted to work on problems and that I wanted to become a mathematician.

My friends and officemates, I say thanks for great conversations, good times (from DDR parties to real analysis parties), and general harassment. Akil, I'll need a bright red phone in my office so I can call when I need numerical assistance.

I thank my parents, who always made opportunities available without applying pressure.

Jin, I'm luckier than I thought possible. I can't express what your support means. What more can I say? Thank you.

Contents

Vitæ iv

Acknowledgements v

List of Figures ix

Chapter 1. Introduction and Background 1
1. Conformal Shape Representation 2
2. Two Classical Models For **Teich**(Δ) 3
2.1. Notation 3
2.2. The Measurable Mapping Theorem 4
2.3. Two Models for the Universal Teichmüller Space 6
2.4. Passing Between the Two Models 7
3. Hyperbolic 3-Space 8
3.1. Models of Hyperbolic Space 8
3.2. Convex Hulls and the Dome 9
3.3. Bending 10
4. Boundary Derivatives and Harmonic Measure 12
4.1. Harmonic Measure 12
4.1.1. Extension of Domain 14
4.2. Extremal Distance 15
5. Summary of Results 18

Chapter 2. Differential Geometry of Smooth Convex Hull Boundaries 22
0.1. Notation 23
1. Overview: Domes over Smooth Domains 24
2. Preliminaries 25
3. The Jacobian of r, the Nearest-Point Retraction Map 32
3.1. Explicit Formulas for the Jacobian 35
4. An ODE for the Isometry $\iota : S_\Omega \to \mathbb{D}$ 39
4.1. The Finitely-Bent Case 39
4.2. The Smooth Case 40
4.3. Boundary Derivatives of ι 44

Chapter 3. Boundary Derivatives in Smooth Domains 46
0.4. Notation 47
1. Background: Extremal Length and Harmonic Measure 47
1.1. The Metric 47
1.2. Lower Bounds on Extremal Length, Upper Bounds on Harmonic Measure 48
1.3. Upper Bounds and Reduced Extremal Distance 49

2. Local Estimates and Boundary Curvature 50
2.1. General Expressions for the Derivative 51
2.2. Proof of Theorem 3.4: Local Estimates for $|f'|$ 55
2.3. Lipschitz Subregions and Upper Bounds 58
3. Long-Range Estimates and the Dome 60
3.1. Notation 61
3.2. Geodesic Distances in S_Ω 61
3.3. Extremal Distances in S_Ω and Ω 65
3.4. Hyperbolic Distances in S_Ω and Ω 67
3.4.1. Relation to the Ahlfors Integral 73
3.5. Long-range Estimates for $|f'|$ 74

Chapter 4. Passing Between the Two Models of $\mathbf{Teich}(\Delta)$ 77
1. Notation 78
2. Linearizing Welding 78
2.1. The Differential at the Identity 78
2.2. Examples 80
2.3. The General Form of the Differential 80
3. A Bound on Distortion via the Weil-Petersson Metric on $\mathbf{Teich}(\Delta)$ . . . 84
3.1. Lie Algebras 85
3.1.1. Example: The Lie Algebra $psl_2(\mathbb{R})$ 85
3.2. The Weil-Petersson Inner Product and $\mathbf{Diff}(S^1)$ 86
3.3. The WP Inner Product and Beltrami Differentials 89
3.4. Distortion of Quasicircles is Bounded Uniformly by Weil-Petersson Norms of Tangent Vectors 89
4. Quasisymmetry and Distortion of Quasicircles 91
4.1. Quasisymmetry and Uniform Approximations to Shapes 91
4.2. Quasisymmetric Approximations to Welding Maps 92

Chapter 5. Compression of 2D Shapes via Teichmüller Theory 96
1. Background: ϵ-Entropy and Coding 97
1.1. Kolmogorov's ϵ-Entropy 97
1.2. Connection with Coding Theory 98
2. Adaptive Uniform Coding of Real-Valued Functions 99
2.1. A First Encoder 99
2.2. Expanding the Domain 106
2.3. Computing a Mesh with Specified Spacing 110
2.4. Examples 111
3. Reducing the Bit Cost 114
3.1. Discretizing the Values: From Interpolants to Approximations 114
3.2. Experiments: A Second Algorithm for Encoding Approximations . . . 118
3.3. Storage 121
3.4. Examples: The Second Algorithm 121
3.5. Examples: Encoding Cost in Bits for Two Algorithms 126
4. Adaptive Quasisymmetric Coding of $\mathbf{Diff}(S^1)$ 130
4.1. Constructing Piecewise Linear Quasisymmetric Approximations to f . 131
4.2. Examples 133

Appendix A. Stereographic Projection 138
1. Formulas for Stereographic Projection 139
2. Stereographic Projection as a Hyperbolic Isometry 139

Appendix B. The Medial Axis 141
1. Formulas for the Medial Axis 141
2. Regularity of the Medial Axis 145

Appendix C. Supporting Calculations for Theorem 3.7 146

Bibliography 150

List of Figures

1.1 The half-space model of $\mathbb{H}^3$. 9
1.2 The dome of a finitely-bent domain. 11
1.3 The nearest-point retraction and stereographic projection. 11
1.4 Gaps and crescents. 12
1.5 Examples of the Riemann map. 13

2.1 Notation for the medial axis. 24
2.2 Transverse coordinates on the dome. 25
2.3 Endpoints of nearby bending lines are almost cocircular. 27
2.4 Overhead and cross-section views of the setup of lemma 2.7. 33
2.5 Notation for the discrete flow 40
2.6 Boundary points flow back to a disk under the ι flow. 44

3.1 The setup for local estimates on $|f'|$ 48
3.2 The setup for lemma 3.2 56
3.3 ι takes bending lines in the dome to geodesics in the disk. 61
3.4 Notation for the medial axis. 62
3.5 The situation for theorem 3.8. 68
3.6 The setup for theorem 3.13. 75

4.1 A perturbed welding map and the resulting shape. 81
4.2 Another perturbed welding map and shape. 82

5.1 C-Lipschitz functions stay within ϵ-corridors. 98
5.2 Two examples of interpolants. 112
5.3 An interpolant for a triangle function. 113
5.4 A piecewise linear approximation to a smooth function. 119

A.1 Stereographic projection from the south pole. 138

B.1 A rectangle and its medial axis. 141
B.2 Notation for the medial axis. 142

C.1 The graph of equation 13. 149

CHAPTER 1

Introduction and Background

1. Conformal Shape Representation

Representation and comparison of shapes is a central problem in computer vision. In the past several decades, many approaches to represent, compare, and classify shapes have been presented (See [**47**], [**34**] for review and discussion). The space of 2D shapes is inherently nonlinear; this poses fundamental difficulties in computer vision when attempting object recognition and statistics. We follow Mumford, Miller, Michor, and others by constructing metric spaces of 2D shapes in which one can compute distances between any two shapes. In this dissertation, we continue investigation of a relatively recent approach, based on conformal mapping, which was first introduced by Mumford and Sharon in [**40**].

Mumford and Sharon represent shapes using a construction from complex analysis and Teichmüller theory. Given a simply-connected planar region Ω bounded by a smooth Jordan curve (this is our definition of a "shape"), one constructs a pair of conformal maps $\Phi_+ : \Delta \to \Omega_+$ and $\Phi_- : \Delta \to \Omega_-$, which map the interior and exterior of the unit disk to the interior and exterior of Ω, respectively. These maps extend continuously to the boundary S^1, and their composition $\Phi_+^{-1} \circ \Phi_-$, restricted to the boundary, is a map $\Psi : S^1 \to S^1$. This construction is almost an isomorphism: the space of shapes, modulo translation and scale, is isomorphic to the group $\mathbf{Diff}(S^1)$, modulo conformal self-maps of the disk. This provides an elegant way of making the space of shapes into a metric space; we take an equivalence class of diffeomorphisms of the circle as a representation of a shape. In [**40**] these diffeomorphisms are called "fingerprints"; in the mathematical literature, elements of the broader class of quasisymmetric homeomorphisms of S^1 are commonly known as "welding maps".

An important part of this dissertation is a study of the way this representation encodes the geometry. One perceptually salient attribute of a shape is its medial axis [**8**]; there is a large body of work which uses the medial axis to represent and classify shapes [**42, 48, 49, 41**]. By careful study of the boundary derivatives of conformal maps, we demonstrate how our representation encodes a sort of continuous version of the medial axis. In addition, we obtain explicit estimates showing that conformal maps encode the local Euclidean curvature of the boundary. The machinery involved in making our geometric estimates comes both from classical function theory and hyperbolic geometry.

Another problem of great interest, both theoretical and applied, is data compression. Given a point in some metric space, one may wish to find a nearby point with the shortest possible description length. We approach this problem by developing an adaptive compressor for plane curves based on the "fingerprint" construction explored by Sharon and Mumford. To discuss the worth of any such scheme, one needs some criterion for optimality. We appeal to Kolmogorov's notion of ϵ-entropy (see [**14, 15, 27, 38**]) to provide this, and we demonstrate that our compressor is optimal on certain classes of functions.

Before we give a detailed summary of our results, we pause to present the necessary background material.

2. Two Classical Models For Teich(Δ)

The isomorphism between shapes and welding maps is the fundamental link between complex analysis and the study of 2D shape. This isomorphism arises in Teichmüller theory, where we have two models for the universal Teichmüller space **Teich**(Δ) (the Teichmüller space of the unit disk). The first model is given by a set of normalized quasicircles; our smooth shapes are a subset of these. The second model is given by normalized elements of $\mathbf{Homeo}_{QS}(S^1)$, the group of quasisymmetric homeomorphisms of the circle; our fingerprints live in the subgroup $\mathbf{Diff}(S^1)$.

2.1. Notation.

Δ – The unit disk $\{|z| < 1\}$

$L^\infty(\Delta)$ – The space of bounded Beltrami differentials on Δ

$L^\infty(\Delta)_1$ – The open unit ball in $L^\infty(\Delta)$

There are two classical models for the universal Teichmüller space: one given by equivalence classes of homeomorphisms of the circle, another given by equivalence classes of quasicircles. Both models depend holomorphically on a parameter $\mu \in L^\infty(\Delta)_1$. Here we construct the two models and describe how to pass between them. We are interested in the differential of this isomorphism between $\mathbf{Homeo}_{QS}(S^1)/SL_2(\mathbb{R})$ and quasicircles/(translation,scale). At an arbitrary point in Teichmüller space, the differential of the map between the two models is complicated. However, the differential at the origin admits an explicit formula which we will develop in chapter 4.

2.2. The Measurable Mapping Theorem. Suppose $\mu(z)$ is a measurable function defined on some domain Ω, and $\|\mu\|_\infty < 1$. The existence of solutions to the Beltrami differential equation

$$f_{\bar{z}}(z) = \mu(z) f_z(z) \tag{1}$$

is guaranteed by the "Measurable Mapping Theorem", which may be stated as follows.

THEOREM 1.1 (Measurable Mapping Theorem). *Equation (1) gives a one-to-one correspondence between the set of quasiconformal homeomorphisms of $\hat{\mathbb{C}}$ that fix the points 0, 1, and ∞ and the set of measurable complex-valued functions μ on $\hat{\mathbb{C}}$ for which $\|\mu\|_\infty < 1$. Furthermore, the normalized solution f^μ to the Beltrami equation depends holomorphically on μ and for any $R > 0$ there exists $\delta > 0$ and $C(R) > 0$ such that*

$$|f^{t\mu}(z) - z - tV(Z)| \leq C(R)t^2$$

for $|z| < R$ and $|t| < \delta$, where

$$V(z) = -\frac{z(z-1)}{\pi} \iint_{\mathbb{C}} \frac{\mu(\xi)}{\xi(\xi-1)(\xi-z)} |d\xi|^2$$

We make a pair of remarks regarding normalizations of the maps.

REMARK. The essential feature of the integral defining $V(z)$ is the convolution $\mu * \frac{1}{\pi z}$. The role of the other terms becomes more clear if we expand the integrand in partial fractions and rewrite it as convolutions evaluated at z, 0, and 1:

$$\begin{aligned}-\frac{1}{\pi}\frac{z(z-1)\mu(\xi)}{\xi(\xi-1)(\xi-z)} &= -\frac{\mu(\xi)}{\pi}\left(\frac{1}{\xi-z}-\frac{1-z}{\xi}-\frac{z}{\xi-1}\right)\\ &= \frac{1}{\pi}\left(\frac{\mu(\xi)}{z-\xi}+(z-1)\frac{\mu(\xi)}{-\xi}-z\frac{\mu(\xi)}{1-\xi}\right)\end{aligned}$$

Thus if we let W be the (non-normalized) vector field $W(z) = \mu * \frac{1}{\pi z}$, we can write

$$V(z) = W(z) + (W(0) - W(1))\, z - W(0)$$

In other words, a vector field V fixing infinity is of the form $V(z) = \mu * \frac{1}{\pi z}$, modulo vector fields of the form $bz + c$ whose coefficients may be chosen so V fixes 0 and 1, as per our statement of the mapping theorem. More generally, we can set

$$V(z) = \left(\mu * \frac{1}{\pi z}\right) + az^2 + bz + c$$

to achieve any normalization desired.

REMARK. Let $\mu \in L^\infty(U)$ satify $\|\mu\|_\infty < 1$ and have compact support in some region Ω. In this case the map $f^{t\mu}$ is conformal in the exterior Ω^*, hence it suffices to normalize the exterior map. If $f^{t\mu}$ the unique solution which can be written at infinity as $f^{t\mu}(z) = z + O\left(\frac{1}{|z|}\right)$, then we have

$$V(z) = \mu * \frac{1}{\pi z}$$

That $f^{t\mu}$ tends to the identity near infinity follows from the fact the V vanishes at infinity like $O(1/|z|)$.

2.3. Two Models for the Universal Teichmüller Space. Solving the welding problem amounts to passing between two models of the universal Teichmuller space. In both cases, let $\mu \in L^\infty(\Delta)_1$. We now define the two models.

(1) $\mathbf{Homeo}_{qs}(S^1)$

Extend μ into $\hat{\mathbb{C}}$ by the reflection

$$\mu\left(\frac{1}{\bar{z}}\right) = \bar{\mu}(z)\frac{z^2}{\bar{z}^2}$$

Denote by f_μ the unique solution to the Beltrami equation

$$(f_\mu)_{\bar{z}} = \mu(f_\mu)_z$$

normalized to preserve $(-1, -i, 1)$. Then due to the reflection symmetry,

$$\frac{1}{f_\mu(z)} = \bar{f}_\mu\left(\frac{1}{\bar{z}}\right)$$

and f_μ preserves the unit circle. Given two $\mu, \nu \in L^\infty(\Delta)_1$, set $\mu \sim \nu$ if $f_\mu|_{S^1} = f_\nu|_{S^1}$. The universal Teichmuller space is the set of equivalence classes of mappings f_μ,

$$Teich(\Delta) = L^\infty(\Delta)_1/\sim$$

One may equally well consider normalized homeomorphisms of the circle: the restriction of f_μ to S^1 is a quasisymmetric homeomorphism of the circle, unique up to elements of $PSL_2(\mathbb{R})$. Define

$$Teich(\Delta) = \mathbf{Homeo}_{qs}(S^1)/PSL_2(\mathbb{R})$$

(2) Quasicircles

Extend μ into $\hat{\mathbb{C}}$ by setting $\mu(z) = 0$ outside the unit disk. Denote by f^μ the solution to the Beltrami equation

$$f^\mu_{\bar{z}} = \mu f^\mu_z$$

normalized so $f^\mu(z) = z + O\left(\frac{1}{|z|}\right)$ near infinity. On the exterior of the unit disk Δ^*, f^μ is a conformal map onto its image D^μ; set $\mu \sim \nu$ if $f^\mu|_{\Delta^*} = f^\nu_{\Delta^*}$. The universal Teichmuller space is the set of equivalence classes of mappings f^μ,

$$Teich(\Delta) = L^\infty(\Delta)_1/\sim$$

As the normalized exterior maps are in one-to-one correspondence with the quasicircles ∂D^μ, this construction is equivalent to one in terms of equivalence classes of quasicircles.

The two definitions of universal Teichmuller space are equivalent, since $f_\mu|_{S^1} = f_\nu|_{S^1} \iff f^\mu|_{\Delta^*} = f^\nu|_{\Delta^*}$

2.4. Passing Between the Two Models. We now observe how to pass from one model to the other.

(1) From welding maps to quasicircles

Given a quasisymmetric $\phi : S^1 \to S^1$, extend ϕ to the interior to produce any quasiconformal map $F : \Delta \to \Delta$. This map has an associated Beltrami differential μ. Extend μ to be 0 on Δ^* and solve the Beltrami equation to produce f^μ. Then $Q = f^\mu(S^1)$ is a quasicircle. It is a short proof to show that Q depends only on the equivalence class of ϕ; i.e. Q is independent of the choice of extension F.

(2) From quasicircles to welding maps

Observe that on Δ, the map $g_- = f^\mu \circ f_\mu^{-1}$ is a normalized conformal map to the interior of $Q = f^\mu(S^1)$. Let $g_+ = f^\mu|_{\Delta^*}$, which is a normalized conformal map of the exterior of the disk to the exterior of Q. To recover the quasisymmetric map $\phi = f_\mu|_{S^1}$, compose the two Riemann maps:

$$g_+^{-1} \circ g_-\big|_{S^1} = \left(f^\mu \circ f_\mu^{-1}\right)^{-1} \circ f^\mu\big|_{S^1} = f_\mu\big|_{S^1}$$

3. Hyperbolic 3-Space

We are interested in conformal structures on a domain Ω lying on the Riemann sphere $\hat{\mathbb{C}}$. In chapter 3, we will see that conformal structures can be approximated very well using constructions from hyperbolic geometry. These hyperbolic constructions have the advantage of being entirely local, unlike the global nature of the Riemann map. To make the link, one regards $\hat{\mathbb{C}}$ as the "boundary at infinity" of hyperbolic 3-space $\mathbb{H}^3$. In this section we describe the constructions we'll need to relate hyperbolic and conformal geometries.

3.1. Models of Hyperbolic Space. Equipping the open unit ball in $\mathbb{R}^n$ with the Poincaré metric $ds^2 = \left(\frac{2}{1-|z|^2}\right)^2 |dz|^2$, where $|z|$ is the distance to the origin and $|dz|$ is the Euclidean distance element, gives a model of hyperbolic space $\mathbb{H}^n$. With this metric, the space is normalized so all sectional curvatures are a constant -1. The isometries of $\mathbb{H}^n$ act on the boundary S^{n-1} as conformal automorphisms.

We are particularly interested in the case $n = 3$. We regard $\hat{\mathbb{C}}$ as the boundary at infinity of hyperbolic 3-space $\mathbb{H}^3$. In this Poincaré model, arcs of circles orthogonal to $\hat{\mathbb{C}}$ are geodesics in the half-space or ball models. The isometries of $\mathbb{H}^3$ act on the boundary as the group of linear fractional maps $SL_2(\mathbb{C})$. Denote the closed unit ball, with the hyperbolic structure on the interior and conformal structure on the boundary by $\mathbb{B}^n$.

One may also realize the same geometry in the half-space model (see figure 1.1); the two models are related by a conformal self-map of $\mathbb{R}^3$. In this model, hyperbolic 3-space is the set $\{(x_1, x_2, x_3) : x_3 > 0\}$ with the metric $ds^2 = \frac{dx_1^2+dx_2^2+dx_3^2}{x_3^2}$. Geodesics

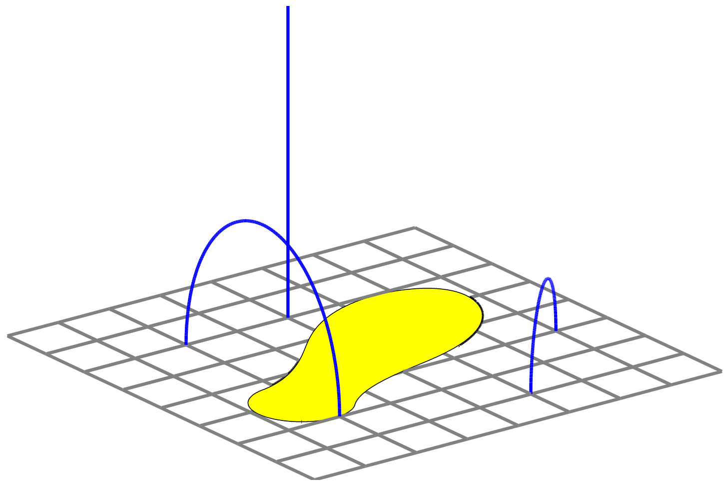

FIGURE 1.1. The half-space model of $\mathbb{H}^3$: Arcs of circles orthogonal to $\hat{\mathbb{C}}$ are geodesics. A planar domain lies in $\hat{\mathbb{C}}$, the boundary of $\mathbb{H}^3$.

are again arcs of circles orthogonal to the (x_1, x_2) plane $\hat{\mathbb{C}}$, and isometries again extend to the boundary and act conformally on $\hat{\mathbb{C}}$.

3.2. Convex Hulls and the Dome.

DEFINITION 1.1 (Convex). A non-empty subset $F \subset \mathbb{B}^n$ is said to be *convex* if, given any two points in F, the geodesic arc joining them is also contained in F.

A *supporting half-space* for a convex set $E \subset \mathbb{B}^n$ is a closed half-space containing E whose boundary meets E. A *support plane* for E at some point $z \in E \cap \mathbb{H}^n$ is the boundary of a supporting half-space which meets E at z. It can be shown (see [**9**]) that support planes exist for all points in the boundary of E.

Given a closed nonempty convex subset $E \subset \mathbb{B}^n$, there is a canonical retraction $r : \mathbb{B}^n \to E$. We define it as follows:

DEFINITION 1.2 (Nearest-point retraction map $r : \mathbb{B}^n \to E$). Let $E \subset \mathbb{H}^n$ be a convex set. For $z \in \mathbb{H}^n$ we define the map $r : HS^n \to \partial E$ as follows.

$$r(z) = \arg\min_{w \in E} \mathrm{d}_h(z, w)$$

For $z \in \partial\mathbb{H}^n$, we define $r(z)$ by inflating a horoball tangent at z until it makes contact with some point $w \in E$ and set $r(z) = w$.

One may also construct the map r by inflating balls centered at z until they make contact with E. By convexity of E, the ball will have a unique first point of contact in ∂E; this unique point is $r(z)$. This geometric construction makes it clear that the extension of r to the boundary of hyperbolic space is natural.

The nearest-point retraction map is both continuous and distance-decreasing; for details and proof, see e.g. [**9**].

Definition 1.3 (Hyperbolic convex hull). The convex hull of a set $F \subset \mathbb{B}^n$ is the smallest convex subset of $\mathbb{B}^n$ containing F.

We will use the notation $C(F)$ for the convex hull of $F \subset \mathbb{B}^n$. The notation $\partial C(F)$ refers to the part of the boundary of $C(F)$ which lies in $\mathbb{H}^n$.

Definition 1.4 (The Dome of a planar domain). Let $\Omega \subset \partial\mathbb{H}^3$ be a proper subset of the plane and $C(\Omega^c)$ be the convex hull of its complement. The "dome" S_Ω is the boundary $\partial C(\Omega^c)$.

We can equip the dome with a natural path metric by restricting the Poincaré metric in $\mathbb{H}^3$ to paths contained in the dome. In fact, this metric makes the dome into a surface of constant negative curvature. There is an explicit construction for the Riemann map $\iota : S_\Omega \to \mathbb{D}$, due to Thurston, which we will describe in more detail in chapter 2. Throughout this thesis we will only need to consider domes of simply-connected regions Ω.

3.3. Bending. If $\Omega \subset \hat{\mathbb{C}}$ is a simply-connected region which is a union of N disks, the dome S_Ω has a particularly simple form. If we consider all support planes P for S_Ω, we see that $P \cap S_\Omega$ is either a line or a piece of a hyperbolic plane. If $P \cap S_\Omega$ is a line, we call it a *bending line*; otherwise $P \cap S_\Omega$ is called a *flat piece*. We say that such a dome is *finitely-bent*. Note that if $z \in S_\Omega$ lies in a bending line it has a set of support planes; if z lies in a flat piece it has only one support plane. The *bending angle* associated with a bending line is angle between the extremal support planes for the line, that is, it is the angle at which the associated flat pieces meet (the angle between their normal vectors).

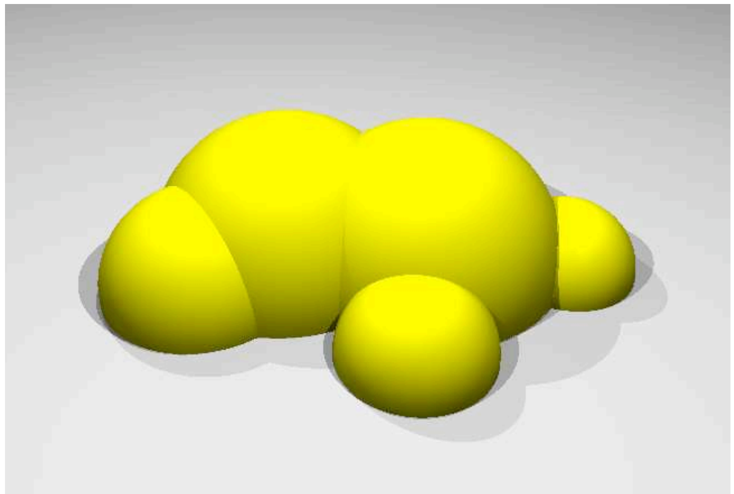

FIGURE 1.2. Above: Ω is a union of disks, shown in the half-space model. The faces of the dome meet at geodesic "bending lines", each with some bending angle β.

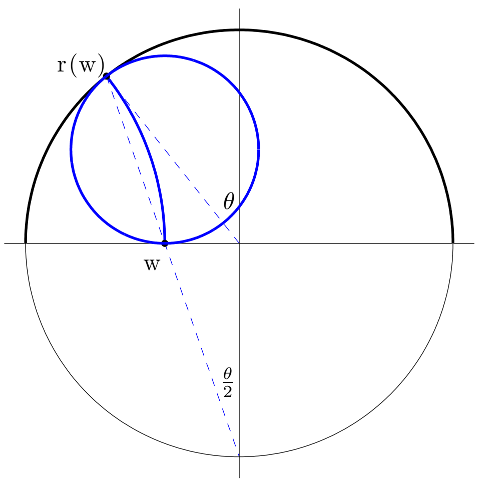

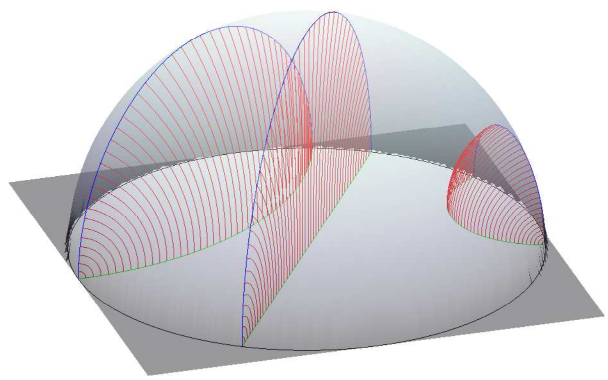

FIGURE 1.3. The nearest-point retraction $r : \Omega \to S_\Omega$ agrees with stereographic projection in the half-space model of $\mathbb{H}^3$ when Ω is a single disk.

The bending at each intersection induces a transverse measure on the dome, called the bending measure, constructed as follows. For $z \in S_\Omega$, let $\beta(z)$ be the bending angle at z. This is zero unless z lies on a bending line. If S_Ω is finitely-bent, we define a measure on embedded intervals γ in S_Ω by setting $\beta(\gamma)$ to be the sum of the bending encountered along γ. For more general domains, we define $\beta(\gamma)$ as an infimum over finitely-bent approximations between the endpoints of γ (see [**9**] for details). Here, we are interested in the case where $\partial\Omega$ is smooth. In this case, the bending measure has a Radon-Nikodym derivative with respect to arc length on transverse intervals on the dome; we will work with this explicitly in chapters 2 and 3.

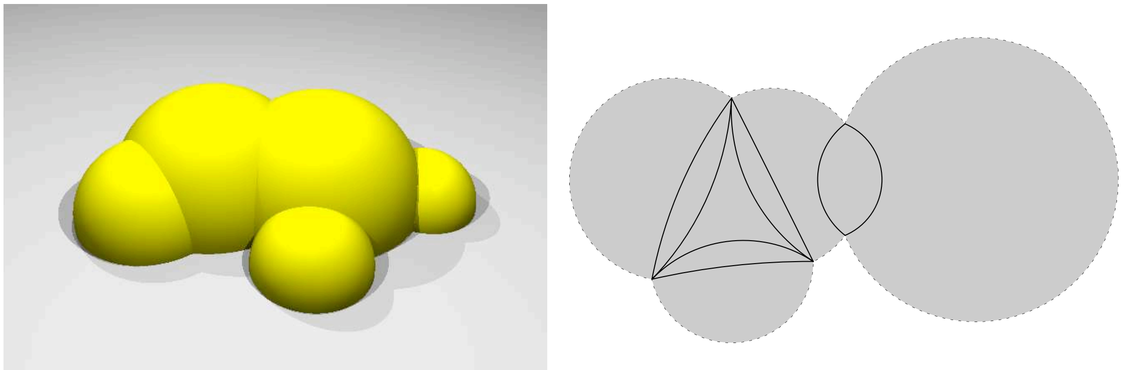

FIGURE 1.4. For finitely-bent domains, preimages of flat pieces under r are called "gaps", preimages of bending lines are "crescents".

4. Boundary Derivatives and Harmonic Measure

It is clear from looking at a few examples that the derivatives of a welding map encode the geometry of a domain. Since the derivatives of the welding map are determined by the derivatives of conformal maps, we wish to obtain estimates on the boundary derivatives of conformal maps which relate the geometry of a domain to the modulus of the derivative. An intuitive understanding is given by classical physics: we know that the derivative $\frac{1}{|f'|}$ of the Riemann map describes heat flow or electrostatic flux through the boundary in a simple model where a point source of heat or charge is placed at $f(0)$ and the boundary is packed with ice or connected to ground. Thus $|f'|$ is largest at points of convexity far from $f(0)$and $|f'|$ is smallest at points of concavity near to $f(0)$, like a lightning rod. To make this concrete, we use some techniques from geometric function theory which provide invariant ways of getting at the question of boundary derivatives.

4.1. Harmonic Measure. Let Ω be a simply-connected planar domain whose boundary is a Jordan curve in $\hat{\mathbb{C}}$, and let $E \subset \partial\Omega$. Choose some $z \in \Omega$. The *harmonic measure* of E in Ω as seen from z, denoted $\omega(z, E, \Omega)$, is a sort of conformally invariant

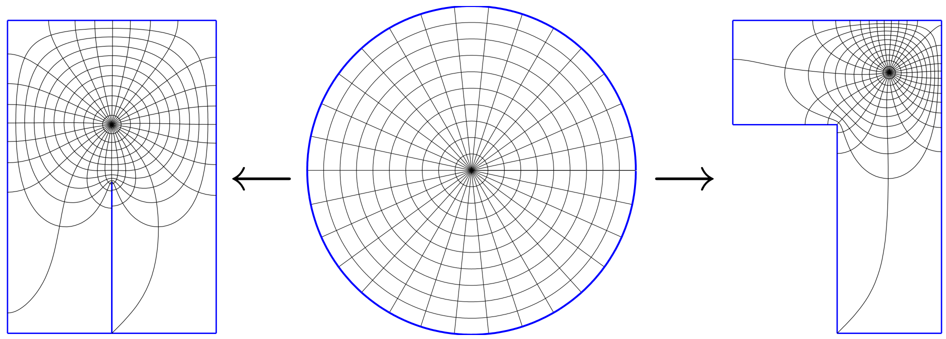

FIGURE 1.5. Images of circles and radial lines under the Riemann map from the the disk to two domains. The behavior of the derivatives is apparent in the spacing.

way of asking how large the arc E is, as seen from the point z. There are 3 equivalent ways of viewing the harmonic measure:

(1) Solutions to the Dirichlet problem.

Let $u : \Omega \to \mathbb{R}$ solve the Dirichlet problem in Ω with boundary conditions

$$\chi_E(w) = \begin{cases} 1 & , w \in E \\ 0 & , otherwise \end{cases}$$

Then $\omega(z, E, \Omega) = u(z)$.

(2) Exit probabilities of Brownian motion.

Let $B_z(t)$ be a standard 2-dimensional Brownian motion starting from z. Define the stopping time

$$\tau = \inf\{t > 0 : B_z(t) \in \partial\Omega\}$$

Then $\omega(z, E, \Omega) = \Pr\{B_z(\tau) \in E\}$.

(3) Arclength on the disk.

Let $f : \Delta \to \Omega$ be conformal with $f(0) = z$. Then $\omega(z, E, \Omega) = \frac{1}{2\pi} L[f^{-1}(E)]$.

Rigorous proof is somewhat lengthy. Consider (1) $\iff$ (3). This follows from two facts: first, that harmonic functions are equal to their average taken on concentric circles, and second, that the solution $u(z)$ is a harmonic function, and hence $u \circ f$ is also harmonic (the composition of an analytic function and a harmonic function is again harmonic).

To see (1) $\iff$ (2), we need to show that $\Pr\{B_z(\tau) \in E\}$ is harmonic in z. The basic idea is a conditioning argument. Before arriving at the boundary, B_z must pass through any circle $C_{z,r}$ centered at z and contained in Ω. Let $\sigma = \inf\{t > 0 : B_z(t) \in C_{z,r}\}$. Using the radial symmetry of Brownian motion, we observe that $B_z(\sigma)$ is distributed uniformly on $C_{z,r}$. Thus our conditioning argument is

$$\begin{aligned}\Pr\{B_z(\tau) \in E\} &= \int_{C_{z,r}} \Pr\{B_w(\tau) \in E\}\Pr\{B_z(\sigma) \in dw\} \\ &= \frac{1}{2\pi r}\int_{C_{z,r}} \Pr\{B_w(\tau) \in E\}|dw|\end{aligned}$$

Since $\Pr\{B_z(\tau) \in E\}$ is equal to its own average on circles $C_{z,r}$, it is a harmonic function. Further, it satisfies the same boundary conditions as u, and hence the two agree.

Interpretation (3) gives us the connection with boundary derivatives. If s is arclength on $\partial\Omega$, θ is the angular coordinate on the circle (with s, θ related by the conformal map f), and ω is harmonic measure (for some Ω and basepoint $z = f(0)$), we can consider the Radon-Nikodym derivative $\frac{d\omega}{ds}$ and we have

$$\frac{d\omega}{ds} = \frac{d\theta}{ds} = \frac{1}{|f' \circ f^{-1}|}$$

4.1.1. *Extension of Domain.* Interpretation (2) has an immediate and useful consequence known as the principle of extension of domain.

PROPOSITION 1.1 (Extension of Domain). *Let $\Omega_1 \subset \Omega_2$ be Jordan domains allowing a nontrivial shared boundary arc $E \subset \partial\Omega_1 \cap \partial\Omega_2 \neq \emptyset$. Then*

$$\omega(z, E, \Omega_1) \leq \omega(z, E, \Omega_2)$$

Consider that some of the random walks which were stopped when they hit $\partial\Omega_1$ are no longer stopped since $\Omega_1 \subset \Omega_2$. Thus, some of them may return and hit E. On the other hand, every trajectory which stops at E in Ω_1 still does so in Ω_2.

Thus boundary derivatives along common boundary arcs will decrease as a domain grows.

4.2. Extremal Distance. Let Γ be a *path family* in a domain Ω, that is, a set of countable unions of rectifiable arcs contained in Ω. We wish to create a conformally-invariant notion of the length of a path family. We will consider metrics on Ω of the form

$$ds^2 = \rho^2(dx^2 + dy^2)$$

where $\rho : \Omega \to \mathbb{R}$ is any non-negative Borel measurable function which assigns finite nonzero area to Ω, i.e.

$$0 < A(\Omega, \rho) \equiv \int_\Omega \rho^2 dx dy < \infty$$

We define the length of a path family Γ with respect to ρ as

$$L(\Gamma, \rho) \equiv \inf_{\gamma \in \Gamma} \int_\gamma \rho |dz|$$

Definition 1.5 (Extremal Length). The *extremal length* of a path family Γ is

$$\lambda_\Omega(\Gamma) = \sup_\rho \frac{L(\Gamma, \rho)^2}{A(\Omega, \rho)}$$

It is often useful to normalize the problem so one considers only metrics such that either $L(\Gamma, \rho) = 1$ or $A(\Omega, \rho) = 1$; since the ratio L^2/A is unchanged when ρ is multiplied by a scalar, either normalization is of course fine.

$\lambda_\Omega(\Gamma)$ is a conformal invariant. Indeed, pulling back the metric defined by $\rho(w)$ through a conformal map $w = f(z)$ results in a metric defined on $f^{-1}(\Omega)$ by the scalar

$$\rho(f(z))|f'(z)|$$

This is also an allowable metric, and hence our definition is invariant with respect to conformal transformations.

DEFINITION 1.6 (Extremal Distance). Let $E, F \subset \overline{\Omega}$. The *extremal distance* $d_\Omega(E, F)$ between E and F is

$$d_\Omega(E, F) \equiv \lambda_\Omega(\Gamma)$$

where Γ is the set of connected arcs in Ω which join E and F.

The conjugate extremal distance $d^*(E, F)$ is the extremal length of the family of curves which separate E and F. In this case, we do not require that the curves be connected – they may be a finite union of disjoint arcs in Ω.

For the case of a rectangle, we can obtain the extremal length between two opposing sides explicitly. We have

PROPOSITION 1.2. *Let Ω be a rectangle with side lengths l and h. If E and F are the two opposing sides of length h, then*

$$d_\Omega(E, F) = \frac{l}{h}$$

and

$$d^*(E, F) = \frac{h}{l}$$

This suggests an alternate characterization of extremal distance when E, F are two disjoint subarcs of $\partial\Omega$. Let $\xi_1, \xi_2, \xi_3, \xi_4$ be the endpoints of E and F listed in standard orientation. One can show that there is a unique conformal map f taking Ω to a rectangle of height 1 such that the ξ_i lie on the vertices. Let l be the length of this rectangle. Then by conformal invariance,

$$d_\Omega(E, F) = l$$

and the extremal metrics are the scalar multiples of $|f'|$.

Extremal distance has several properties which make it a useful tool. First is the fact that it is defined as a supremum over a famiy of metrics, so any choice of metric provides an estimate for extremal distance. (Further, note that we have $dd^* = 1$.

Thus, lower bounds on d^* give upper bounds on d.) Some other key properties, no less practical, are summarized here.

(1) The extension rule.

Let $\Omega_1 \subset \Omega_2$ be domains and let Γ a path family in Ω. Then

$$\lambda_{\Omega_2}(\Gamma) = \lambda_{\Omega_1}(\Gamma)$$

and if Γ_2 is a path family in Ω_2 such that every $\gamma \in \Gamma_2$ contains some path in Γ then

$$\lambda_{\Omega_2}(\Gamma_2) \geq \lambda_{\Omega}(\Gamma)$$

(2) The serial rule.

Consider two path families Γ_1, Γ_2 contained in disjoint open sets Ω_1, Ω_2. Let Γ be a third path family contained in $\Omega \supseteq \Omega_1 \cup \Omega_2$ such that every $\gamma \in \Gamma$ contains a path in Γ_1 and a path in Γ_2. Then

$$\lambda(\Gamma) \geq \lambda(\Gamma_1) + \lambda(\Gamma_2)$$

(3) The parallel rule.

Consider two path families Γ_1, Γ_2 contained in disjoint open sets Ω_1, Ω_2. Let Γ be a third path family contained in $\Omega \supseteq \Omega_1 \cup \Omega_2$ such that every $\gamma \in \Gamma_1 \cup \Gamma_2$ contains a path in Γ . Then

$$\frac{1}{\lambda(\Gamma)} \geq \frac{1}{\lambda(\Gamma_1)} + \frac{1}{\lambda(\Gamma_2)}$$

(4) The symmetry rule.

Let $T : \Omega \to \Omega$ satisfy $T \circ T(z) = z$ with either T or $\overline{T}$ analytic. If Γ is a path family in Ω such that $T(\Gamma) = \Gamma$, then

$$\lambda(\Gamma) = \sup \left\{ \frac{L^2(\Gamma, \rho)}{A(\Omega, \rho)} : \rho = (\rho \circ T)|J_T| \right\}$$

where $|J_T| = |T'|$ when T is analytic and $|\overline{T}'|$ when $\overline{T}$ is analytic.

The serial rule suggests an estimate for extremal distances in strip domains, i.e domains of the form:

$$\Omega = \{(x, y) : |y - m(x)| < \theta(x)/2, a < x < b\}$$

To see why this should be true, choose a partition of $[a, b]$ by choosing some integer $n > 0$ and setting

$$x_k = \frac{k}{n}(b - a)$$

for $0 \leq k \leq n$.

Let $I_k = \Omega \cap \{(x, y) : x = x_k\}$. By the serial rule,

$$d_\Omega(I_0, I_n) \geq \sum_1^n d(I_{k-1}, I_k)$$

As $n \to \infty$, the regions between successive I_k become approximately rectangular, so $d(I_{k-1}, I_k) \approx \frac{\Delta x}{\theta(x_k)}$, where $\Delta x = (b - a)/n$. Thus

$$d_\Omega(I_0, I_n) \geq \int_a^b \frac{dx}{\theta(x)}$$

After proper proof, this result is sometimes known as the Ahlfors Distortion Theorem.

There is a method, due to Beurling, for estimating harmonic measures of boundary arcs in terms of extremal distances between particular arcs in a domain. We will describe this in more detail in chapter three, where we apply the method to obtain results in domains with smooth boundaries.

5. Summary of Results

We can now describe the main results in this thesis.

In chapter 2, we develop the differential geometry of convex hull boundaries in the case when Ω has a smooth boundary. In the context of 3-manifolds, convex hull boundaries are typically studied when the planar domain Ω has a highly non-smooth boundary, typically with dimension > 1. In the smooth case, it emerges that Thurston's bending measure is essentially the principal hyperbolic curvature of the dome S_Ω. In the smooth case, the nearest-point retraction map is a bijection and piecewise C^1; we obtain explicit formulas for the Jacobian and the quasiconformal factor. Finally, we develop a differential equation for the conformal map from the convex hull boundary to the disk. The flow generated by this ODE acts on the domain as a retraction along the medial axis; this is one demonstration of how the conformal structure of the hyperbolic convex hull can be understood in terms of the medial axis.

In chapter 3, we obtain estimates on the modulus of boundary derivatives in smooth domains. The main theme is that given a conformal map $f : \Delta \to \Omega$ and some point $\xi \in \partial\Omega$, the boundary derivative $|f' \circ f^{-1}(\xi)|$ factors into two terms: the first term accounts for the local geometry of $\partial\Omega$ near ξ and is stated in terms of κ, the boundary curvature at ξ, and R, the radius of the medial circle tangent at ξ. The second term says that boundary derivatives increase exponentially with hyperbolic distance. Thus, one can think of the boundary derivatives as factoring into the form

$$|f' \circ f^{-1}(\xi)| \approx \frac{R}{2 - R\kappa} e^d$$

The $\frac{R}{2-R\kappa}$ is an application of Beurling's method (see [**25**]) to the case of a smooth boundary. The exponential term is obtained using constructions from hyperbolic geometry.

It is a famous theorem of Sullivan that the conformal structure of the convex hull boundary approximates the conformal structure of the domain; one might state the theorem as follows: "Given any domain Ω, there is a universal $K > 1$ such that there exists a K-quasiconformal map $\sigma : \Omega \to S_\Omega$ which is the identity on the common boundary". In chapter 3, we develop explicit estimates that allow us to approximate hyperbolic distances and extremal distances in Ω in terms of the same quantities on S_Ω. These explain the exponential dependence of boundary derivatives on hyperbolic distance, and also connect hyperbolic distance to the geometry of the domain. Using the material in chapter 2, we show that these estimates have natural interpretations in terms of the medial axis. In particular, we have a medial-axis based analog of the

Ahlfors distortion theorem. The famous estimate $\int \frac{dx}{\theta}$ is exchanged for an analogous integral taken along the medial axis. We also produce a new method of proof, and a refinement of, a conjecture due to Thurston that the nearest-point retraction is 2-Lipschitz in the hyperbolic metrics.

Chapter 4 begins to pave the way for data compression. Our eventual goal in chapter 5 is to develop a compressor for simple closed plane curves; rather than working directly with the curves we work with the associated welding maps. This means we need to understand how perturbations in welding maps will affect the corresponding quasicircles. In chapter 4 we study the differential of the isomorphism between the two models of the universal Teichmüller space. We develop explicit formulas, given in terms of Hilbert transforms, for the differential. The formula simplifies greatly at the identity. We also develop estimates showing how Weil-Petersson norms of tangent vectors can be used to obtain bounds in the Hausdorff metric on distortion of quasicircles. However, even when the tangent vector is too irregular to admit a finite WP norm, we can still obtain good bounds on distortion.

In chapter 5, we develop our compressor. We introduce Kolmogorov's ϵ-entropy and describe some results on ϵ-entropy of Lipschitz functions. We then introduce a compressor which produces piecewise linear ϵ-approximations to a more general class of functions in the uniform norm. We demonstrate that it gives optimal results when one restricts the functions under consideration to be Lipschitz. The final task is developing a compressor for shapes. Uniform approximations to welding maps are not sufficient; we show that quasisymmetry is the essential feature. That is, consider a welding map h and an approximation $\tilde{h}$ with associated quasicircles Q and $\tilde{Q}$ such that

$$K_{qc}(h \circ \tilde{h}^{-1}) \leq 1 + \epsilon$$

where $K_{qc}(h \circ \tilde{h}^{-1})$ is the constant of quasisymmetry of the composition. We obtain bounds on the Hausdorff distance between the quasicircles Q and $\tilde{Q}$ which depend only on ϵ. Finally, we develop a heuristic for constructing quasisymmetric approximations $\tilde{h}$, and provide some experimental results showing the effectiveness of the compressor.

CHAPTER 2

Differential Geometry of Smooth Convex Hull Boundaries

0.1. Notation.

Ω – a domain

S_Ω – hyperbolic convex hull boundary (dome) of Ω

β – bending measure on S_Ω

$L[\gamma], L_h[\gamma], L_\rho[\gamma]$ – length of an arc γ in the Euclidean, hyperbolic, or other metric ρ

$d_h(p, q)$ – hyperbolic distance between points p and q.

$\kappa(\gamma, h), \kappa(\gamma, e)$ – curvature of a curve γ in hyperbolic or Euclidean space

$\kappa_n(v, h), \kappa_n(v, e)$ – hyperbolic or Euclidean normal curvature of a surface in direction v

On a smooth branch of the medial axis we adopt the following notation. See figure 2.1.

$m(t)$ – an arc-length parametrization of the medial axis.

$a(t), b(t)$ – points of tangency of the medial circle at time t.

$B_t \subset S_\Omega$ – bending line whose endpoints at infinity are $a(t), b(t)$.

$F_t \subset \Omega$ – the arc $r^{-1}(B_t)$

$c(t)$ – center of the arc F_t

$R(t)$ – radius of the medial circle at time t.

$\kappa_m, \kappa_a, \kappa_b$ – Euclidean curvatures of $a(t), b(t), m(t)$

τ_a, τ_b, τ_m – tangent angle of $a(t), b(t), m(t)$

ν_a, ν_b, ν_m – angle of normal to $a(t), b(t), m(t)$

ϕ – the angle $\arg(b - m) - \tau_m = \tau_m - \arg(a - m)$

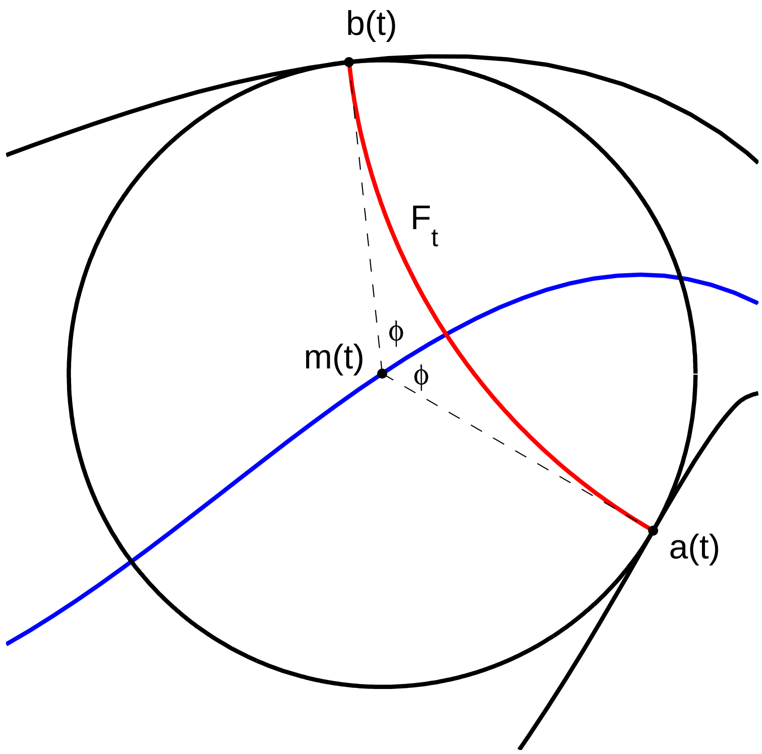

FIGURE 2.1. Notation for the medial axis. The axis is shown in blue; $m(t)$ is a parametrization of the medial axis. $a(t), b(t)$ are points of tangency. The red arc $F_t = r^{-1}(B_t)$ is the foliating arc connecting $a(t)$ and $b(t)$. $\phi = \arg(b - m) - \tau_m$ is the angle between one of the dashed lines and the tangent to the medial axis at m.

1. Overview: Domes over Smooth Domains

Throughout this paper we will work on a domain whose medial axis consists of one smooth branch with smooth boundary arcs. The dome S_Ω of such a domain is also smooth (as we will show), unlike the case when the medial axis has branch points. At branch points, the dome will generally be no more than C^1 no matter how smooth the boundary arcs are.

A few remarks are in order on the geometry of S_Ω. First, there is a natural "transverse" coordinate system $S(t, v)$ on S_Ω (see figure 2.2: for fixed t, $S_t(v) = S(t, v)$ is a parametrization of B_t and for fixed v, $S_v(t) = S(t, v)$ is a transverse arc, i.e. an arc orthogonal to all bending lines B_t. Call the t and v directions "transverse" and "parallel" respectively.

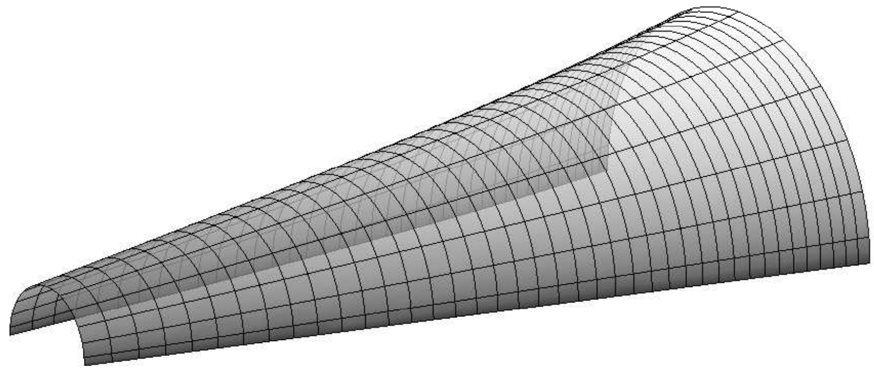

FIGURE 2.2. Transverse coordinates on a smooth section of S_Ω are constructed from bending lines and the family of arcs transverse to the bending lines. Under the nearest-point retraction, these coordinates retract to a transverse coordinate system on the domain Ω.

These coordinates also give principal coordinates at each point of S_Ω. The dome is a hyperbolic developable surface with zero hyperbolic principal curvature along each geodesic B_t and hence maximal hyperbolic principal curvature in the transverse direction. Each transverse arc is thus a line of hyperbolic principal curvature.

Let $r : \Omega \to S_\Omega$ be the hyperbolic nearest-point retraction map. In the situation we are considering, it is a bijection. Transverse coordinates retract under r^{-1} to an orthogonal coordinate system on Ω. This is obvious when the point of interest is the midpoint of a bending line whose endpoints at infinity are diametrically opposed on the relevant medial circle, and it follows in general by conjugation with a conformal self-map of $\mathbb{H}^3$. Hence the Jacobian is diagonal in transverse coordinates. In the parallel direction, r agrees with stereographic projection onto any bending line.

2. Preliminaries

In this section we define the basic quantities we need to develop the theory.

DEFINITION 2.1 (Cross-ratio). Let (a, b, c, d) be 4 points in the complex plane. Their cross-ratio is defined to be

$$\chi(a, b, c, d) = \frac{(b-a)}{(d-a)}\frac{(d-c)}{(b-c)}$$

Definition 2.2 (Path of nearest points). Define the path of "nearest points"

$$p^*(t) = \lim_{\epsilon \searrow t} \arg\min_{p \in B_t} \mathrm{d}_h(p, B_{t+\epsilon})$$

and the infinitesimal distance between them

$$d^*(t) = \lim_{\epsilon \to 0} \frac{1}{\epsilon} d_h(B_t, B_{t+\epsilon})$$

We would like geometric estimates for d^*. Our first step is a formula for the infinitesimal cross-ratio of endpoints of adjacent bending lines.

Proposition 2.1 (Cross-ratio of Endpoints). *Let a, b be the endpoints of some bending line at $t = 0$. Then the infinitesimal cross-ratio $\chi_{inf}(t)$ satisfies*

$$\chi_{inf}(t) \equiv \lim_{\epsilon \searrow 0} \frac{1}{t^2} \chi(a_t, a_{t+\epsilon}, b_{t+\epsilon}, b_t) = -\frac{|\dot{a}\dot{b}|}{|b-a|^2}$$

where $\dot{a} = \frac{da}{dt}\Big|_t$, similar for $\dot{b}$.

Proof. We lose nothing by considering $\chi_{inf}(0)$. Then

$$\begin{aligned}
\chi(a, a_t, b_t, b) &= \frac{a_t - a}{b-a} \cdot \frac{b - b_t}{a_t - b_t} \\
&= \frac{t\dot{a} + O(t^2)}{b-a} \cdot \frac{-t\dot{b} + O(t^2)}{(a-b) + t(\dot{a} - \dot{b}) + O(t^3)} \\
&= \frac{t^2 \dot{a}\dot{b} + O(t^3)}{(b-a)^2 + t(\dot{a} - \dot{b})(b-a) + O(t^3)}
\end{aligned}$$

From the geometry of the medial axis one sees that $\arg \dot{a}\dot{b} = 2\arg(b-a) - \pi$, and it is then straightforward to verify that the right-hand-side becomes real and negative in the limit. $\square$

The next lemma is stated in non-invariant terms; it connects the Euclidean geometry of Ω to invariant quantities. We make the following definition:

Definition 2.3 (Midpoint of B_t). Fix a chart for the half-space model of H^3. Then the midpoint of a bending line B_t for a given domain $\Omega \subset \hat{\mathbb{C}}$ is the midpoint of B_t viewed a Euclidean semicircle in this chart.

Lemma 2.1 (Location of p^*). *Let $a, b \in \partial\Omega$ be the endpoints of some bending line B_0. Then p^* lies at hyperbolic distance $\frac{1}{2}\log\left|\frac{\dot{a}}{\dot{b}}\right|$ from the midpoint of B_0. Positive distances indicate motion towards b.*

Proof. First, conjugate with a hyperbolic ϕ with fixed points a, b to create a domain $\widetilde{\Omega}$ where $|\dot{\tilde{a}}| = |\dot{\tilde{b}}|$ (see figure 2.3). This will imply that $\kappa_{\tilde{a}} = \kappa_{\tilde{b}}$, and hence ϕ

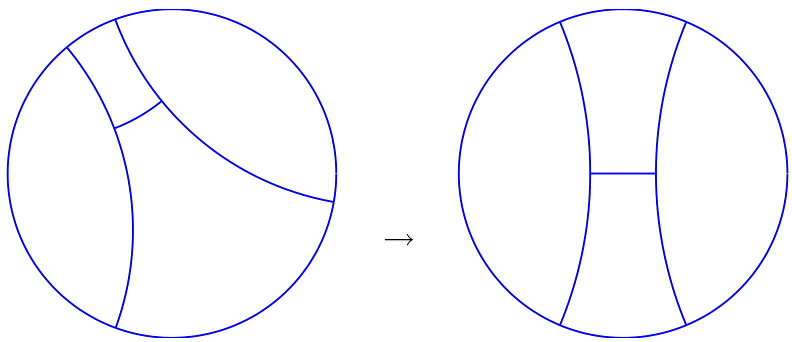

Figure 2.3. Endpoints of nearby bending lines are almost cocircular. This figure shows the action of the map ϕ in lemma 2.1 on the retracts of a nearby pair of bending lines. The arc joins the retracts of the nearest points on each bending line.

takes p^* to the midpoint of B_0. We claim that that ϕ satisfies

$$|\phi'(a)| = e^d$$

$$|\phi'(b)| = e^{-d}$$

where d is the hyperbolic translation distance along B_0 towards b. Indeed, assume for the moment that $a = -1$ and $b = 1$ and our medial circle is the unit circle. Then a hyperbolic taking some point $r \in (-1, 1)$ to 0 has the form

$$\sigma(z) = \frac{z - r}{1 - rz}$$

with

$$\sigma'(z) = \frac{1 - r^2}{(1 - rz)^2}$$

and thus $\sigma'(1) = \frac{1+r}{1-r}$ and $\sigma'(-1) = \frac{1-r}{1+r}$. But $\mathrm{d}_h(0,r) = \log\frac{1+r}{1-r}$, so our claim holds in this case. If a and b are arbitrary points, we can always consider the composition $\phi = \psi \circ \sigma \circ \psi^{-1}$ where $\psi \in SL_2(\mathbb{C})$ normalizes things to the situation just described. But $\phi'(a) = \sigma'(-1)$ and $\phi'(b) = \sigma'(1)$ since σ fixes 0 and 1. The claim is proven.

Now by our claim, we have $|\dot{\tilde{a}}| = e^d|\dot{a}|$ and $|\dot{\tilde{b}}| = e^{-d}|\dot{b}|$, and since we chose d so that $|\dot{\tilde{a}}| = |\dot{\tilde{b}}|$, we have:

$$e^d|\dot{a}| = e^{-d}|\dot{b}|$$

$$e^d = \sqrt{\left|\frac{\dot{b}}{\dot{a}}\right|}$$

and the conclusion follows, since p^* lies at distance $-d$ from the midpoint.

□

Lemma 2.2 (Infinitesimal distance between bending lines).

$$d^*(t) = 2\frac{\sqrt{|\dot{a}\dot{b}|}}{|b-a|}$$

Proof. Let B_t and $B_{t+\epsilon}$ be two bending lines. Normalize so their endpoints at infinity form a rectangle of some height h and width w. By definition, the cross-ratio $|\chi|$ of their endpoints is w^2/h^2.

Further, we already showed that

$$\lim_{\epsilon\to 0}\frac{1}{\epsilon^2}\left|\chi(a_t, a_{t+\epsilon}, b_{t+\epsilon}, b_t)\right| = |\chi_{inf}(t)| = \frac{|\dot{a}\dot{b}|}{|b-a|^2}$$

That is, as $\epsilon \to 0$, we have

$$\frac{w^2}{h^2} \to \epsilon^2\frac{|\dot{a}\dot{b}|}{|b-a|^2}$$

After normalization, the nearest points on B_t and $B_{t+\epsilon}$ are clearly their midpoints. The metric at the midpoints tends to $2/h$, so

$$d_h(B_t, B_{t+\epsilon}) \to w\cdot\frac{2}{h} = 2\epsilon\frac{\sqrt{|\dot{a}\dot{b}|}}{|b-a|}$$

Therefore

$$d^*(t) \equiv \lim_{\epsilon \to 0} \frac{1}{\epsilon} d_h(B_t, B_{t+\epsilon}) = 2\frac{\sqrt{|\dot{a}\dot{b}|}}{|b-a|}$$

□

This next invariant is useful when understanding how Euclidean curvatures transform under linear fractional maps. It is also closely related to the curvature of S_Ω, as we will show later.

LEMMA 2.3. *The quantity*

$$\chi_\kappa = \sin^2 \phi \, (1 - R\kappa_a)\, (1 - R\kappa_b)$$

is invariant under linear fractional maps.

PROOF. Let $C(t)$ be a medial circle and let A and B be the circles of curvature at $a(t)$ and $b(t)$. If we extend the arc F_t to a circle, it will intersect A and B at 2 additional points p and q. χ_κ is the cross-ratio $\frac{b-p}{a-p}\frac{a-q}{b-q}$. □

We now show that the bending measure, in the smooth case, is given by the nonzero hyperbolic principal curvature of S_Ω which we will denote by κ_1.

LEMMA 2.4. *Let $\tau : [0, T] \to S_\Omega$ be an arclength parametrization of a transverse path. Then*

$$\frac{d\beta}{dh}\Big|_\tau = \kappa_1\Big|_\tau$$

where $\frac{d\beta}{dh}$ is the density of β with respect to hyperbolic length along τ and κ_1 is the principal hyperbolic normal curvature at point $\tau(t)$.

PROOF. Along a transverse arc τ, β is a measure which gives the total turning of the normal to S_Ω along a segment of τ. Consider a finitely-bent approximation to S_Ω. When τ crosses a bending line, the unit normal changes discontinuously according to the bending angle. The change has no component parallel to the bending line. In the smooth limit, the analogous construction is the turning of the normal along a path without geodesic torsion. In fact, τ is a line of principal curvature (hence geodesic torsion vanishes) and

$$D_{\dot{\tau}}(\hat{\mathbf{n}}) = \begin{pmatrix} \frac{d\beta}{dh} \\ 0 \end{pmatrix}$$

in principal coordinates. Thus

$$\begin{aligned} \frac{d\beta}{dh} &= \langle D_{\dot{\tau}}\hat{\mathbf{n}}, \dot{\tau} \rangle \\ &\equiv \kappa_1 \end{aligned}$$

REMARK. Note that lemma 2.4 only holds along transverse paths. Along an arbitrary path σ,

$$\frac{d\beta}{dh} = \langle D_{\dot{\tau}}\hat{\mathbf{n}}, \dot{\tau} \rangle \cos\phi = \kappa_1 \cos\phi$$

where ϕ is the angle between $\dot{\sigma}$ and the normal to the bending lines. However, this is no longer the normal hyperbolic curvature: by the Euler formula, the hyperbolic normal curvature $\kappa_n(\dot{\sigma})$ is

$$\kappa_n(\dot{\sigma}) = \kappa_1 \cos^2\phi$$

$\square$

We also have a formula for the area element in transverse coordinates.

LEMMA 2.5 (Area Element). *Let (t, θ) be transverse coordinates on S_Ω where t is hyperbolic arclength along p^* and $\theta \in (-\pi/2, \pi/2)$ is the angular coordinate on each B_t. Then the hyperbolic area element is*

$$dA_{hyp} = \frac{1}{y_3^2}\left(\frac{d\theta dt}{|\phi'|}\right)$$

where $\phi \in PSL_2(\mathbb{C})$ fixes $a(t), b(t)$ and takes $p^*(t)$ to the midpoint of B_t.

PROOF. θ is the angular coordinate on B_t, which is a semicircular arc of radius $|b-a|$, so clearly the hyperbolic length of $d\theta$ is $\frac{d\theta}{|b-a|y_3}$.

Now let $\gamma_p(t)$ be the transverse coordinate arc through $p \in B_t$ and let $\tilde{\gamma}_p(t) = \phi(\gamma_p(t))$. Since $\gamma_{p^*}(t)$ is hyperbolic unit-speed, we have $|\frac{\partial}{\partial t}\tilde{\gamma}_{p^*}(t)| = |b-a|$. In fact, by symmetry of the situation after applying the normalizing map ϕ, all $|\frac{\partial}{\partial t}\tilde{\gamma}_p(t)|$ are equal. Since $|\frac{\partial}{\partial t}\tilde{\gamma}_p(t)| = |\phi'(p)| \cdot |\frac{\partial}{\partial t}\gamma_p(t)|$, we have $|\frac{\partial}{\partial t}\gamma_p(t)| = \frac{|b-a|}{|\phi'|}$. Hence the hyperbolic length of the coordinate vector dt is $\frac{|b-a|dt}{y_3|\phi'|}$.

The lemma follows by multiplying the two hyperbolic lengths, since the coordinate system is orthogonal.

□

Finally, we address the smoothness of the dome. This is a corollary of known results relating smoothness properties of the medial axis to smoothness properties of the boundary curves.

LEMMA 2.6 (Smoothness of S_Ω). *If $(m(t), R(t))$ be a C^p, $p \geq 2$ branch of the medial axis satisfying $R > 0$, $|\dot{R}| < 1$ and $|\kappa_m| < \frac{1-\dot{R}^2-R\ddot{R}}{R\left(1-\dot{R}^2\right)}$, then S_Ω is also C^p.*

PROOF. Fix a chart for $\mathbb{H}^3$ and parametrize S_Ω in transverse (t,θ) coordinates where the θ coordinate indicates distance along B_t, measured in radians from the midpoint of the circular arc B_t . These coordinates can be written

$$y_1 = \mathrm{Re}\left(\frac{a+b}{2} + \frac{b-a}{2}\sin\theta\right)$$
$$y_2 = \mathrm{Im}\left(\frac{a+b}{2} + \frac{b-a}{2}\sin\theta\right)$$
$$y_3 = \frac{|a-b|}{2}\cos\theta$$

These depend analytically on the boundary curves $a(t), b(t)$, which are known to be C^p given the assumptions [**31**].

□

3. The Jacobian of r, the Nearest-Point Retraction Map

We first compute the Jacobian in a simple situation and then derive the general formula by conjugation. We'll work in terms of r^{-1}, which is a bijection in our situation, and has the advantage that the differential geometry of the dome is very simple.

Throughout this section we'll work in transverse coordinates (see figure 2.2) and adopt the notations

κ_1, κ_2 – principal hyperbolic normal curvatures of S_Ω in the transverse and parallel directions, respectively. ($\kappa_2 \equiv 0$)

J_{ij} – i, j-th component of the Jacobian of r

J_{ij}^{-1} – i, j-th component of the Jacobian of r^{-1}

Lemma 2.7. *At the midpoint of a bending line B_{t_0} whose endpoints at infinity are diametrically opposed on C_{t_0},*

$$J_{11}^{-1} = \frac{1+\kappa_1}{2}$$

where J_{11}^{-1} is the transverse component of J^{-1}.

Proof. Normalize so the endpoints of B_t are $\pm R(t_0)$. Let $q(t)$ be the path of midpoints of bending lines, parametrized by "Euclidean" distance in the half-space chart. At $t = t_0$, this path is transverse to B_{t_0}. We have (see figure 2.4)

$$r^{-1}(q(t)) = m(t) + R(t)\tan\frac{\theta}{2}e^{i\tau_m}$$

where $\theta(t)$ is the angle between the normal to S_Ω and the vertical axis, and τ_m is the tangent to the medial axis. Thus

$$\frac{d}{dt}r^{-1}(q(t)) = \dot{m} + \dot{R}\tan\frac{\theta}{2}e^{i\tau_m} + R\frac{\dot{\theta}}{2}\sec^2\frac{\theta}{2}e^{i\tau_m} + R\tan\frac{\theta}{2}ie^{i\tau_m}\dot{\tau}_m$$

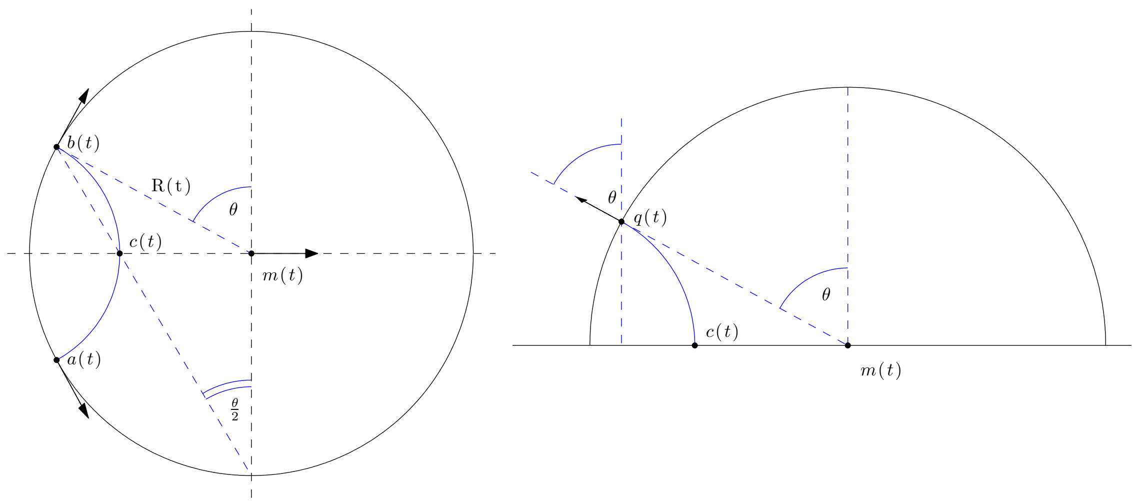

FIGURE 2.4. Overhead and cross-section views of the setup of lemma 2.7. The circle on the left is the medial circle tangent at $a(t), b(t)$; the circle on the right is part of the support plane of S_Ω tangent at q. The point $r^{-1}(q(t))$ lies at $c(t) = m(t) + R(t)\tan\frac{\theta}{2}e^{i\tau_m}$

.

At time $t = t_0$, we have $\theta = 0$, $\dot{R} = 0$, and $\tau_m = 0$, so

$$\begin{aligned}\frac{d}{dt}r^{-1}(q(t)) &= \dot{m} + \frac{R\dot{\theta}}{2}\\ &= 1 + \frac{R\dot{\theta}}{2}\end{aligned}$$

where we assumed a unit-speed parametrization of $m(t)$, so $\dot{m} = 1$. Further, at $t = t_0$ we have $|\dot{a}| = \frac{\sqrt{1-\dot{R}^2}}{1-R\kappa_a} = 1$ and $|\dot{b}| = \frac{\sqrt{1-\dot{R}^2}}{1-R\kappa_b} = 1$, so $\dot{q} = 1$ as well. Hence

$$\begin{aligned}J_{11}^{-1} = \left|\frac{d(r^{-1}(q))}{dq}\right| &= 1 + \frac{R\dot{\theta}}{2}\\ &= 1 + \frac{R\kappa_n(\dot{q}, e)}{2}\\ &= \frac{1+\kappa_1}{2}\end{aligned}$$

since $\kappa_1 \equiv \kappa_n(\dot{q}, h) = 1 + R\kappa_n(\dot{q}, e)$ by lemma 2.8. $\square$

THEOREM 2.1 (Jacobian of r^{-1}). *At a point $p = (y_1, y_2, y_3) \in S_\Omega$, the Jacobian of the inverse of the nearest-point retraction is*

$$J^{-1} = \begin{bmatrix} \frac{1+\kappa_1}{1+y_3/R} & 0 \\ 0 & \frac{1}{1+y_3/R} \end{bmatrix}$$

in transverse coordinates on S_Ω and Ω. κ_1 is the principal curvature of the dome in the transverse direction.

PROOF. The proof is by conjugation to the situation in lemma 2.7. Let $p = (y_1, y_2, y_3)$ be any point on some bending line B_t. Apply a Möbius map ϕ to normalize so that the endpoints of B_t are diametrically opposed on a circle of radius $R(t)$ and $\phi(p)$ lies at the midpoint. Then

$$r^{-1} = \phi^{-1} \circ r^{-1} \circ \phi$$

Hence

$$J^{-1}\Big|_p = |\phi^{-1\prime}(r^{-1} \circ \phi(p))| \begin{bmatrix} \frac{1+\kappa_1}{2} & 0 \\ 0 & \frac{1}{2} \end{bmatrix} |\phi'(p)|$$

The entry J^{-1}_{22} is equal to $1/2$ since r agrees with stereographic projection along bending lines; $1/2$ is simply the derivative of stereographic projection at the origin.

We now compute the derivatives of our map ϕ. Since ϕ is an isometry of $\mathbb{H}^3$ we have $\frac{1}{R}|\phi'(p)| = \frac{1}{y_3}$ hence

$$|\phi'(p)| = \frac{R}{y_3}$$

On B_t, r^{-1} agrees with stereographic projection in the disk of radius R. From the formulas for stereographic projection, we compute that $r^{-1}(p)$ lies at distance $R\sqrt{\frac{1-y_3/R}{1+y_3/R}}$ from the center of the disk. Since ϕ^{-1} acts isometrically on the disk of radius R taking the center to $r^{-1}(p)$, we have

$$|\phi^{-1\prime}| = 2\frac{y_3/R}{1+y_3/R}$$

and the lemma follows. $\square$

REMARK. The quantity $\frac{1+y_3/R}{2}$ which appears in the lemma is the spherical metric at $r^{-1}(p)$ in the disk of radius R:

$$\frac{1+y_3/R}{2} = \frac{1+\frac{1-(s/R)^2}{1+(s/R)^2}}{2} = \frac{1}{1+(s/R)^2}$$

where we used the fact that $r^{-1}(p)$ lies at some distance $s = R\sqrt{\frac{1-y_3/R}{1+y_3/R}}$, or equivalently $\frac{y_3}{R} = \frac{1-(s/R)^2}{1+(s/R)^2}$. Thus the Jacobian is a product of two terms: the spherical metric and a correction given in terms of bending.

3.1. Explicit Formulas for the Jacobian. We now develop some formulas for κ_1 in terms of the geometry of Ω.

Calculating curvatures generally involves taking second derivatives of curves in some chart. This next lemma may be viewed as a shortcut for taking some second derivatives of curves in $\mathbb{H}^3$ when their "Euclidean" curvatures, i.e. their curvatures as curves in some chart with the Euclidean metric, are easy to come by. For example, in the standard half-space model for hyperbolic 3-space $\mathbb{H}^3$, a circular arc of radius R orthogonal to the boundary has Euclidean curvature $1/R$ in the chart, but 0 hyperbolic curvature.

Let $\gamma(t)$ be a hyperbolic unit-speed parametrization of a smooth curve in $\mathbb{H}^3$. We will use these notations; the subscript $'e'$ implies a fixed choice of chart.

$\mathbf{n_h}$	principal hyperbolic unit normal to the curve in $\mathbb{H}^3$
$\mathbf{n_e}$	principal "Euclidean" unit normal to the curve in chart coordinates
$\kappa_n(\gamma, h) = \langle D_t\dot\gamma, \mathbf{n_h}\rangle_h$	curvature of γ in $\mathbb{H}^3$
$\kappa_n(\gamma, e) = \dfrac{\langle\ddot\gamma, \mathbf{n_e}\rangle_e}{\lvert\dot\gamma\rvert_e^2}$	curvature of γ in the chart, as $\mathbb{E}^3$

We remark that $\mathbf{n_h}$ and $\mathbf{n_e}$ are identical up to a factor of length. If $1/y_3$ is the hyperbolic metric in the half-space model $\{(y_1, y_2, y_3) : y_3 > 0\}$ for $\mathbb{H}^3$, then $\mathbf{n_h} = y_3\mathbf{n_e}$.

LEMMA 2.8. *Let $\gamma(t)$ be a hyperbolic unit-speed parametrization of a curve in $\mathbb{H}^3$ and let $\alpha(t) = \exp(t\dot{\gamma}(t_0))$. Then*

$$\kappa(\gamma, h) = y_3 \left(\kappa(\gamma, e) - \kappa(\alpha, e) \cos\theta\right)$$

at time t_0, where θ is the angle between the acceleration vector $\ddot{\alpha}$ and $\mathbf{n_e}$.

PROOF. We need a formula for the covariant acceleration.

$$\begin{aligned} D_t\dot{\gamma} &= (\ddot{\gamma}^k + \dot{\gamma}^i\dot{\gamma}^j\Gamma^k_{ij})\partial_k \\ &= (\ddot{\gamma}^k + \dot{\alpha}^i\dot{\alpha}^j\Gamma^k_{ij})\partial_k && \text{at time } t_0 \\ &= (\ddot{\gamma}^k - \ddot{\alpha}^k)\partial_k && \text{by the geodesic equation} \end{aligned}$$

The h- and e- normals and inner products agree up to a scalar factor. We compute the h-curvature of γ in terms of the e-curvatures:

$$\begin{aligned} \langle D_t\dot{\gamma}, \mathbf{n_h}\rangle_h &= \langle \ddot{\gamma} - \ddot{\alpha}, \mathbf{n_h}\rangle_h \\ &= \langle \ddot{\gamma} - \ddot{\alpha}, y_3\mathbf{n_e}\rangle_h && \text{since } \mathbf{n_e} = \frac{1}{y_3}\mathbf{n_h} \\ &= \frac{1}{y_3}\langle \ddot{\gamma} - \ddot{\alpha}, \mathbf{n_e}\rangle_e && \text{since } \langle\rangle_h = \left(\frac{1}{y_3}\right)^2 \langle\rangle_e \\ &= \frac{1}{y_3}\left(\langle \ddot{\gamma}, \mathbf{n_e}\rangle_e - \langle \ddot{\alpha}, \mathbf{n_e}\rangle_e\right) \\ &= \frac{1}{y_3}\left(\kappa(\gamma, e)|\dot{\gamma}|^2 - \kappa(\alpha, e)|\dot{\alpha}|^2\cos\theta\right) \\ &= y_3\left(\kappa(\gamma, e) - \kappa(\alpha, e)\cos\theta\right) && \text{since } |\dot{\gamma}| = |\dot{\alpha}| = y_3^2 \end{aligned}$$

as claimed. □

A similar calculation relates "Euclidean" and hyperbolic normal curvatures of a surface $S \subset \mathbb{H}^3$:

LEMMA 2.9. *The normal curvature to S in direction v satisfies*

$$\kappa_n(v, h) = y_3 \left(\kappa_n(v, e) - \kappa(\alpha, e) \cos\theta\right)$$

where θ is now the angle between $\ddot{\alpha}$ and the surface normal.

PROOF. Apply the method of lemma 2.8 to a geodesic in S with initial velocity v and project the result onto the surface normal. □

Applying our corollary yields an explicit expression for the principal curvature of the dome.

PROPOSITION 2.2.

$$\kappa_1(q) = \frac{\sin\phi}{\cosh(d)}\sqrt{(1 - R\kappa_a)(1 - R\kappa_b)}$$

where $d = d_h(q, p^*)$ is hyperbolic distance between q and p^*.

PROOF. Apply a normalizing map so the endpoints of B_t are diametrically opposed on C_t and $\kappa_a = \kappa_b = \kappa$ for some κ. Let u be a transverse-pointing vector at some $q = (y_1, y_2, y_3) \in B_t$. In this chart, the Euclidean transverse principal curvature $\kappa_n(u, e)$ of S_Ω satisfies

$$\kappa_n(u, e) = -\kappa \qquad , \forall q \in B_t$$

The difference in sign is due to the choice of inward-pointing normals both on the convex hull boundary and on the boundary of Ω. By corollary 2.9,

$$\begin{aligned} \kappa_1(q) &= \kappa_n(u, h) \\ &= y_3\left(\kappa_n(u, e) - \kappa(\alpha, e)\cos\theta\right) \\ &= -y_3\left(\kappa + \frac{1}{y_3}\cos\theta\right) \end{aligned}$$

In this chart, p^* is at the midpoint of B_t and q lies at some angular distance α from p^*, measured in radians along the circular arc B_t. If θ is the angle between the normal to S_Ω and the vector $\ddot{\alpha}$, we have

$$\cos\alpha = -\cos\theta = \frac{y_3}{R}$$

Hence

$$\kappa_1(q) = \cos\alpha\,(1 - R\kappa)$$
$$= \cos\alpha\sqrt{\chi_\kappa}$$

Now we need to express $\cos\alpha$ in terms of hyperbolic distance. It is a standard calculation in hyperbolic geometry that

$$d_h(p^*, q) = \tanh^{-1}\sin\alpha$$

Indeed, to compute $d_h(p^*, q)$, change coordinates so B_t has endpoints lying on the unit circle at infinity and p^* lies at $(0, 0, 1)$. Then integration along the geodesic joining p^* and q gives

$$d_h(p^*, q) = \int_0^\alpha \frac{1}{y^3}d\theta = \int_0^\alpha \frac{d\theta}{\cos\theta}$$

Direct evaluation of the integral gives the result. Hence

$$\sin\alpha = \tanh d$$
$$\implies \cos\alpha = \sqrt{1 - \tanh^2 d}$$
$$= \operatorname{sech}\, d$$

So combining,

$$\kappa_1(q) = \frac{\sin\phi}{\cosh d}\sqrt{\chi_\kappa}$$

This completes the proof. $\square$

We state two corollaries; both follow immediately from the formulas for the Jacobian and κ_1.

Corollary 2.2. *Let* $\kappa_1^*(t) = \max_{q\in B_t}\kappa_1(q)$. *Then*

$$\kappa_1^* = \sin\phi\sqrt{(1 - R\kappa_a)(1 - R\kappa_b)}$$

achieved at p^*.

Corollary 2.3. *The quasiconformal factor of the map $r : \Omega \to S_\Omega$ is*

$$K = 1 + \kappa_1$$

with a maximum on each B_t of

$$K^*(t) = 1 + \sin\phi\sqrt{(1 - R\kappa_a)(1 - R\kappa_b)}$$

achieved at p^*. The infimum, $K^*(t) = 1$, is attained at the endpoints at infinity.

4. An ODE for the Isometry $\iota : S_\Omega \to \mathbb{D}$

Thurston gave an explicit construction for the Riemann map $\iota : S_\Omega \to \mathbb{D}$. Here we work out an ODE for the boundary values of ι along a smooth branch of the medial axis. We review the construction in the finitely-bent case and then construct the map in the smooth case.

4.1. The Finitely-Bent Case. Let $\Omega \subset \mathbb{C}$ be a domain with smooth boundary; further assume its medial axis has only a single branch. Let $O = \bigcup_1^K D_j$ be a finite union of discs approximating Ω, say by choosing a connected subset of the discs whose centers form the medial axis (See figure 2.5). Let $\{D_1, D_2, ..., D_K\}$ be an enumeration of the discs along the medial axis starting at one leaf D_1 and ending at the last disc D_K. We take D_K as the final disc for our map $\iota : \partial O \to \partial D_K$.

Each disc D_k contains a gap, on which the nearest-point retraction is a bijection, and this gap is bounded by two circular arcs orthogonal to ∂D_k. Let F_k^- be the arc whose endpoints intersect ∂D_{k-1} and let F_k^+ be the arc which intersects ∂D_{k+1}. Let E_k be the closure of the gap, minus F_k^+.

The dome of the approximation is finitely-bent, and in the finitely-bent case, the map ι can be realized as a composition of elliptic mobius maps $\{\eta(k)\}_1^{K-1}$, where η_k has fixed points at $D_k \cap D_{k+1}$ and rotation angle equal to the bending angle at the intersection of D_k and D_{k+1}.

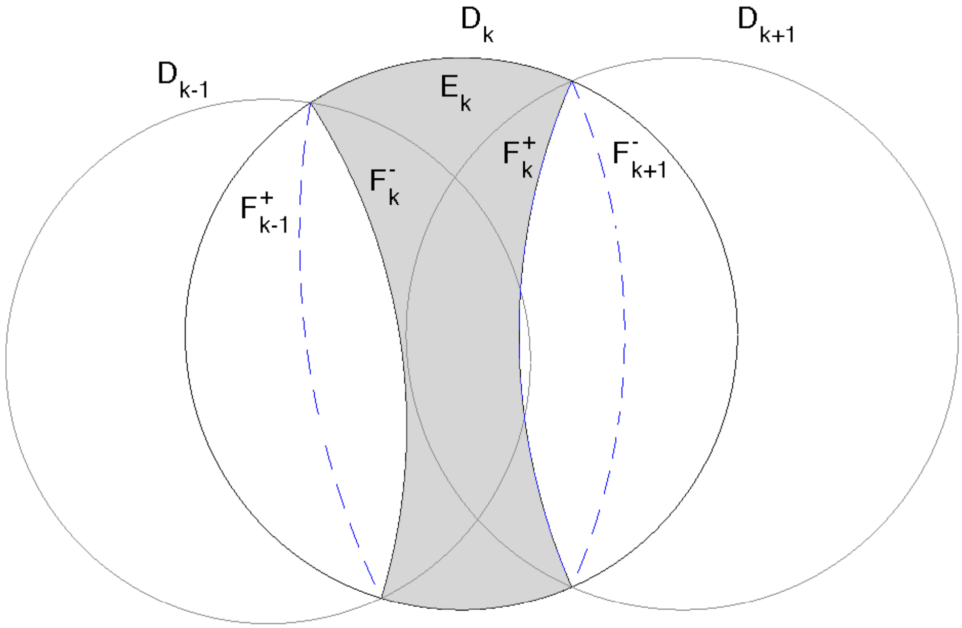

FIGURE 2.5. Notation for the discrete flow

We can imagine this process evolving in stages given by a family of maps $f(w,k):O\to\bigcup_{k+1}^{K}$ for $0\leq k<K$ with the property that

$$f(w,k)=\begin{cases}\eta_k\circ\eta_{k-1}\circ\ldots\circ\eta_1 & ,w\in\bigcup_1^k E_j\\ \mathrm{Id} & ,\text{otherwise}\end{cases}\tag{2}$$

and $f(w,0)$ is taken to be the identity.

4.2. The Smooth Case. By successively refining our approximation O we obtain in the limit a smooth flow $\psi(w,t):\Omega\to\Omega_t$ for $0\leq t\leq T$, where $m(t)$ is some parametrization of the medial axis of Ω, $\{D_0,D_T\}$ are the interiors of the medial circles at $t=0$ and $t=T$, and $\{\Omega_t\}_0^T$ is a decreasing family of subsets of Ω. Using standard orientation, we let $\Omega_t\subset\Omega$ be the region bounded by ∂D_t between $a(t),b(t)$ and $\partial\Omega$ between $b(t),a(t)$.

By considering the limit of the finitely-bent case we see that the derivatives of our flow must be 0 for $x\in F_s, s\geq t$. For $x\in F_s, s<t$, the flow must be given by a vector field $v_t\in sl(2,\mathbb{C})$: the generator of an elliptic rotation with fixed points $a(t),b(t)$ and rotation velocity corresponding to the infinitesimal change in bending angle at time

t, namely the Radon-Nikodym derivative $\frac{d\beta}{dt}$. Such a vector field has the form

$$v_t = -i\frac{d\beta}{dt}\frac{(w-a_t)(w-b_t)}{a_t-b_t}$$

Thus we can write

$$v_t(\psi(w)) = \begin{cases} \mathrm{Id} & w \in F_s, \quad s \geq t \\ -i\frac{d\beta}{dt}\frac{(\psi(w)-a_t)(\psi(w)-b_t)}{a_t-b_t} & w \in F_s, \quad s < t \end{cases}$$

We obtain the flow at time t by integration:

$$\psi(w,t) = \int_0^t v_s(\psi(w,s))ds$$

The next task is working out the bending along the medial axis.

THEOREM 2.4. *Along a smooth branch of the medial axis,*

$$\frac{d\beta}{dt} = \frac{\sqrt{1-\dot{R}^2}}{R}$$

PROOF. Along the path $p^*(t)$ we have

$$\frac{d\beta}{dh} = \kappa_1 = \sin\phi\sqrt{(1-R\kappa_a)(1-R\kappa_b)}$$

and

$$\begin{aligned} \frac{dh}{dt} \equiv d^* &= 2\frac{\sqrt{|\dot{a}\dot{b}|}}{|b-a|} \\ &= \frac{2}{|b-a|}\sqrt{\frac{1-\dot{R}^2}{(1-R\kappa_a)(1-R\kappa_b)}} \\ &= \frac{1}{R\sin\phi}\sqrt{\frac{1-\dot{R}^2}{(1-R\kappa_a)(1-R\kappa_b)}} \end{aligned}$$

where we used identities for $\dot{a}, \dot{b}$ from the geometry of the medial axis and the fact that $\frac{|a-b|}{2R} = \sin\phi$. Combining,

$$\begin{aligned} \frac{d\beta}{dt} &= \frac{d\beta}{dh}\frac{dh}{dt} \\ &= \frac{\sqrt{1-\dot{R}^2}}{R} \end{aligned}$$

as claimed.

□

We can now present the flow equations.

THEOREM 2.5 (The ι flow equations). *The flow* $\psi : \Omega \times [0,T] \to \Omega$ *given by*

$$\psi(w,t) = \int_0^t v_s(\psi(w,s))ds$$

where

$$v_t(\psi(w)) = \begin{cases} \mathrm{Id} & w \in F_s, \quad s \geq t \\ -i\frac{\sqrt{1-\dot{R}^2}}{R}\frac{(\psi(w)-a_t)(\psi(w)-b_t)}{a_t-b_t} & w \in F_s, \quad s < t \end{cases}$$

satisfies

$$\psi_0 = \mathrm{Id}$$

$$\psi_T = \iota$$

We point out that these equations are now expressed in terms of Ω, without appeal to the convex hull boundary S_Ω or its bending.

In a particular moving frame, this vector field is seen as a hyperbolic element of $psl_2(\mathbb{R})$.

PROPOSITION 2.3 (ι in a moving rotational frame). *In coordinate* $z(w) = \frac{w-m(t)}{R(t)}e^{-i\theta_m(t)}$ *the vector field generating the* ι *flow is the hyperbolic*

$$\tilde{v}_t(z) = \frac{1}{2R}\left(z^2 - i\left(|\dot{a}| - |\dot{b}|\right) - 1\right)$$

and the hyperbolic fixed points lie on the unit circle.

PROOF. Taking $\frac{\partial}{\partial t}$ of $z(w)$ leads to

$$\begin{aligned}\dot{z} &= -\frac{\dot{R}}{R}z + \frac{1}{R}\left(\dot{w} - \dot{m}\right)e^{-i\theta_m} - iz\kappa_m \\ &= -\frac{\dot{R}}{R}z + \frac{1}{R}\left(\frac{\sqrt{1-\dot{R}^2}}{R}\frac{(w-a)(w-b)}{a-b} - e^{i\theta_m}\right)e^{-i\theta_m} - iz\kappa_m\end{aligned}$$

Writing $\tilde{a} = z(a)$, etc. and using $e^{-i\theta_m} = -i\frac{|a-b|}{a-b}$ and $\sqrt{1-\dot{R}^2} = \frac{|b-a|}{2R}$ we find

$$\begin{aligned}\dot{z} &= -\frac{\dot{R}}{R}z + \frac{1}{R}\left(\frac{(z-\tilde{a})(z-\tilde{b})}{2} - 1\right)e^{-i\theta_m} - iz\kappa_m \\ &= \frac{1}{2R}\left(z^2 - (2\dot{R} + (\tilde{a}+\tilde{b}) + 2iR\kappa_m)z + \tilde{a}\tilde{b} - 2\right)\end{aligned}$$

Since $\tilde{a}\tilde{b} = 1$ and $\tilde{a} + \tilde{b} = 2\cos\phi = -2\dot{R}$, we have

$$\dot{z} = \frac{1}{2R}\left(z^2 - 2iR\kappa_m z - 1\right)$$

and since $\kappa_m = \frac{|\dot{a}|-|\dot{b}|}{2R}$, the formula follows.

Further, $\tilde{v}_t$ is a polynomial of the form $z^2 - i\lambda z - 1$, whose zeros are $\frac{1}{2}\left(i\lambda \pm \sqrt{4-\lambda^2}\right)$. Such points lie on the unit circle and the theorem is proven. □

From the hyperbolic formula above, it is not difficult to work out the vector field in angular coordinates. Computationally, angular coordinates are far more convenient to work with. We present the resulting formulas in the next proposition.

PROPOSITION 2.4 (The vector field in angular coordinates). *In a moving, non-rotational polar coordinate frame (r, θ) centered at $m(t)$, the restriction of the vector field v_t to the boundary of Ω_t is tangential to $\partial\Omega_t$ and satisfies*

$$v_t(r,\theta) = \begin{cases} \frac{\sin(\theta-\theta_m)}{R}\hat{\theta} & (r,\theta) \in (R, (\theta_b, \theta_a)) \\ 0 & \textit{otherwise} \end{cases}$$

where $\hat{\theta}$ is the unit tangent vector to $\partial D_t \cap \partial\Omega_t$ in radians. In a rotating frame where angular coordinate $\theta = 0$ corresponds to the direction of the tangent to the medial *axis, we have*

$$v_t(r,\theta) = \begin{cases} \left(\frac{\sin\theta}{R} - \kappa_m\right)\hat{\theta} & (r,\theta) \in (R,(\theta_b,\theta_a)) \\ 0 & \textit{otherwise} \end{cases}$$

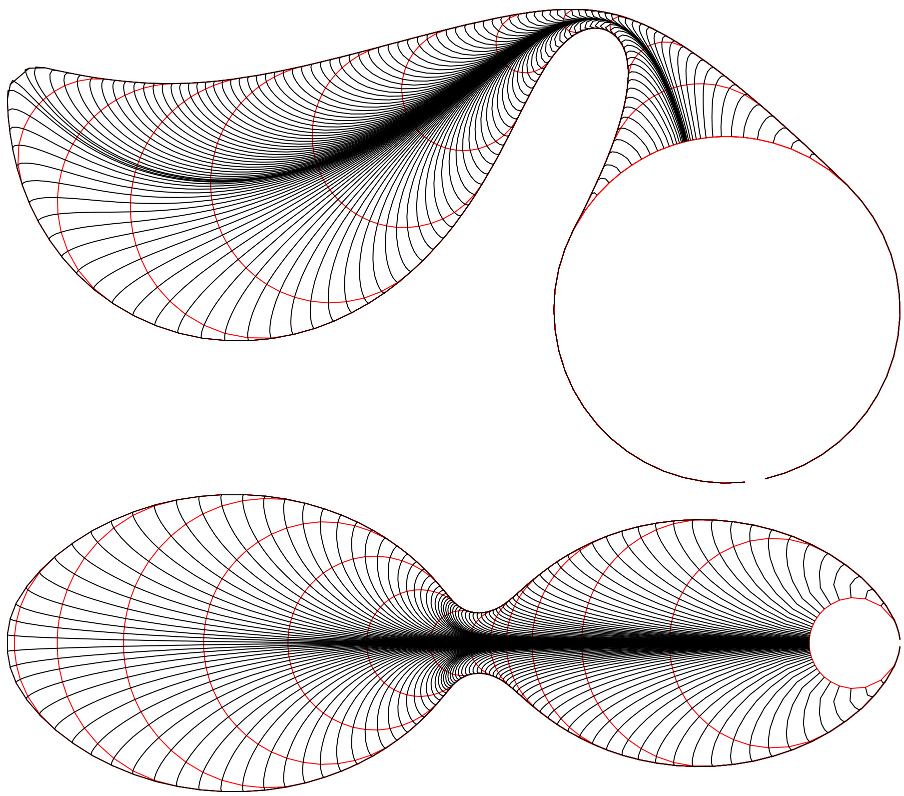

FIGURE 2.6. Boundary points flow back to a disk under the ι flow. The light red circles inside the domain Ω indicate the boundary of the domains Ω_t for times $0 < t < T$.

4.3. Boundary Derivatives of ι. The boundary derivatives of the map $\iota : \partial\Omega \to D_T$ are particularly simple. This next proposition may be viewed as essentially the observation that ι is just an infinitesimal rotation near its fixed points.

PROPOSITION 2.5. *Let $\iota : \partial\Omega \to \partial D_T$ map $\partial\Omega$ to some medial circle ∂D_T. Then ι is differentiable with*

$$\left|\frac{\mathrm{d}\iota}{\mathrm{d}s}\right| = 1$$

at iota's fixed points $a(T)$ and $b(T)$, where s is the arclength parameter along $\partial\Omega$.

PROOF. This follows from basic ODE theory. The flow ψ satisfies an equation of the form

$$\frac{\partial \psi}{\partial t} = f(w,t)$$

where $f(x,t) = v(\psi(w,t),t)$ is C^0 and piecewise C^1 in w, and hence uniformly Lipschitz for all t. It follows that our solution ψ is C^1, and since v vanishes at the fixed points for all t, the arclength derivative of ι at the fixed points is 1.

$\square$

REMARK. It is worth noting that smoothness of $\partial\Omega$ is not used in the proposition. Indeed, the conclusion still holds as a limiting case in, for example, the case of a domain with a cusp.

Away from the fixed points, the flow acts by linear fractional maps. That is, $\psi_{tT} = \psi_T \circ \psi_t^{-1}$ acts on $\partial D_t \cap \partial\Omega_t$ as a linear fractional map σ_t which takes $\partial D_t \cap \partial\Omega_t$ into ∂D_T. Thus the derivatives at any point $a(t)$, $b(t)$ are given by the map σ_t.

CHAPTER 3

Boundary Derivatives in Smooth Domains

0.4. Notation.

Ω – a domain

$f : \mathbb{D} \to \Omega$ – a conformal map

$L[\gamma], L_h[\gamma], L_\rho[\gamma]$ – length of an arc γ in the Euclidean, hyperbolic, or other metric ρ

$\omega(w, E, \Omega)$ – harmonic measure of $E \subset \partial\Omega$ w.r.t. the basepoint $w \in \Omega$

$d_\Omega(E, F)$ – extremal distance between $E, F \subset \partial\Omega$ w.r.t. paths in Ω

$d_h(p, q)$ – hyperbolic distance between points p and q

1. Background: Extremal Length and Harmonic Measure

We recall the main theorems relating extremal distance and harmonic measures in this section. For details and proof, see the excellent book [**25**] of Garnett and Marshall (2005) for a careful exposition.

1.1. The Metric. Extremal distance may be defined as a supremum over a family of metrics on Ω; hence constructing metrics is an important method in estimating extremal distances. Very useful estimates follow from the map and metric defined in this subsection. Let Ω be a domain containing a point $w_0 \in \Omega$ and $\xi \in \partial\Omega$. Writing $d = |w_0 - \xi|$, define $E_r \subset \{w \in \Omega : |w - \xi| = r\}$, $0 < r < d$, to be the shortest circular crosscut separating w_0 from ξ (see figure 3.1). These crosscuts form a region

$$\bigcup_{r=0}^{d} E_r = \{\xi + re^{i\phi} : 0 < r < d, |\phi - \mu(r)| < \theta(r)\}$$

where $\mu(r)$ and $\theta(r)$ are the angular midpoint and width of E_r. The (non-analytic) map

$$\psi(re^{i\phi}) = -\int_r^d \frac{dt}{t\theta(t)} + i\frac{\phi - \mu(r)}{\theta(r)}$$

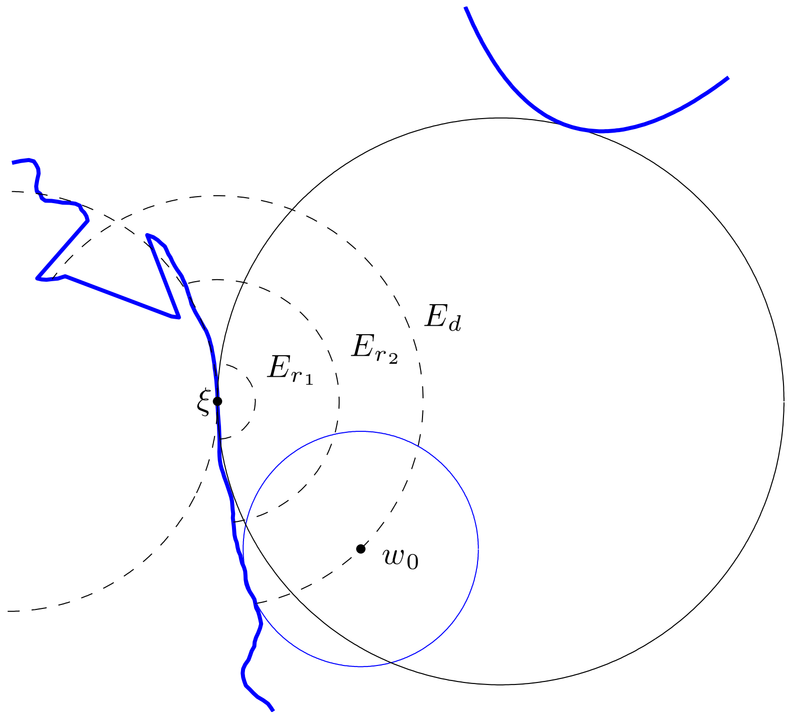

FIGURE 3.1. The setup for the local estimates on $|f'|$. The circle of curvature and two of the separating arcs $\{E_r : 0 < r < d\}$, are shown dashed; the medial circle is solid black. A maximal disk contained in Ω surrounds $w_0 = f(0)$.

takes $\bigcup E_r$ onto the semi-infinite strip $\{(x, y) : -\infty < x < 0, -1/2 < y < 1/2\}$.

Taking $ds^2 = |\nabla \mathrm{Re}(\psi)|^2(dx^2 + dy^2)$ as a metric on some domain Ω leads to the following remarkable estimate for extremal distance.

THEOREM 3.1. *For* $0 < r < d$,

$$d_\Omega(E_r, E_d) \geq \int_r^d \frac{1}{t\theta(t)} dt \tag{3}$$

1.2. Lower Bounds on Extremal Length, Upper Bounds on Harmonic Measure. Take some domain Ω, some point $w_0 \in \Omega$, and a boundary arc $F \subset \partial\Omega$. Consider all Jordan arcs $\sigma \subset \Omega$ which join w_0 to $\partial\Omega \setminus F$ and define

$$\lambda(w_0, F) = \sup_\sigma d_{\Omega\setminus\sigma}(\sigma, F)$$

where we take the supremum over all such σ.

The following theorem of Beurling relates extremal distance and harmonic measure.

THEOREM 3.2. *Let Ω be a domain. Let $w_0 \in \Omega$ and $F \subset \partial\Omega$. Then*

$$e^{-\pi\lambda(w_0,\Omega)} \leq \omega(w_0, F, \Omega) \leq \frac{8}{\pi} e^{-\pi\lambda(w_0,\Omega)}$$

Any choice of the arc σ gives a lower bound on λ and hence an upper bound on harmonic measure.

In the setup of theorem 3.1, let F be the boundary arc containing ξ which lies between the endpoints of some arc E_s for $s < d$. Choose E_d as the arc σ; theorems 3.1 and 3.2 together yield

$$\omega(w_0, F, \Omega \leq \frac{8}{\pi} \exp\left\{-\pi \int_s^d \frac{dt}{t\theta(t)}\right\}$$

1.3. Upper Bounds and Reduced Extremal Distance. While Beurling's theorem yields both upper and lower bounds on harmonic measure, we obtain better lower bounds on harmonic measure by considering reduced extremal distances.

Let $F \in \partial\Omega$ and $w_0 \in \Omega$, and denote by $\delta(w_0, F)$ the reduced extremal distance

$$\delta(w_0, F) \equiv \lim_{\epsilon \longrightarrow 0} \left(d_{\Omega\backslash B_\epsilon}(\partial B_\epsilon, F) - d_{\Omega\backslash B_\epsilon}(\partial B_\epsilon, \partial\Omega)\right)$$

where $B_\epsilon = \{|w - w_0| < \epsilon\}$

We will use the following theorem.

THEOREM 3.3. *If Ω is a Jordan domain and $F \subset \partial\Omega$ is a single arc, then*

$$\omega(w_0, F, \Omega) \geq \frac{2}{\pi} e^{-\pi\delta(w_0,F)}$$

This theorem, along with smoothness assumptions and a metric derived from

$$|\nabla \mathrm{Im}(\psi)| = \sqrt{\left(\frac{1}{r\theta}\right)^2 + \left(\frac{(\phi - \mu)\theta' + \theta\mu'}{\theta^2}\right)^2}$$

yields a lower bound on harmonic measure which complements theorem 3.2. We develop this in the next section. The smoothness assumptions are not too severe; one may mollify the domain by shrinking it slightly to produce another domain with smooth μ, θ. Shrinking the domain will only increase the boundary derivative, so any upper bound which applies to the smaller mollified domain will also apply to the larger original domain. See section 2.3 for a particularly convenient way of doing this.

2. Local Estimates and Boundary Curvature

We are interested in explicit estimates for $|f' \circ f^{-1}(\xi)|$ in terms of the local geometry of Ω. Consider the the following situation (See figure 3.1):

Let Ω be a domain containing a medial circle of radius R, tangent at some $\xi \in \partial\Omega$. Assume further that $\partial\Omega$ is C^2, with boundary curvature κ at ξ. Let $f : \mathbb{D} \to \Omega$ be a conformal map with $f(0)$ lying on the separating crosscut E_d.

Let $F_r \subset \{|w - \xi| = r\}$ be the shortest circular arc passing through $\xi + r\mathbf{n}_\xi$ whose endpoints lie on the circle of curvature at ξ. We can now state the main theorem:

Theorem 3.4 (Local estimates for $|f'|$). *Let $f : \mathbb{D} \to \Omega$ be a conformal map to a domain Ω containing a medial circle of radius R tangent at $\xi \in \partial\Omega$. If $f(0) = \xi + d\mathbf{n}_\xi$ for $d < R$, then $\exists$ constants C_2, C_3 independent of Ω such that*

$$C_2 \frac{d}{2 - \kappa d} \exp\{-A(d)\} \leq |f' \circ f^{-1}(\xi)| \leq C_3 \frac{d}{2 - \kappa d} \exp\left\{ \left(\frac{d}{d(w_0, \partial\Omega)} \right)^2 (B(d) - A(d)) \right\}$$

where

$$A(d) = \pi \int_0^d \frac{L[E_r] - L[F_r]}{L[E_t]L[F_t]} dt$$
$$B(d) = \pi \int_0^d \frac{\mu'(t)^2 + \frac{1}{12}\theta'(t)^2}{L[E_t]} t^2 dt$$

and $d(w_0, \partial\Omega)$ is the Euclidean distance to the boundary. We assume Ω admits $\mu, \theta \in C^1$, by mollification if necessary.

Remark. The method of proof does not yield sharp constants. We obtain constants $C_2 = .453...$ and $C_3 = 1.04....$

The proof will proceed in stages. In the next two subsections we first work out expressions for the derivative and then apply our geometric assumptions to make explicit estimates.

2.1. General Expressions for the Derivative. In this section we work out expressions for the boundary derivative in a domain with smooth boundary. Beurling's method allows us to estimate harmonic measures for the separating arcs E_r. This first lemma allows us to pass to the harmonic measure of a boundary arc in the limit as $r \to 0$.

LEMMA 3.1. *Let $I_r \subset \partial\Omega$ be the boundary arc containing ξ which shares its endpoints with some E_r. Let $\Omega_r = \Omega \setminus B_{\xi,r}$. Then*

$$\lim_{r\to 0} \frac{\omega(w_0, I_r, \Omega)}{\omega(w_0, E_r, \Omega_r)} = \frac{1}{2}$$

PROOF. Let $B_t(y)$ be a 2-dimensional brownian motion in Ω starting from $y \in \Omega$. Let τ be the first hitting time $\tau = \min_{t\geq 0}\{B_t(y) \in \partial\Omega\}$. Since $\omega(w_0, I_r, \Omega) = \int_{E_r} \Pr\{B_\tau(y) \in I_r\} d\omega(w_0, y, \Omega_r)$, the lemma will follow if we can show that $\lim_{r\to 0} \Pr\{B_\tau(re^{i\theta}) \in I_r\} = 1/2$ for any $re^{i\theta} \in E_r$.

Indeed, fix some y and consider the mobius maps β_r taking E_r to the line segment $[-i, i]$, normalized to send the midpoint of E_r to 0. Then $\beta_r(I_r)$ tends to $S^1 \cap \{x < 0\}$ and $\beta_r(\partial\Omega \setminus I_r)$ tends to $S^1 \cap \{x > 0\}$. Since $\beta_r(y) \in [-i, i]$ the claim follows by symmetry. $\square$

THEOREM 3.5. *In the setup of theorem 3.4*

$$|f' \circ f^{-1}(\xi)| \geq \frac{1}{4} \lim_{r\to 0} \exp\left\{\log r + \pi \int_r^d \frac{1}{\theta(t)} \frac{dt}{t}\right\}$$

PROOF. Let $I_r \subset \partial\Omega$ be the boundary arc containing ξ which shares its endpoints with some E_r.

$$\begin{aligned} |f' \circ f^{-1}(\xi) &= \lim_{r\to 0} \frac{L[I_r]}{2\pi\omega(w_0, I_r, \Omega)} \\ &= \frac{1}{\pi} \lim_{r\to 0} \frac{r}{\omega(w_0, I_r, \Omega)} \\ &\geq \frac{1}{4} \lim_{r\to 0} r \exp\left\{\pi\lambda(w_0, E_r, \Omega_r)\right\} \end{aligned}$$

The last inequality is a consequence of lemma 3.1 and theorem 3.2 combined, i.e.

$$\lim_{r\to 0} \omega(w_0, I_r, \Omega) \exp\left\{-\pi\lambda(w_0, E_r, \Omega_r)\right\} \leq \frac{4}{\pi}$$

Applying theorem 3.1 completes the proof.

□

REMARK. In order to obtain a lower bound on the derivative, the essential assumption on $f(0)$ is that the arcs $\{E_r\}_0^d$ separate ξ from $f(0)$; not much other information was used in the proof. However, the upper bound requires us to use more information about the location of $f(0)$. In particular, we need to ensure that $f(0)$ is not too near other points on $\partial\Omega$, since nearby boundary points consume harmonic measure. We'll do this now.

Upper bounds follow from a related metric. As before, consider a domain Ω containing a medial disk D tangent at some $\xi \in \partial\Omega$, and also containing the crosscuts

$$\bigcup_{r=0}^{d} E_r = \{\xi + re^{i\phi} : 0 < r < d, |\phi - \mu(r)| < \theta(r)\}$$

where $\mu(r)$ and $\theta(r)$ are the angular midpoint and width of E_r. The (non-analytic) map

$$\psi(re^{i\phi}) = -\int_r^d \frac{dt}{t\theta(t)} + i\frac{\phi - \mu(r)}{\theta(r)}$$

takes $\bigcup E_r$ onto the semi-infinite strip $\{(x, y) : -\infty < x < 0, -1/2 < y < 1/2\}$.

THEOREM 3.6. *In the setup of theorem 3.4, there exists a constant* $C_1 > 0$ *such that*

$$|f' \circ f^{-1}(\xi)| \leq C_1 \lim_{r \to 0} \exp\left\{ \log r + \pi \left(\frac{d}{d(w_0, \partial\Omega)} \right)^2 \left(\int_r^d \frac{1}{\theta(t)} \frac{dt}{t} + \int_r^d t \frac{\mu'(t)^2 + \frac{1}{12}\theta'(t)^2}{\theta(t)} dt \right) \right\}$$

We may take $C_1 = 1$.

PROOF. Let D be the maximal disk contained in Ω with center w_0. By extension of domain, we may assume Ω consists only of the union $D \bigcup \{E_s\}_0^d$. Indeed, enlarging the domain will only decrease $|f' \circ f^{-1}(\xi)|$.

For some arc E_s, consider the reduced extremal distance

$$\delta(w_0, E_s) \equiv \lim_{\epsilon \to 0} \left(d_{\Omega \setminus B_\epsilon}(\partial B_\epsilon, E_s) - d_{\Omega \setminus B_\epsilon}(\partial B_\epsilon, \partial\Omega) \right)$$

Clearly

$$d_{\Omega \setminus B_\epsilon}(\partial B_\epsilon, \partial\Omega) \geq d_{\Omega \setminus B_\epsilon}(\partial B_\epsilon, \partial D) = \frac{1}{2\pi} \log \frac{d}{\epsilon}$$

by the extension rule for extremal distance. An upper bound on $d_{\Omega \setminus B_\epsilon}(\partial B_\epsilon, E_s)$ will follow from a lower bound on $d^*_{\Omega \setminus B_\epsilon}(\partial B_\epsilon, E_s)$: the length of the family of closed curves in Ω which separate ∂B_ϵ and E_s.

Without loss of generality, assume $w_0 = 0$. Let $r = r(w) = |w - w_0|$, $\phi = \phi(w) = \arg(w - w_0)$ and define

$$\rho_B(w) = \left(\frac{d}{d(w_0, \partial\Omega)} \right) \sqrt{ \left(\frac{1}{r\theta} \right)^2 + \left(\frac{(\phi - \mu)\theta' + \theta\mu'}{\theta^2} \right)^2 }$$

Define the metric $ds^2 = \rho^2(w)|dw|^2$ in $\Omega \setminus B_\epsilon$ where $B_\epsilon = \{|w_0| < \epsilon\}$ and

$$\rho(w) = \begin{cases} \rho_B & w \in \bigcup E_r \setminus D \\ \sqrt{\rho_B^2 + \left(\frac{1}{2\pi|w|} \right)^2} & w \in \bigcup E_r \cap D \\ \frac{1}{2\pi|w|} & w \in D \setminus \bigcup E_r \end{cases}$$

We need to measure the area of Ω and the lengths of closed curves separating ∂B_ϵ and E_s in the metric ρ. We claim that any closed separating curve has length at least

1. Note that $\rho(w) \geq \frac{1}{2\pi|w|}$ for all $w \in \Omega$: indeed, if $w \in \bigcup E_r \setminus D$,

$$\frac{1}{2\pi|w|} \leq \frac{1}{2\pi d(w_0, \partial\Omega)} \leq \frac{d}{2\pi r d(w_0, \partial\Omega)} \leq \frac{d}{\theta r d(w_0, \partial\Omega)} \leq \rho_B(w)$$

and elsewhere it is immediate from the definition of ρ. Hence, any closed arc γ separating ∂B_ϵ and E_s must have length $L_\rho[\gamma] \geq 1$.

The area of Ω under the metric ρ is

$$\begin{aligned}\int_\Omega \rho^2 dxdy &= \int_{\bigcup E_r \setminus D} \rho_B^2 dxdy + \int_{\bigcup E_r \cap D} \rho_B^2 + \left(\frac{1}{2\pi|w|}\right)^2 dxdy + \int_{D \setminus \bigcup E_r} \left(\frac{1}{2\pi|w|}\right)^2 dxdy \\ &= \int_{\bigcup E_r} \rho_B^2 dxdy + \frac{1}{2\pi} \log \frac{d}{\epsilon}\end{aligned}$$

Hence

$$d_{\Omega \setminus B_\epsilon}(\partial B_\epsilon, E_s) = \frac{1}{d^*_{\Omega \setminus B_\epsilon}(\partial B_\epsilon, E_s)} \leq \int_{\bigcup E_r} \rho_B^2 dxdy + \frac{1}{2\pi} \log \frac{d}{\epsilon}$$

and

$$\delta(w_0, E_s) \leq \int_{\bigcup E_r} \rho_B^2 dxdy$$

Let I_s be the boundary arc which lies between the endpoints of E_s and contains ξ. Forming the derivative,

$$\begin{aligned}|f' \circ f^{-1}(\xi)| &= \lim_{s \to 0} \frac{L[I_s]}{2\pi\omega(w_0, I_s, \Omega)} \\ &= \lim_{s \to 0} \frac{L[I_s]}{\pi\omega(w_0, E_s, \Omega)} && \text{by lemma 3.1} \\ &= \frac{2}{\pi} \lim_{s \to 0} \frac{s}{\omega(w_0, E_s, \Omega)} \\ &\leq \lim_{s \to 0} s \exp\left\{\pi \int_{\bigcup_{r=s}^d E_r} \rho_B^2 dxdy\right\}\end{aligned}$$

We can compute this explicitly:

$$\int_r^d \int_{\mu-\theta/2}^{\mu+\theta/2} \rho_B^2 dxdy = \left(\frac{d}{d(w_0,\partial\Omega)}\right)^2 \int_r^d \int_{\mu-\theta/2}^{\mu+\theta/2} \left(\frac{1}{r\theta}\right)^2 + \left(\frac{(\phi-\mu)\theta' + \theta\mu'}{\theta^2}\right)^2 dxdy$$
$$= \left(\frac{d}{d(w_0,\partial\Omega)}\right)^2 \int_r^d \frac{1}{r\theta(r)} + \int_r^d \frac{\mu'(r)^2 + \frac{1}{12}\theta'(r)^2}{\theta(r)} rdr$$

The proof is complete upon substitution. □

2.2. Proof of Theorem 3.4: Local Estimates for $|f'|$. We return to the main theorem and apply our assumptions. The proof makes use of a calculation and an estimate which we formulate as lemmas.

Lemma 3.2. *Let $\kappa \in \mathbb{R}$, let I be a circular arc of curvature κ, and let K_r be a circle of radius $r < 2/|\kappa|$ whose center lies on I. Then I divides K_r into two circular arcs of lengths $2r \arccos \pm \frac{r\kappa}{2}$.*

Proof. See figure 3.2. Assume $\kappa < 0$. Let P be the center of K_r. Extend I to a circle of radius $R = 1/\kappa$ whose center lies at some point Q. Let S be one of the points of intersection of K_r and I and let T be the midpoint of the line joining S to the other point of intersection. Then QTS is a right triangle.

Let $2r\phi$ be the length of the segment of the circle lying to the left of the arc. Then $QS = R$, $ST = r\sin\phi$, and $QT = R - r\cos\phi$. Apply the Pythagorean theorem to the right triangle QTS:

$$(r\sin\phi)^2 + (R - r\cos\phi)^2 = R^2$$
$$\implies \phi = \arccos\left(\frac{r}{2R}\right)$$
$$\phi = \arccos\frac{r\kappa}{2}$$

A similar calculation yields the conclusion in the positively curved case. □

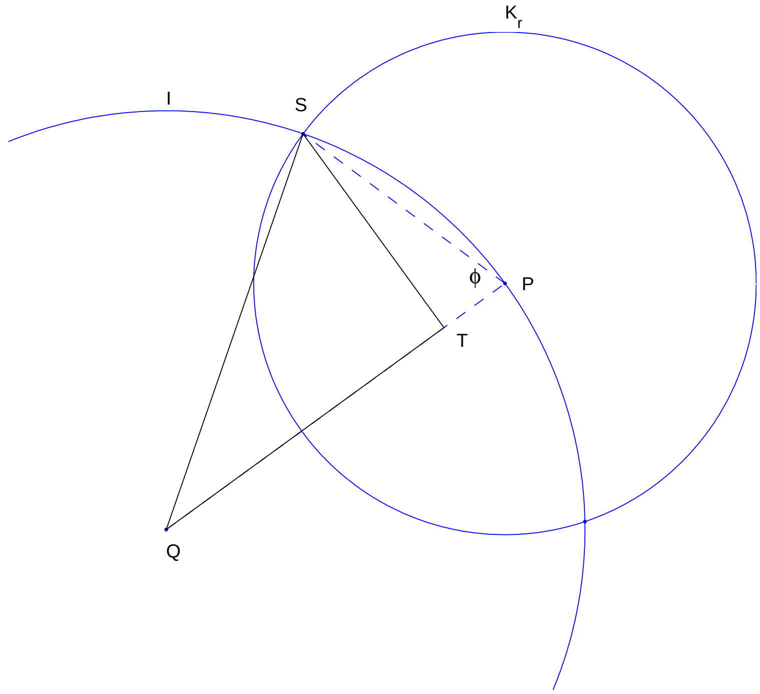

FIGURE 3.2. The setup for lemma 3.2

LEMMA 3.3. *There exist constants* A_1, A_2 *so that for any* $\kappa \in (-\infty, \infty)$ *and* $0 < \epsilon < d \leq 1/|\kappa|$,

$$-A_1 \leq \frac{1}{\pi}\int_\epsilon^d \frac{dr}{r\left(1-\frac{r\kappa}{2}\right)} - \int_\epsilon^d \frac{dr}{2r\arccos\frac{r\kappa}{2}} \leq A_2$$

We may take $A_1 = .0411...$ *and* $A_2 = .0987...$

PROOF. For $0 \leq x \leq 1$, we have

$$\frac{\pi}{2}(1-x) \leq \arccos(x) \leq \frac{\pi}{2} - x$$

Consider the case $\kappa > 0$. In this case, it follows immediately that the difference in the lemma is non-negative. Applying the upper bound,

$$\begin{aligned}\frac{1}{\pi}\int_\epsilon^d \frac{dr}{r\left(1-\frac{r\kappa}{2}\right)} - \int_\epsilon^d \frac{dr}{2r\arccos\frac{r\kappa}{2}} &\leq \frac{1}{\pi}\int_\epsilon^d \frac{dr}{r\left(1-\frac{r\kappa}{2}\right)} - \frac{1}{\pi}\int_\epsilon^d \frac{dr}{r\left(1-\frac{r\kappa}{\pi}\right)} \\ &= \frac{1}{\pi}\left(\int_\epsilon^d \frac{1}{r} + \frac{\kappa}{2-r\kappa} - \int_\epsilon^d \frac{1}{r} + \frac{\kappa}{\pi - r\kappa}\right) \\ &= \frac{1}{\pi}\log\frac{2-\kappa\epsilon}{2-\kappa d}\frac{\pi-\kappa d}{\pi-\kappa\epsilon}\end{aligned}$$

This is decreasing in ϵ and increasing in d. In fact, it is convex in d. The second derivative in d is

$$\kappa^2\left(\frac{1}{(2-\kappa d)^2} - \frac{1}{(\pi-\kappa d)^2}\right) > 0$$

Under the conditions of the lemma, the maximum is achieved at $\epsilon = 0$ and $d = 1/\kappa$. Hence

$$A_2 = \frac{1}{\pi}\log 2\left(1-\frac{1}{\pi}\right) = .0987...$$

This completes the proof of the lemma in the case $\kappa > 0$. A similar argument handles the case of $\kappa < 0$. In this case, the difference in the lemma is nonpositive and the rest of the proof proceeds similarly to produce the estimate for A_1. The case $\kappa = 0$ is trivial. This completes the proof of the lemma.

$\square$

We now prove the main theorem.

Proof of theorem 3.4. We first show the lower bound. By theorem 3.5,

$$|f' \circ f^{-1}(\xi)| \geq \frac{1}{4}\lim_{\epsilon\to 0}\exp\left\{\log\epsilon + \pi\int_\epsilon^d \frac{dr}{L[E_r]}\right\}$$

Define the function $\eta : (0, d] \to (-\pi, \pi]$ by $r\eta(r) = L[E_r] - L[F_r]$. Then by lemma 3.2,

$$\begin{aligned} r\eta(r) &\equiv L[E_r] - L[F_r] \\ &= L[E_r] - 2r \arccos\left(\frac{r\kappa}{2}\right) \end{aligned}$$

and therefore

$$\begin{aligned} \int_\epsilon^d \frac{dr}{L[E_r]} &= \int_\epsilon^d \frac{dr}{r(2\arccos(\frac{r\kappa}{2}) + \eta(r))} \\ &= \int_\epsilon^d \frac{1}{2r \arccos \frac{r\kappa}{2}} - \frac{\eta(r)}{2r \arccos \frac{r\kappa}{2}\left(2\arccos\frac{r\kappa}{2} + \eta(r)\right)} dr \\ &= \int_\epsilon^d \frac{1}{2r\arccos\frac{r\kappa}{2}} - \frac{r\eta(r)}{L[F_r]L[E_r]} dr \end{aligned} \tag{4}$$

Now apply lemma 3.3 to the first term in the integrand.

(5)

$$\int_\epsilon^d \frac{1}{2r\arccos\frac{r\kappa}{2}} + A_2 \geq \frac{1}{\pi}\int_\epsilon^d \frac{1}{\pi\left(1 - \frac{r\kappa}{2}\right)} dr = \frac{1}{\pi}\int_\epsilon^d \frac{1}{r} + \frac{\kappa}{2 - r\kappa} dr = \frac{1}{\pi}\log\frac{d}{\epsilon}\frac{2-\kappa\epsilon}{2-\kappa d}$$

Combining the above expressions,

$$\begin{aligned} |f' \circ f^{-1}(\xi)| &\geq \frac{1}{4}\lim_{\epsilon \to 0} \epsilon \exp\left\{\log\epsilon + \log\frac{d}{\epsilon}\frac{2-\kappa\epsilon}{2-\kappa d} - \pi\int_\epsilon^d \frac{r\eta(r)}{L[F_r]L[E_r]}dr - A_2\right\} \\ &= C_1 \frac{d}{2-\kappa d}\exp\left\{-\pi\int_0^d \frac{r\eta(r)}{L[F_r]L[E_r]}dr\right\} \end{aligned}$$

where the integral converges under our geometric assumptions and $C_2 = \frac{1}{2}e^{-A_2} = .453...$. This completes the lower bound. The proof of the upper bound is nearly identical: beginning from theorem 3.6 and applying the lower bound in lemma 3.3 completes the theorem with constant $C_3 = C_1 e^{A_1} = 1.04...$ $\square$

2.3. Lipschitz Subregions and Upper Bounds. The term

$$B(d) = \pi\int_0^d \frac{\mu'(t)^2 + \frac{1}{12}\theta'(t)^2}{L[E_t]}t^2 dt$$

is not as well-behaved as one might hope; in particular, the term $\theta'(t)^2$ will increase without bound as θ' approaches a delta function. This is particularly unfortunate since the boundary derivatives will not, in general, blow up simply because $\theta(t)$ has become discontinuous. There is a nice construction [1] which allows us to consider a logarithmic measure of area, rather than the boundary behavior, of a subregion in order to obtain upper bounds on extremal distance. We can then convert this estimate, as before, into an upper bound on the derivative. Our presentation follows [**25**].

Assume we're in a situation where $\xi = 0$ and $f(0) = d$. We first normalize by applying the linear fractional map

$$\phi(z) = \frac{z}{1 - \kappa z/2}$$

which sends the circle of curvature to the imaginary axis and preserves the reals. ϕ fixes 0, has $|\phi'(0)| = 1$, and $\phi(d) = \frac{2d}{2-\kappa d}$. Taking the logarithm, we map the right half-plane to the strip. Our domain Ω has been transformed so it now contains the real axis and is asymptotically strip-like as one approaches $-\infty$.

Let $Tr(M)$ be the set of isoceles triangles T such that

(1) $T \subset \Omega$,

(2) T has base on $\mathbb{R}$, and

(3) T has sides of slope $\pm M$,

and define the subregion

$$\widetilde{\Omega} = \bigcup \{T : T \in Tr(M)\}$$

$\widetilde{\Omega}$ is the largest subregion of Ω containing the real axis with M-Lipschitz boundary.

Assume that $\partial\widetilde{\Omega}$ can be written as two curves $y_+(x) = h_1(x) + \pi/2$ and $y_-(x) = -h_2(x) - \pi/2$, with $h_1, h_2 > -\pi/2$. Under our assumptions, both $h_1, h_2 \to 0$ as $x \to -\infty$.

The key lemma is

[1] See [**25**]; thanks to Don Marshall for suggesting this method.

Lemma 3.4 (Sastry). *If* $|h_j(x)| \le \pi M^2$ *for* $s < x < t$*, then*

$$d_{\widetilde{\Omega}}(F_s, F_t) \le \frac{t-s}{\pi} + \frac{4M^2+2}{\pi^2}\text{Area}(S \setminus \widetilde{\Omega}_M)_{s,t} - \frac{1}{(4M^2+2)\pi^2}\text{Area}(\widetilde{\Omega}_M \setminus S)_{s,t}$$

where $E_{s,t} = E \cap \{z : s < \text{Re}z < t\}$*,* $S = \{z = x+iy : -\pi/2 < y < \pi/2\}$*, and* F_s *is the component of* $\widetilde{\Omega}_M \cap \{z : \text{Re}z = s\}$ *intersecting the real axis.*

Thus we have a bound on extremal distance in terms of logarithmic areas, which does not involve boundary regularity. In our setup, we find ourselves integrating from $s = \epsilon$ to $t = \log \frac{2d}{2-\kappa d}$, leaving us with a similar estimate on extremal distance as before, but with the error term $B(d)$ now replaced by

$$\widetilde{B}(d) = \frac{4M^2+2}{\pi^2}\text{Area}(S \setminus \widetilde{\Omega}_M)_{s,t} - \frac{1}{(4M^2+2)\pi^2}\text{Area}(\widetilde{\Omega}_M \setminus S)_{s,t}$$

This estimate is given solely in terms of measures of areas, and does not suffer when the boundary is irregular. This construction also gives a subregion to which the existing estimates $B(d)$ could be applied, without losing too much in terms of the original geometry.

3. Long-Range Estimates and the Dome

We now show that certain extremal and hyperbolic distances in Ω can be approximated by the same quantities on S_Ω. This is advantageous as the Riemann map $\iota : S_\Omega \to \mathbb{D}$ from the dome to the unit disk admits an explicit construction, easily understood in terms of the medial axis of Ω. In particular, we exploit the fact that ι almost immediately gives extremal distances between pairs of bending lines: if B_s and B_t, together with the arcs of $\partial\Omega$ joining their endpoints, bound a generalized quadrilateral $Q \in S_\Omega$, then up to a normalization by some map in $PSL_2(R)$, the map

$$\log\left(\frac{1+\iota}{1-\iota}\right) : S_\Omega \to \{(x,y) : -\infty < x < \infty, -\pi/2 < y < \pi/2\}$$

takes Q to a rectangle in the strip (see figure 3.3).

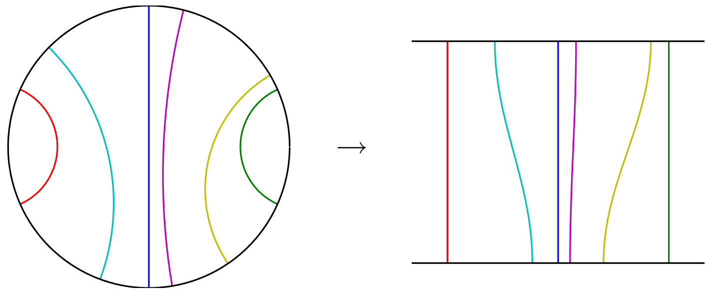

FIGURE 3.3. ι takes bending lines in the dome to geodesics in the disk. After mapping the disk to the strip, we immediately obtain hyperbolic distance d_h and extremal distance d_{S_Ω} between bending lines B_s and B_t: that is, $d_{S_\Omega}(B_s, B_t) = \frac{1}{\pi} d_h(B_s, B_t)$

.

3.1. Notation. Along a smooth branch of the medial axis we adopt the following notation. See figure 3.4.

$m(t)$ – an arc-length parametrization of the medial axis.

$a(t), b(t)$ – points of tangency of the medial circle at time t.

$\kappa_m, \kappa_a, \kappa_b$ – Euclidean curvatures of $a(t), b(t), m(t)$

τ_a, τ_b, τ_m – tangent angle of $a(t), b(t), m(t)$

ν_a, ν_b, ν_m – angle of normal to $a(t), b(t), m(t)$

ϕ – the angle $\arg(b - m) - \tau_m = \tau_{m-} \arg(a - m)$

S_Ω – the dome of Ω

$B_t \subset S_\Omega$ – the bending line whose endpoints at infinity are $a(t), b(t)$.

$F_t \subset \Omega$ – $r^{-1}(B_t)$, a foliating arc.

3.2. Geodesic Distances in S_Ω. As in the previous chapter, let

$$p^*(t) = \arg \min_{p \in B_t} \lim_{\epsilon \searrow t} \mathrm{d}(p, B_{t+\epsilon})$$

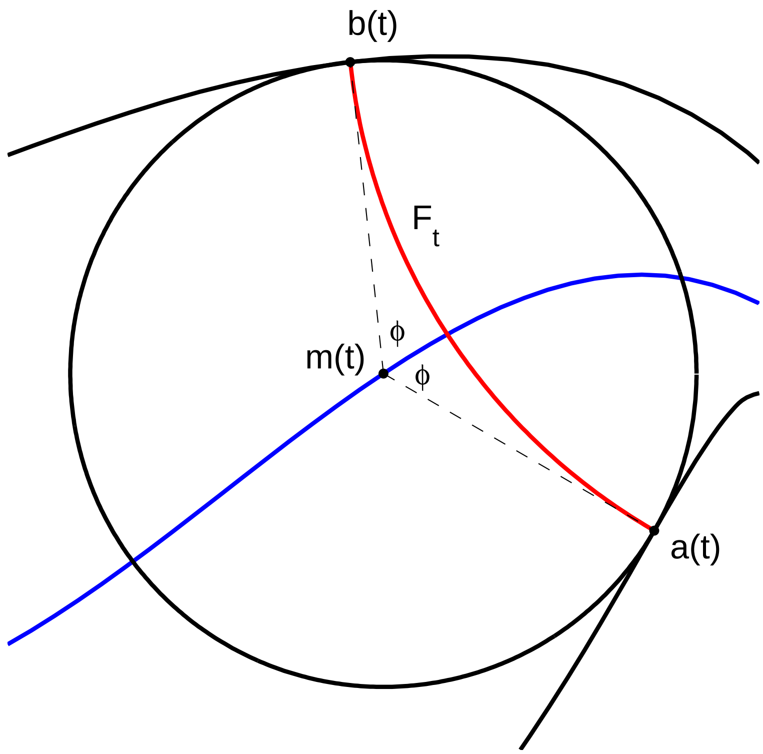

FIGURE 3.4. Notation for the medial axis. The axis is shown in blue; $m(t)$ is a parametrization of the medial axis. $a(t), b(t)$ are points of tangency. The red arc $F_t = r^{-1}(B_t)$ is the foliating arc connecting $a(t)$ and $b(t)$. ϕ is the angle between the dashed lines and the tangent to the medial axis at m.

and

$$d^*(t) = \lim_{\epsilon \to 0} \frac{1}{\epsilon} d_h(B_t, B_{t+\epsilon})$$

LEMMA 3.5 (χ_{inf} invariant under ι).

$$\lim_{\epsilon \to 0} \frac{1}{\epsilon^2} \chi(a_t, a_{t+\epsilon}, b_{t+\epsilon}, b_t) = \lim_{\epsilon \to 0} \frac{1}{\epsilon^2} \chi(\iota(a_t), \iota(a_{t+\epsilon}), \iota(b_{t+\epsilon}), \iota(b_t))$$

PROOF. Assume ι fixes the endpoints of B_t so ι is a retraction into the disk D_t. In this case

$$\frac{\partial}{\partial t} a(t) = \frac{\partial}{\partial t} \iota(a(t))$$
$$\frac{\partial}{\partial t} b(t) = \frac{\partial}{\partial t} \iota(b(t))$$

since the tangent to D_t agrees with the tangent to $\partial\Omega$ at the fixed points and the moduli of the derivatives agree by proposition 2.5. In this case the lemma follows as per the proof of proposition 2.1.

Since any two versions of ι differ only by a Möbius map, the general case follows from invariance of the cross-ratio.

$\square$

LEMMA 3.6 (Length of geodesics in S_Ω). *Let $\gamma \subset S_\Omega$ be the shortest geodesic joining some B_s and B_t, $s < t$. Then*

$$2\int_s^t \frac{\sqrt{|\dot{a}\dot{b}|}}{|b-a|}du \leq L_h[\gamma] \leq 2\int_s^t \sqrt{\frac{|\dot{a}\dot{b}|}{|b-a|^2} + \frac{1}{4}\left(\frac{\kappa_m \dot{R}}{\sqrt{1-\dot{R}^2}} + \frac{\partial}{\partial m}\frac{1}{2}\log\left|\frac{\dot{b}}{\dot{a}}\right|\right)^2}\,du$$

whenever the curve p^* is continuous. ∂_m and dot notation both denote differentiation with respect to the distance along the medial axis.

PROOF. Choose any path $p(u)$ joining B_s and B_t. The lower bound is simply the observation that

$$||\dot{p}(u)||_h \equiv \lim_{\epsilon\to 0}\frac{1}{\epsilon}||p(u+\epsilon)-p(u)||_h \geq \lim_{\epsilon\to 0}\frac{1}{\epsilon}d_h(B_u, B_{u+\epsilon}) \equiv d^*(u)$$

for any choice of path $p(u)$.

The upper bound follows from integrating $||\dot{p}^*||_h$ along the path $p^*(u)$. Decompose $\dot{p}^*(u)$ into components $\dot{p}^*_T(u)$, $\dot{p}^*_\perp(u)$ tangential and orthogonal to the bending line B_u.

Let $c(u)$ be the midpoint of B_u and let $\{\gamma_u(r)\}_{u=s}^t$ be a family of geodesics, each parametrized by hyperbolic distance r such that

$$c(u) + \gamma_u(r)$$

is a point on B_u at signed distance r from the midpoint. Then

$$p^*(u) = c(u) + \gamma_u\left(\log\sqrt{\left|\frac{\dot{b}}{\dot{a}}\right|}\right)$$

and the tangential component $\dot{p}_T^*$ of $||\dot{p}^*||_h$ is given by

$$\begin{aligned}
||\dot{p}_T^*||_h &= ||\dot{c}_T||_h + \frac{\partial}{\partial m} \log \sqrt{\left|\frac{\dot{b}}{\dot{a}}\right|} \\
&= \operatorname{Im} \frac{\dot{b} + \dot{a}}{2|b-a|} + \frac{\partial}{\partial m} \frac{1}{2} \log \left|\frac{\dot{b}}{\dot{a}}\right| \\
&= \frac{(|\dot{a}| - |\dot{b}|)\cos\theta_b}{|b-a|} + \frac{\partial}{\partial m} \frac{1}{2} \log \left|\frac{\dot{b}}{\dot{a}}\right| \\
&= \kappa_m \frac{\dot{R}}{\sqrt{1-\dot{R}^2}} + \frac{\partial}{\partial m} \frac{1}{2} \log \left|\frac{\dot{b}}{\dot{a}}\right|
\end{aligned}$$

where κ_m is the curvature of the medial axis, θ_b is the angle $\arg(b-m) - \tau_m$, τ_m is the angle of the tangent to the medial axis, and m is the center of the medial circle of radius R, all at time u.

The orthogonal component is simply d^*. Since the metric is conformal we have

$$||\dot{p}^*||_h^2 = ||\dot{p}_T^*||_h^2 + ||\dot{p}_\perp^*||_h^2$$

and hence

$$L_h[p^*] = \int_s^t ||\dot{p}^*(t)||_h du = 2 \int_s^t \sqrt{\frac{|\dot{a}\dot{b}|}{|b-a|^2} + \frac{1}{4}\left(\frac{2\kappa_m \dot{R}}{\sqrt{1-\dot{R}^2}} + \frac{\partial}{\partial m}\frac{1}{2}\log\left|\frac{\dot{b}}{\dot{a}}\right|\right)^2}\, du$$

□

Remark. This estimate is sharp, i.e. the path $p^*(u)$ is the geodesic joining B_s and B_t, when $\frac{d}{dt} \log \sqrt{\frac{|\dot{b}|}{|\dot{a}|}} = 0$ and either κ_m or $\dot{R}$ is zero. The first happens exactly when $|\dot{b}/\dot{a}|$ is constant, and using some facts from the medial axis, this condition is equivalent to

$$\frac{\dot{b}}{\dot{a}} = \frac{1 - R\kappa_a}{1 - R\kappa_b} = k$$

Both conditions are satisfied in, for example, a strip-like domain consisting of two curves symmetric about a straight axis, or a section of an annulus.

3.3. Extremal Distances in S_Ω and Ω.

THEOREM 3.7 (Extremal distance comparable). *Let $F_s, F_t \subset \Omega$ be two foliating arcs. Then*

$$\mathrm{d}_{S_\Omega}(B_s, B_t) \le \mathrm{d}_\Omega(F_s, F_t) \le \mathrm{d}_{S_\Omega}(B_s, B_t) + \frac{2}{\pi^2}\int_s^t \mathrm{d}\beta \tag{6}$$

where $\beta(t)$ is the bending measure associated with S_Ω.

PROOF. We appeal to the the finitely-bent case. Let ρ_S be the extremal metric for S_Ω. Observe that the nearest-point retraction r^{-1} maps each facet of the dome conformally onto its image in Ω. Define the metric ρ_Ω on Ω to be $r^*\rho_S$ (the pullback under the nearest-point retraction), where this is defined, and let $\rho_\Omega = 0$ elsewhere. This metric achieves the lower bound.

We explicitly construct a metric to produce the upper bound. Consider two bending lines B_j and B_k, $k > j$. The region of the dome between these lines is a generalized quadrilateral, and there is some extremal map taking this quadrilateral to a rectangle. In fact, this map is simply ι followed by the transformation $z \longrightarrow \log \frac{1+z}{1-z}$ and a normalizing conformal self-map of the strip. Hence we see that the extremal map takes bending lines to geodesics in the strip model.

Let ϕ_n be the restriction of this extremal map to the n-th facet of the dome; ϕ_n takes the facet to a region in the strip bounded by a pair of geodesics. The map $\phi_n \circ r$ takes a subset of each medial disk in Ω to the strip.

Now let C_n be the crescent between faces n and $n+1$ and note that on each bending line, ϕ_n and ϕ_{n+1} agree. On C_n, define coordinates $0 < r < \infty$, $0 < \theta < \beta$ by sending the two endpoints of the crescent to 0 and ∞ and the center to (say) 1, and taking standard polar coordinates in this frame. The map

$$\sigma_n(z) = (\phi_n \circ r)(z) + \theta(z)$$

takes C_n to a region of the strip bounded by two geodesics; σ_n agrees with ϕ_n and ϕ_{n+1} on the boundary, up to translation. One may verify that the map σ_n is equivalent to the map

$$re^{i\theta} \mapsto \theta + i \arctan r$$

taking the crescent to a rectangle of height π and width β, followed by a self-map of the strip applied separately to each vertical line in the rectangle.

Now let R be a rectangle of height π and width $\pi^2 \mathrm{d}_{S_\Omega}(B_s, B_t) + \sum_n \beta(n)$, and define the continuous map $\Psi : \Omega \to R$ by gluing together the images of adjacent maps $\phi_1, \sigma_1, \phi_2, \sigma_2, ..., \phi_n$ along the sides of length π.

Define the metric ρ_Ω on R to be $|\nabla \mathrm{Im}\Psi|$. Clearly the length L_{ρ_Ω} of any path joining the top and bottom of the rectangle is at least π. We need an upper bound on the area. Since this metric is the extremal metric on each face of the dome, we have that the combined area of all faces is $\pi^2 \mathrm{d}_{S_\Omega}(B_j, B_k)$.

On each crescent C_n, the map Ψ is given by $(r, \theta) \mapsto \theta + i \arctan r$ followed by a self-map of the strip applied to each vertical line. If the self-map is the identity, we have

$$\begin{aligned} A_{\rho_\Omega}(C_n) &= \int_0^{\beta(n)} \int_0^\infty |\nabla \mathrm{Im}\Psi|^2 r dr d\theta \\ &= \int_0^{\beta(n)} \int_0^\infty \frac{r}{(1+r^2)^2} dr d\theta \\ &= -\beta(n) \frac{1}{2(1+r^2)} \Big|_0^\infty \\ &= \frac{\beta(n)}{2} \end{aligned}$$

It remains to be shown that area is nonincreasing when the self-map is other than the identity. This is in fact the case, see appendix C for the calculations.

Therefore the conjugate extremal distance satisfies

$$\mathrm{d}^*_\Omega(F_j, F_k) \geq \frac{\pi^2}{\pi^2 \mathrm{d}_{S_\Omega}(B_j, B_k) + \frac{1}{2}\sum_n \beta(n)}$$

Hence

$$d_\Omega(F_j, F_k) \leq d_{S_\Omega}(B_j, B_k) + \frac{2}{\pi^2}\sum_n \beta(n)$$

This completes the proof in the finitely-bent case; the smooth case follows under refinement. ☐

3.4. Hyperbolic Distances in S_Ω and Ω. We now obtain a similar result relating hyperbolic distances in Ω and S_Ω. We first bound the hyperbolic metric on Ω.

PROPOSITION 3.1 (Koebe $\frac{1}{2}$). *If $f : \mathbb{D} \to \Omega$ contains a disc of radius R about $f(0)$ and the boundary of this disc has two diametrically opposed points of tangency with $\partial\Omega$, then $|f'(0)| \leq 2R$.*

PROOF. After an affine map, we may assume the points of tangency are -1 and 1. Let $\sigma : \mathbb{C} \to \mathbb{C}$ be the Möbius map $\sigma(z) = R\frac{R+z}{R-z}$. We have:

$$\sigma(-1) = 0$$

$$\sigma(0) = R$$

$$\sigma(1) = \infty$$

$$\sigma'(z) = \frac{2}{(1-z)^2}$$

$$|\sigma'(0)| = 2R$$

By the Koebe 1/4 theorem

$$4R \geq |(\sigma \circ f)'(0)| = |\sigma' \circ f(0)| \cdot |f'(0)| = 2|f'(0)| \tag{7}$$

☐

Lemma 3.7 (A medial metric). *Let Ω be a domain with foliating arcs $\{F_t\}$. Then for $z \in F_t$*

$$\frac{1}{2}\rho_{D_t}(z) \leq \rho_\Omega(z) \leq \rho_{D_t}(z)$$

where ρ_Ω and ρ_{D_t} are scalars defining the hyperbolic metric on Ω and the Poincaré metric on D_t respectively.

Proof. The upper bound follows from extension of domain. To show the lower bound, assume without loss of generality that D_t is the unit disk and let $f : \mathbb{D} \to \Omega$ conformal with $f(0) = z \in F_t$. Apply a Möbius map ϕ which preserves D_t and sends z to the center of D_t. Observe that such a map also takes F_t to a diameter of D_t. By the preceeding proposition,

$$2 \geq |(\sigma \circ f)'(0)| = |\sigma'(z)| \cdot |f'(0)|$$

And hence

$$\frac{2}{|f'(0)|} \geq |\sigma'(z)|$$

But $\frac{2}{|f'(0)|} = \rho_\Omega(z)$ and $|\sigma'(z)| = \frac{1}{2}\rho_{D_t}(z)$. This completes the proof. $\square$

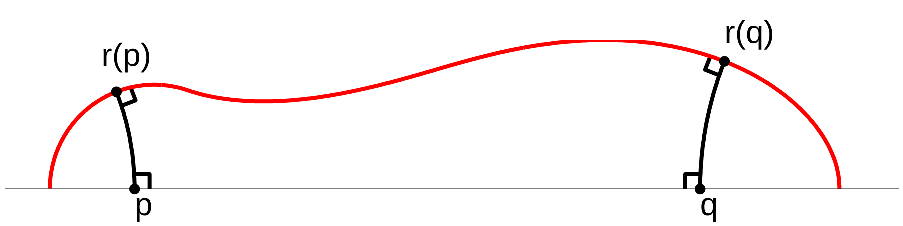

Figure 3.5. The situation for theorem 3.8. One imagines the domain Ω lying in the plane with the dome above; we see this here in cross-section with the points p, q mapped to the dome via the nearest-point retraction.

Theorem 3.8 (Hyperbolic distances comparable). *Let $\gamma : [0,T] \to \Omega$ be path in Ω and $\sigma = r(\gamma)$. Then the hyperbolic velocities of γ and σ satisfy*

$$\frac{1}{2}\|\dot\sigma\|_{S_\Omega}\frac{1+\kappa_1}{1+\kappa_1\sin\theta} \le \|\dot\gamma\|_\Omega \le \|\dot\sigma\|_{S_\Omega}\left(1+\kappa_1\cos\theta\right)$$

where θ is the angle between $\dot\sigma$ and the bending line on which σ lies, κ_1 is the hyperbolic principal curvature of S_Ω, and the norms $\|\cdot\|_\Omega$ and $\|\cdot\|_{S_\Omega}$ denote hyperbolic length on Ω and S_Ω.

Proof. By conformal invariance, we need only consider a single point where $\gamma = 0$ with velocity $\dot\gamma = \frac{\partial}{\partial t}\gamma$, the maximal circle is the unit circle, and the points of tangency are $a = -i, b = i$. Hence $r(\gamma) = (0,0,1)$. In this case, we have

$$1 \le \rho_\Omega(\gamma) \le 2$$

by lemma 3.7, and $\rho_{S_\Omega}(r(\gamma)) = 1$. Let $\dot\sigma = r_*\dot\gamma$ and in transverse coordinates on Ω and S_Ω write

$$\dot\gamma = (|\dot\gamma|\cos\theta, |\dot\gamma|\sin\theta)$$
$$\dot\sigma = (|\dot\sigma|\cos\theta, |\dot\sigma|\sin\theta)$$

We evaluate the upper bound

$$\begin{aligned}\|\dot\gamma\|_\Omega &= \rho_\Omega|J^{-1}\dot\sigma| \\ &\le 2\sqrt{\left(\frac{\dot\sigma_1}{2}\right)^2(1+\kappa_1)^2 + \left(\frac{\dot\sigma_2}{2}\right)^2} \\ &= \sqrt{|\dot\sigma|^2 + \dot\sigma_1^2(2\kappa_1+\kappa_1^2)} \\ &= |\dot\sigma|\sqrt{1+\cos^2\theta(2\kappa_1+\kappa_1^2)}\end{aligned}$$

We now need the inequality $\sqrt{1+a^2(2b+b^2)} \le 1+ab$, for $0 \le a < 1, b > 0$. Indeed,

$$(1+ab)^2 = 1 + 2ab + a^2b^2 \ge 1 + 2a^2b + a^2b^2$$

Hence,

$$\begin{aligned}\|\dot{\gamma}\|_{\Omega} &\le |\dot{\sigma}|(1+\kappa_1\cos\theta)\\ &= \|\dot{\sigma}\|_{S_\Omega}\,(1+\kappa_1\cos\theta)\end{aligned}$$

We now address the lower bound:

$$\begin{aligned}\|\dot{\sigma}\|_{S_\Omega} &= \rho_{S_\Omega}|J\dot{\gamma}|\\ &= \sqrt{\left(\frac{2\dot{\gamma}_1}{1+\kappa_1}\right)^2+(2\dot{\gamma}_2)^2}\\ &= \frac{2}{1+\kappa_1}\sqrt{\dot{\gamma}_1^2+\dot{\gamma}_2^2(1+\kappa_1)^2}\\ &= \frac{2|\dot{\gamma}|}{1+\kappa_1}\sqrt{1+\sin^2\theta(2\kappa_1+\kappa_1^2)}\\ &\le \frac{2\|\dot{\gamma}\|_{\Omega}}{1+\kappa_1}\sqrt{1+\sin^2\theta(2\kappa_1+\kappa_1^2)}\\ &\le 2\|\dot{\gamma}\|_{\Omega}\frac{1+\kappa_1\sin\theta}{1+\kappa_1}\end{aligned}$$

□

REMARK. The lower estimate in theorem 3.8 implies that the nearest-point retraction is 2-Lipschitz in the hyperbolic metrics:

$$\|\dot{\sigma}\|_{S_\Omega} \le 2\|\dot{\gamma}\|_{\Omega}\frac{1+\kappa_1\sin\theta}{1+\kappa_1} \le 2\|\dot{\gamma}\|_{\Omega}$$

This 2-Lipschitz result is sharp in the case of a "folded" surface. For example, take Ω to be the complement in the complex plane of the negative part of the real axis. The dome of this domain consists of two half planes, glued together. This dome has only one bending line. By the Koebe 1/4 theorem, the hyperbolic metric in Ω is exactly 1/2 at $z = 1$. It is easy to see that in this example the nearest point retraction is 2-Lipschitz.

REMARK. The quantity $\kappa_1 \cos\theta$ is the amount of bending encountered per unit hyperbolic length in the direction $\dot\sigma$. The upper bound can then be rewritten as

$$\|\dot\gamma\|_\Omega \leq \|\dot\sigma\|_{S_\Omega} + d\beta$$

Or in integrated form, for a path γ, we have

$$L_h[\gamma] \leq L_h[r(\gamma)] + \int_{r(\gamma)} d\beta$$

The lower bound admits a similar interpretation; the quantity $\kappa_1 \sin\theta$ is measuring how much time the path spends "in the gaps", so to speak. The next corollary gives a situation where the bounds simplify.

COROLLARY 3.9. *Let $\sigma : [0,T] \to S_\Omega$ be a transverse arc. Then*

$$\frac{1}{2}\left(L_h[\sigma] + \int_\sigma d\beta\right) \leq L_h[\gamma] \leq L_h[\sigma] + \int_\sigma d\beta$$

where $\gamma = r^{-1}(\sigma)$.

PROOF. As we remarked, the upper bound holds in general. By theorem 10, we have

$$\begin{aligned}\|\dot\gamma\|_\Omega &\geq \frac{1}{2}\|\dot\sigma\|_{S_\Omega}\frac{1+\kappa_1}{1+\kappa_1\sin\theta} \\ &= \frac{1}{2}\|\dot\sigma\|_{S_\Omega}(1+\kappa_1) \\ &= \frac{1}{2}\left(\|\dot\sigma\|_{S_\Omega} + d\beta\right)\end{aligned}$$

Where the first equality uses the fact that σ is a transverse arc implies $\theta \equiv 0$. The corollary follows by integration. □

Lurking behind the estimates on hyperbolic distances is a nice interpretation of crescents in the finitely-bent case. The previous corollary showed that up to constants, hyperbolic lengths of transverse arcs agreed up to the amount of bending encountered along the path. In the finitely-bent case, one can view the crescents (the preimages of bending lines under r) as ideal strips of approximately constant hyperbolic width. We present a proof in the finitely-bent case.

Lemma 3.8 (Width of crescents). *In a finitely-bent domain, let $B \subset S_\Omega$ be a bending line with bending angle β and let $C \subset \Omega$ be the associated crescent $r^{-1}(B)$. Let F^- and F^+ be the two circular arcs bounding C. Then*

$$\frac{1}{2}\beta \leq d_h(F^-, F^+) \leq \beta$$

where d_h is hyperbolic distance in Ω.

Proof. Let a and b be the two points in $\partial C \cap \partial\Omega$. We consider C as a disjoint union of circular arcs F_θ, $0 < \theta < \beta$, where F_θ joins a to b and meets F^- at angle θ. By lemma 3.7,

$$\frac{1}{2}\rho_{D_\theta} \leq \rho_\Omega \leq \rho_{D_\theta}$$

on F_θ, where ρ_Ω defines the hyperbolic metric on Ω and $D_\theta \subset \Omega$ is the disk containing F_θ as an ideal geodesic in the Poincaré metric ρ_{D_θ}. Let σ be any Möbius map taking a to 0 and b to ∞. Then $\sigma(C)$ is a sector of angular width β and $\sigma(F_\theta)$ is a straight line extending from 0 to ∞. For any θ, the pushforward under σ of ρ_{D_θ} is simply the metric given by $1/r$ in polar coordinates, and we see that

$$\frac{1}{2r} \leq \sigma_*\rho_\Omega \leq \frac{1}{r}$$

If we show that arcs of circles centered at 0 are geodesic in the metric $1/r$, the conclusion will follow. This is indeed the case: Under the map $\phi(z) = \log(z)$, the sector maps to a strip and the metric $\rho = 1/r$ pushes forward to the metric on the strip given by

$$(\phi_*\rho)(w) \equiv \frac{\rho(\phi^{-1}(w))}{|\phi' \circ \phi^{-1}(w)|} = \frac{1}{e^w} \cdot e^w = 1$$

Thus any two points on the boundary of the strip are joined by the Euclidean straight line between them, the shortest such paths have length β, and the conclusion follows. $\square$

The next result allows us to pass between hyperbolic distances and extremal distances between bending lines on the dome.

LEMMA 3.9 (Extremal and hyperbolic distances coincide for $\{B_t\}$). *Let $B_s, B_t \subset S_\Omega$, $s < t$ be two bending lines. Then the extremal distance d_{S_Ω} and the hyperbolic distance d_h satisfy*

$$\mathrm{d}_{S_\Omega}(B_s, B_t) = \frac{1}{\pi}\mathrm{d}_h(B_s, B_t) \tag{8}$$

PROOF. The ι map takes B_s and B_t to a pair of geodesics $\iota(B_s)$, $\iota(B_t)$ in the disk. Then for some angle $0 < \phi < \pi/2$, there is a map $\sigma : \mathbb{D} \to \mathbb{D}$ taking the endpoints of $\iota(B_t)$ to $\{e^{-i\phi}, e^{i\phi}\}$ and the endpoints of $\iota(B_s)$ to $\{e^{i(\pi-\phi)}, e^{-i(\pi-\phi)}\}$. For such a σ, the map $z \to \log\frac{1+\sigma(z)}{1-\sigma(z)}$ takes the disk to the strip $\{x + iy : -\pi/2 < y < \pi/2\}$ and takes $\iota(B_s)$ and $\iota(B_t)$ to the vertical sides of a rectangle of height π. Since the map is an isometry between the hyperbolic metrics on the disk and the strip, the proof is complete. $\square$

3.4.1. *Relation to the Ahlfors Integral.* The preceeding sections show that on a regular branch of the medial axis there is a natural analog for the $\int \frac{dx}{\theta(x)}$ estimate for extremal distances in strip domains. This follows from the geodesic length estimates of lemma 3.6, combined with the fact that extremal and hyperbolic distances between bending lines coincide.

COROLLARY 3.10. *Let B_s, B_t, $s < t$ be two bending lines in S_Ω. Then*

$$\frac{2}{\pi}\int_s^t \frac{\sqrt{\dot{a}\dot{b}}}{|b-a|}du \le d_\Omega(B_s, B_t) \le \frac{2}{\pi}\int_s^t \sqrt{\frac{|\dot{a}\dot{b}|}{|b-a|^2} + \frac{1}{4}\left(\frac{2\kappa_m \dot{R}}{\sqrt{1-\dot{R}^2}} + \frac{\partial}{\partial m}\frac{1}{2}\log\left|\frac{\dot{b}}{\dot{a}}\right|\right)^2}\, du$$

Proof.

$$d_{S_\Omega}(B_s, B_t) = \frac{1}{\pi} d_h(B_s, B_t)$$

$\square$

Remark. This estimate is sharp when the geodesic joining B_t and B_s coincides with the axis of "nearest points", $p^*(u)$, $s \le u \le t$.

The lower estimate applies without modification to the domain Ω; this is our analog for the integral estimate $\int \frac{dx}{\theta}$ in strip domains.

Corollary 3.11. *Let F_s, F_t, $s < t$ be two foliating arcs in Ω. Then*

$$d_\Omega(F_s, F_t) \ge \frac{2}{\pi} \int_s^t \frac{\sqrt{\dot{a}\dot{b}}}{|b-a|} dm$$

Proof.

$$d_\Omega(F_s, F_t) \ge d_{S_\Omega}(B_s, B_t)$$

$\square$

There is also an upper bound, which requires a correction given in terms of the bending.

Corollary 3.12. *Let F_s, F_t, $s < t$ be two foliating arcs in Ω. Then*

$$d_\Omega(F_s, F_t) \le \frac{2}{\pi} \int_s^t \sqrt{\frac{|\dot{a}\dot{b}|}{|b-a|^2} + \frac{1}{4}\left(\frac{2\kappa_m \dot{R}}{\sqrt{1-\dot{R}^2}} + \frac{\partial}{\partial m}\frac{1}{2}\log\left|\frac{\dot{b}}{\dot{a}}\right|\right)^2}\, du + \frac{2}{\pi^2}\int_s^t \mathrm{d}\beta$$

Proof. Apply theorem 3.7 $\square$

3.5. Long-range Estimates for $|f'|$. We apply the results of the preceding sections to obtain long-range estimates on the boundary derivative. We state the results in terms of hyperbolic distance.

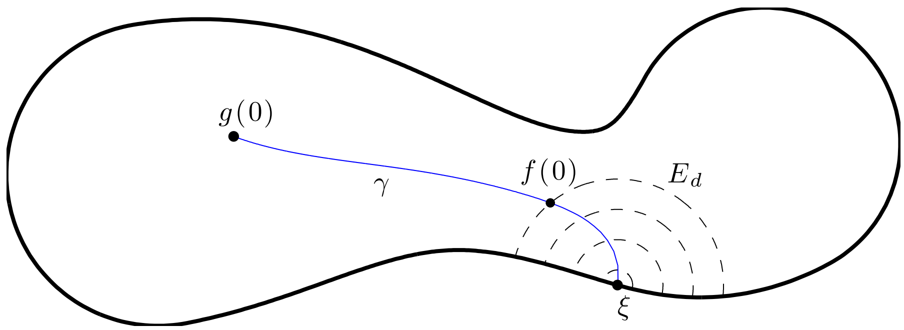

FIGURE 3.6. The setup for theorem 3.13. The geodesic arc γ joins $g(0)$ and $f(0)$ to $\xi \in \partial\Omega$. $f(0)$ lies at the intersection of γ and the separating arc E_d.

THEOREM 3.13. *Let Ω be a domain with $\xi \in \partial\Omega$. Let $f : \Delta \to \Omega$ and $g : \Delta \to \Omega$ be conformal maps with $f(0)$ lying on a separating arc E_d. Let γ be the ideal geodesic joining ξ and $f(0)$, and let $g(0)$ be a point further along γ (see figure 3.6). Then*

$$|g' \circ g^{-1}(\xi)| \geq C_2 e^{d_h(f(0),g(0))} \frac{d}{2-\kappa d} \exp\{-A(d)\}$$
$$|g' \circ g^{-1}(\xi)| \leq C_3 e^{d_h(f(0),g(0))} \frac{d}{2-\kappa d} \exp\left\{\left(\frac{d}{d(f(0),\partial\Omega)}\right)^2 B(d) - A(d)\right\}$$

where

$$A(d) = \pi \int_0^d \frac{L[E_r] - L[F_r]}{L[E_t]L[F_t]} dt$$
$$B(d) = \pi \int_r^d \frac{\mu'(t)^2 + \frac{1}{12}\theta'(t)^2}{L[E_t]} t^2 dt$$

and C_2, C_3 are as before.

PROOF. Assume without loss of generality that $f(1) = g(1) = \xi$ and write

$$g(z) = f \circ \phi(z)$$

for $\phi : \mathbb{D} \to \mathbb{D}$ with $\phi(0) = f^{-1} \circ g(0)$. Since $f(0), g(0)$, and ξ lie on a common geodesic, their preimages must lie on a common geodesic in the disk. (In fact, the preimages all lie on the real axis, given our normalization.) Thus ϕ is a hyperbolic whose axis is the common geodesic. It is a simple calculation to verify that $|\phi'(1)| = \exp\{d_h(0, f^{-1} \circ g(0))\}$. Thus

$$\begin{aligned} |g' \circ g^{-1}(\xi)| &= |f'(1)| \cdot |\phi'(1)| \\ &= |f'(1)| \exp\{d_h(0, f^{-1} \circ g(0))\} \\ &= |f'(1)| \exp\{d_h(f(0), g(0))\} \end{aligned}$$

and the theorem follows from the local estimates.

$\square$

REMARK. The estimates of the preceeding sections can be applied to $d_h(f(0), g(0))$. For example, let $r(f(0))$ and $r(g(0))$ lie on the bending lines B_s and B_t respectively. Then we have immediately

$$\begin{aligned} d_h(f(0), g(0)) &\geq \frac{1}{2} \left(d_h \left(r(f(0)), r(g(0))\right)\right) \\ &\geq \frac{1}{2} \left(d_h(B_s, B_t)\right) \end{aligned}$$

CHAPTER 4

Passing Between the Two Models of Teich(Δ)

1. Notation

Δ – The unit disk $\{|z| < 1\}$

$L^{\infty}(\Delta)$ – The space of bounded Beltrami differentials on Δ

$L^{\infty}(\Delta)_1$ – The open unit ball in $L^{\infty}(\Delta)$

2. Linearizing Welding

In this section we work out the relationship between tangent vectors to **Teich**(Δ) in the two classical models. We wish to know how small changes in welding maps affect quasicircles, and vice-versa. We are able to obtain an explicit formula which has a particularly simple form at the origin.

2.1. The Differential at the Identity. In this section we work on the half plane rather than the disk. The half-plane is conformal to the disk via a linear fractional map, and nothing essential is lost.

Let $\mu \in L^{\infty}(\mathcal{H})_1$ be real analytic [1]. To construct a homeomorphism of the circle we form the symmetric extension

$$\sigma(z) = \begin{cases} \mu(z) & z \in \mathcal{H} \\ \bar{\mu}(\bar{z}) & z \in \mathcal{H}^* \end{cases}$$

and to produce a quasicircle we form the 'zero' extension

$$\beta(z) = \begin{cases} \mu(z) & z \in \mathcal{H} \\ 0 & z \in \mathcal{H}^* \end{cases}$$

In both cases, the real axis is a set of measure zero and the values there are unimportant. By the measurable mapping theorem,

$$\frac{\partial}{\partial t} f^{t\mu}\Big|_{t=0} = \mu_0 * \frac{1}{\pi z}$$

[1]We assume μ is real analytic so the maps become differentiable and we can use more convenient notation; the conclusions carry over to the general case when suitably interpreted.

when $f^{t\mu}$ is normalized so near infinity $f^{t\mu}(z) = z + O\left(\frac{1}{|z|}\right)$. Similarly, we have

$$\left.\frac{\partial}{\partial t} f_{t\mu}\right|_{t=0} = \mu_S * \frac{1}{\pi z} + Q(z)$$

Where $Q(z)$ is a quadratic polynomial with real coefficients achieving a desired normalization (say, fixing 0, 1, and ∞, in which case $Q(z) = az + b$ for $a, b \in \mathbb{R}$). We can now work out the relationship between the two vector fields $\frac{\partial}{\partial t} f^{t\mu}$ and $\frac{\partial}{\partial t} f_{t\mu}$ at a point $x \in \mathbb{R}$.

Proposition 4.1 (The differential along the real line). *Let $\mu \in L^\infty(\mathcal{H})_1$. Then at $t = 0$*

$$\frac{\partial}{\partial t} f^{t\mu} = \frac{1}{2}\left(\frac{\partial}{\partial t} f_{t\mu} - Q - iH\left(\frac{\partial}{\partial t} f_{t\mu} - Q\right)\right)$$

at any point $x \in \mathbb{R}$. H denotes the Hilbert transform.

Proof. At time t=0,

$$\begin{aligned}
\frac{\partial}{\partial t} f_{t\mu}(x) - Q(z) &= \frac{1}{\pi}\iint_{\hat{\mathbb{C}}} \frac{\mu_S(\xi)}{x - \xi}|d\xi|^2 \\
&= \frac{1}{\pi}\iint_{H} \frac{\mu_S(\xi)}{x - \xi}|d\xi|^2 + \frac{1}{\pi}\iint_{H^*} \frac{\mu_S(\xi)}{x - \xi}|d\xi|^2 \\
&= \frac{1}{\pi}\iint_{H} \frac{\mu_S(\xi)}{x - \xi}|d\xi|^2 + \frac{1}{\pi}\iint_{H} \frac{\bar{\mu}_S(\xi)}{x - \bar{\xi}}|d\xi|^2 \\
&= 2\mathrm{Re}\left(\frac{1}{\pi}\iint_{H} \frac{\mu_S(\xi)}{x - \xi}|d\xi|^2\right) \\
&= 2\mathrm{Re}\left(\frac{1}{\pi}\iint_{\hat{\mathbb{C}}} \frac{\mu_0(\xi)}{x - \xi}|d\xi|^2\right) \\
&= 2\mathrm{Re}\left(\frac{\partial}{\partial t} f^{t\mu}\right)
\end{aligned}$$

Further, $f^{t\mu}$ is conformal in H^*. Thus the vector field $\frac{\partial}{\partial t} f^{t\mu}$ is holomorphic in H^* and its imaginary part can be reconstructed as the Hilbert transform of the real part.

□

Remark. On the circle, the analogous conclusion holds: the real and imaginary parts of $\frac{\partial}{\partial t} f^{t\mu}$ become the normal and tangential components, respectively.

2.2. Examples. The examples in figures 4.1 and 4.2 were produced by choosing a smooth vector field $V \in Vec(S^1)$, removing coefficients -1, 0, and 1 from its Fourier series to obtain the non-Möbius part $\mu * \frac{1}{\pi z}$, and constructing a welding map $\theta \mapsto \epsilon V(\theta)$. In this case, we have

$$\frac{\partial}{\partial t} f^{t\mu} = \frac{1}{2}(V - iHV)$$

100 points were sampled uniformly on the unit circle and the welding was performed using a variant of the 'Zipper' algorithm. The resulting vector field was estimated using the difference between the image of $e^{i\theta}$ after the weld and $e^{i\theta}$.

Remark. Small numerical errors in the welding cause distortions of the estimated vector field. A slight rotation of the curve adds a constant term to the tangential component of V and a slight translation will add $\sin(\theta)$ and $\cos(\theta)$ terms to both normal and tangential components. This makes the choice of ϵ somewhat tricky. We must choose ϵ small so our linearization is a good approximation for V (and to ensure the welding map is a homeomorphism). However, if ϵ is too small the estimated V is dominated by numerical noise from the welding. To produce the examples, some trial and error was required on a case-by-case basis.

2.3. The General Form of the Differential. Away from the origin, we can still obtain a formula which relates tangent vectors in the two models of **Teich**(Δ). We'll need the following observation:

Proposition 4.2. *If $N : \partial\Omega \to \mathbb{R}$ is the restriction to the boundary of the normal part of a holomorphic vector field on Ω, then the tangential part is given by $T = H_\Omega N + v$, where H_Ω is the Hilbert transform in the domain Ω and v is any vector field in $psl_2(\mathbb{R})$ acting on $\partial\Omega$.*

Proof. It suffices to prove this for Ω equal to the unit disk. Parametrize N by the angular coordinate θ. Then $N(\theta) + iHN(\theta)$ is the restriction to S^1 of some function F holomorphic in Δ. The function $zF(z)$ is also holomorphic in Δ, and it

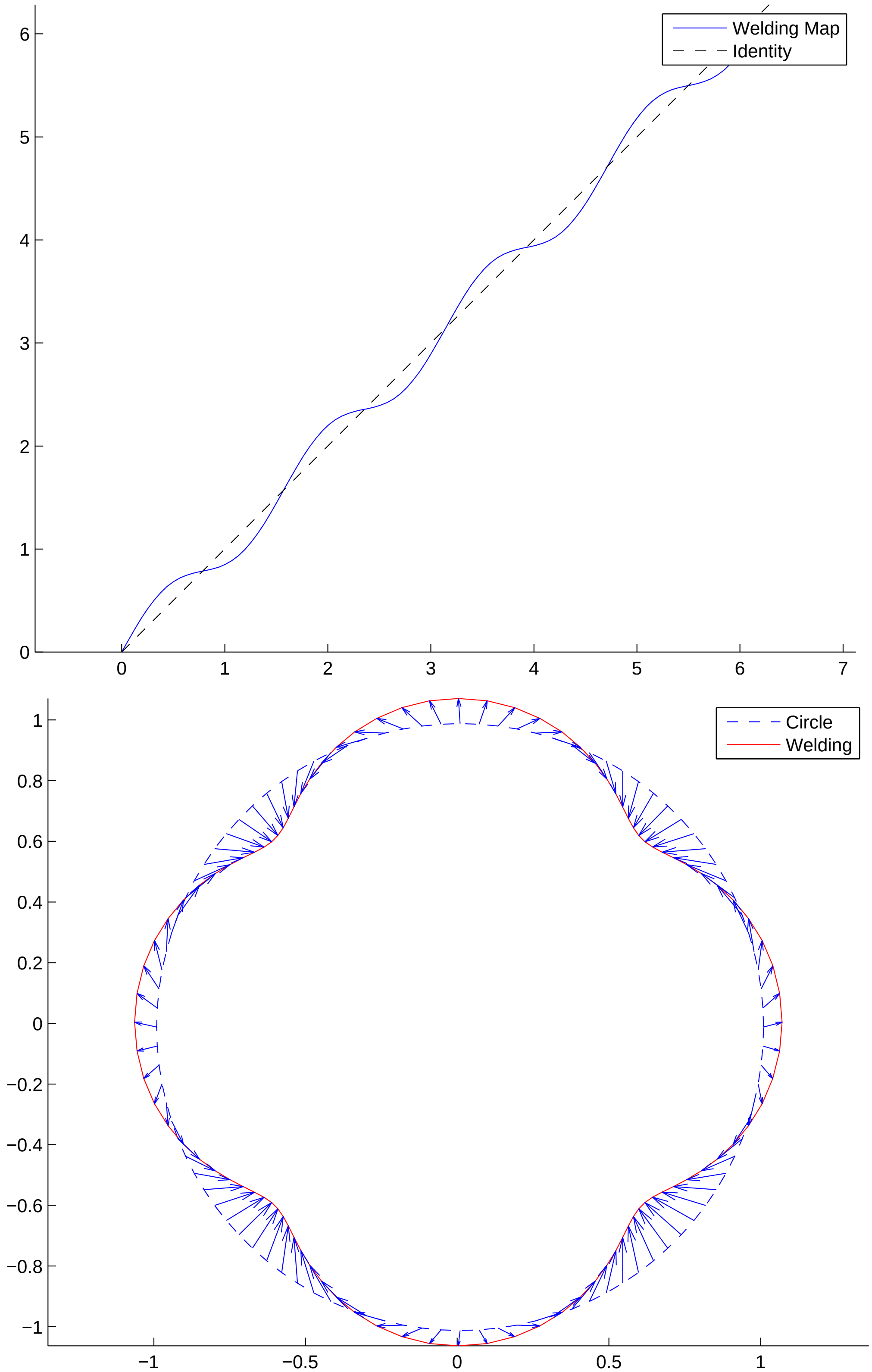

FIGURE 4.1. The welding map $\theta \mapsto \theta + \epsilon \sin(4\theta)$ and perturbed circle (arrows indicate the flow of points) for $\epsilon = .2$.

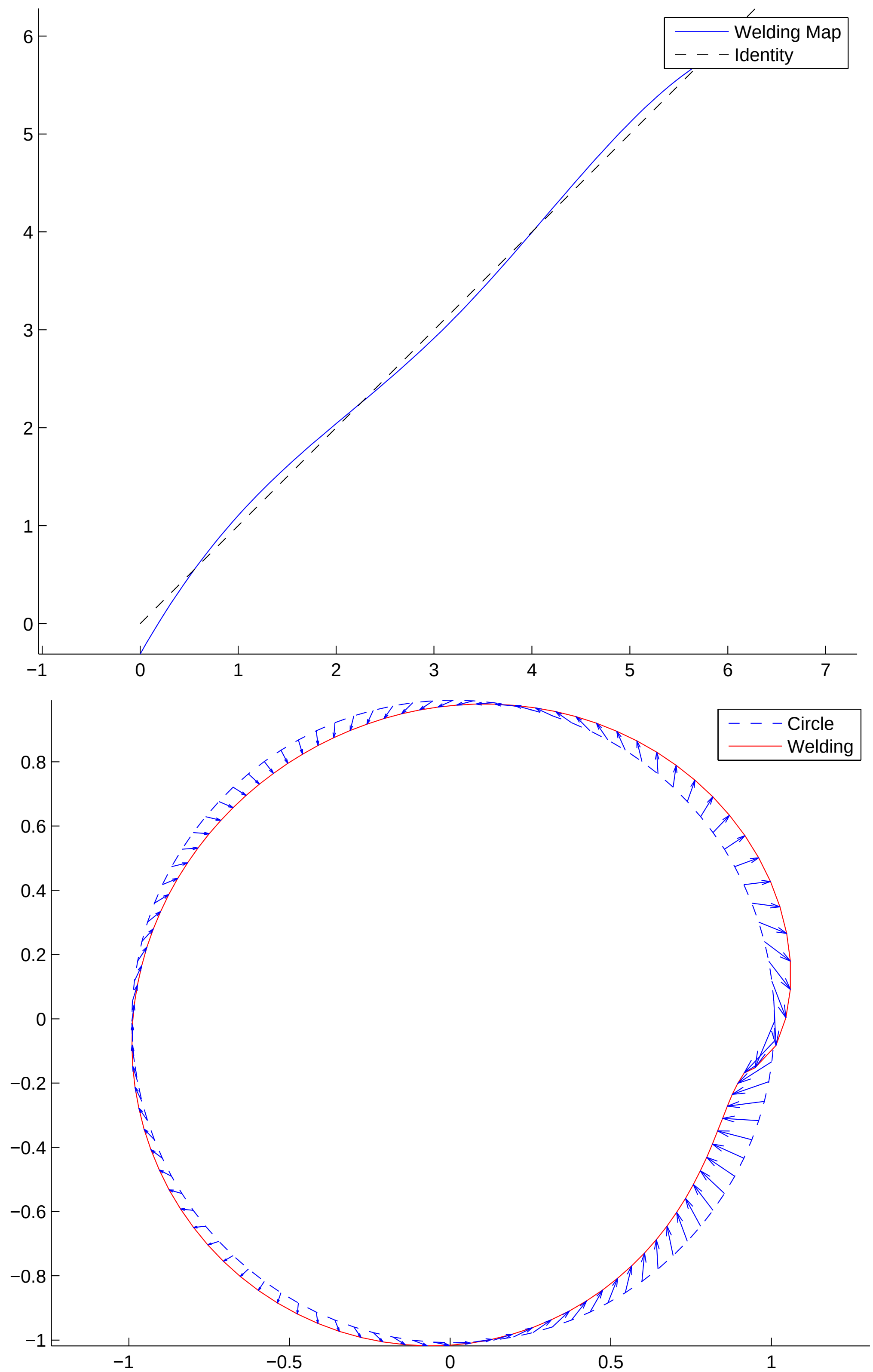

FIGURE 4.2. The welding map $\theta \mapsto \theta + \epsilon V(\theta)$ and perturbed circle for $\epsilon = .8$ and V a normalized version of $1 - |\frac{\theta}{\pi} - 1|^3$.

has boundary values

$$zF(z)\Big|_{z=e^{i\theta}} = Ne^{i\theta} + ie^{i\theta}HN$$

The right-hand side may be viewed as a holomorphic vector field with normal part N and tangential part HN. Clearly adding any vector field $v \in psl_2(\mathbb{R})$ will not change the normal part, and since $psl_2(\mathbb{R})$ consists of exactly those vector fields holomorphic on Δ with no normal part, this completes the proof. $\square$

Now we move towards the general formula. Let Ω be some simply-connected planar domain, with the interior and exterior conformal maps $\phi_- : \Delta \to \Omega$ and $\phi_+ : \Delta^* \to \Omega^*$. Let $h = \phi_-^{-1} \circ \phi_+\big|_{S^1}$ be a welding map for Ω. We have the following.

Lemma 4.1. *Modulo $psl_2(\mathbb{R})$, we have*

$$\dot{h} \circ h^{-1} = \phi_-^* \left(H_+ N - H_- N\right)$$

where the function $N : \partial\Omega \to \mathbb{R}$ is the component of $\dot{\phi}_- \circ \phi_-^{-1}$ normal to $\partial\Omega$, ϕ_-^* is the pullback operator, and H_+, H_- are the Hilbert transforms on the exterior and interior domains.

Proof. By direct computation,

$$\begin{aligned}
\frac{\partial h}{\partial t} &= \left(\frac{\partial}{\partial t}\phi_-^{-1}\right) \circ \phi_+ + D_{\phi_-^{-1}} \left(\frac{\partial}{\partial t}\phi_+\right) \\
&= -\frac{\dot{\phi}_-}{\phi_-'}\bigg|_h + \frac{\dot{\phi}_+}{\phi_-' \circ h} \\
&= \frac{1}{\phi_-' \circ h}\left(\dot{\phi}_+ - \dot{\phi}_- \circ h\right)
\end{aligned}$$

Adopting the notation $\dot{\phi}_+ = v_+ \circ \phi_+$ and $\dot{\phi}_- = v_- \circ \phi_-$ for vector fields v_+, v_-, we have

$$\begin{aligned}\dot{h} \circ h^{-1} &= \frac{1}{\phi'_-}\left(\dot{\phi}_+ \circ h^{-1} - \dot{\phi}_-\right) \\ &= \frac{1}{\phi'_-}\left(v_+ \circ \phi_- - v_- \circ \phi_-\right) \\ &= \phi^*_-\left(v_+ - v_-\right)\end{aligned}$$

Since h is purely tangent to the unit circle, we see that the normal parts of v_+ and v_- must cancel, i.e. the normal parts are identical. So given a function $N : \partial\Omega \to \mathbb{R}$ representing a specified normal perturbation of the boundary, we can recover the tangential parts of the interior and exterior maps via the Hilbert transform on the interior and exterior domains, which we will denote H_- and H_+ respectively. That is,

$$\dot{h} \circ h^{-1} = \phi^*_-\left(H_+N - H_-N\right)$$

$\square$

At the origin, the symmetry of the interior and exterior domains means H_+ and H_- agree (up to choice of sign due to orientation). Plugging this in to our formula, one recovers the earlier formula for the differential at the origin which we worked out in terms of Beltrami forms.

3. A Bound on Distortion via the Weil-Petersson Metric on Teich(Δ)

In this section we introduce the Weil-Petersson Metric and use it to obtain a bound on distortion of quasicircles in terms of the Weil-Petersson norm of a tangent vector to **Teich**(Δ). We begin by reviewing the construction of left- and right- invariant metrics on Lie groups. We construct the Weil-Petersson Riemannian metric on **Teich**(Δ) by placing an inner product on the tangent space at the identity. Classically, this inner product is computed in terms of Beltrami differentials; in [**35**] Nag showed that this definition agrees with a Kähler metric on **Diff**(S^1) which has a convenient representation in terms of Fourier series. Finally, we state and prove our distortion theorem.

3.1. Lie Algebras. Let G be a Lie group. The Lie algebra of G, denoted $\mathfrak{g}$, is the tangent space to the group at the identity. Given a group element $g \in G$, define the conjugation map $\Phi_g : G \to G$

$$\Phi_g(h) = g^{-1} \circ h \circ g$$

for any $h \in G$. The differential of Φ_g at the identity is a Lie algebra automorphism; this automorphism is called the adjoint action, denoted Ad_g.

3.1.1. *Example: The Lie Algebra $psl_2(\mathbb{R})$.* We first compute the Lie algebra of $PSL_2(\mathbb{R})$, which acts on the complex plane as the group of linear fractional maps which preserve the unit disk. The $\mathbb{R}$ in the name reflects the isomorphism with the group of linear fractional maps which preserve the upper half-plane, which have real coefficients. Elements of $PSL_2(\mathbb{R})$ acting on the disk have the form

$$\frac{az+b}{\bar{b}z+\bar{a}} \qquad \text{, with } |a|^2 - |b|^2 = 1$$

To compute the Lie algebra we take a smooth path through the identity and differentiate. Let $a = a(t), b = b(t)$ be smooth complex-valued functions of t with $a(0) = b(0) = 1$. Then at time $t = 0$ we have

$$\begin{aligned}
\frac{\partial}{\partial t}\frac{az+b}{\bar{b}z+\bar{a}} &= \frac{(\dot{a}z+\dot{b})(\bar{b}z+\bar{a}) - (\dot{\bar{b}}z+\dot{\bar{a}})(az+b)}{(\bar{b}z+\bar{a})^2} \\
&= -\dot{\bar{b}}z^2 + (\dot{a}-\dot{\bar{a}})z - \dot{b} \\
&= \left(i\dot{\bar{b}}z + \mathrm{Im}\dot{a} + i\dot{b}z^{-1}\right) iz
\end{aligned}$$

That is, we have a vector field of the form

$$v(z) = \left(a_{-1}z^{-1} + a_0 + a_1 z\right) iz\frac{\partial}{\partial z}$$

where $a_{-1} = \bar{a}_1$. For $z = e^{i\theta}$ this vector field is tangent to the unit circle. If we write this in coordinate θ on the circle, we have

$$v(\theta) = \left(a_{-1}z^{-1} + a_0 + a_1 z\right)\frac{\partial}{\partial\theta}$$

since $\frac{\partial}{\partial\theta}$ pushes to $iz\frac{\partial}{\partial z}$ under the embedding $\theta \mapsto e^{i\theta}$. It remains to be shown that every vector field of this form is in the Lie algebra; this is clear since the integral of a holomorphic vector field is a holomorphic map, and these vector fields preserve the unit circle.

The adjoint action can also be computed explicitly. Let h_t be a smooth path in $\mathbf{Diff}(S^1)$ with $h_0 = \mathrm{Id}$ and $\frac{\partial}{\partial t}h_t = v \in \mathbf{Vec}(S^1)$. Let $g \in \mathbf{Diff}(S^1)$. Then at $t = 0$,

$$\begin{aligned}\frac{\partial}{\partial t}g^{-1}\circ h_t \circ g &= (g^{-1})'\Big|_{h_t\circ g}\cdot\frac{\partial}{\partial t}h_t\Big|_g\\ &= \frac{v\circ g}{g'\circ g^{-1}\circ h_t\circ g}\\ &= \frac{v\circ g}{g'}\end{aligned}$$

This is identical to the pullback of v through g.

3.2. The Weil-Petersson Inner Product and Diff(S^1). Let $v \in \mathbf{Vec}(S^1)$ be a smooth vector field on the unit circle with Fourier series representation

$$v(\theta) = \sum_{-\infty}^{\infty} a_n e^{in\theta}\frac{\partial}{\partial\theta}$$

where $a_{-n} = \bar{a}_n$ since the vector field is real. The Weil-Petersson norm on $\mathbf{Vec}(S^1)$ is defined by

$$\|v\|_{WP}^2 = \sum_{2}^{\infty}(n^3 - n)|a_n|^2$$

Note that for any $w \in psl_2(\mathbb{R})$, we have $\|w\|_{WP} = 0$. One may verify that for $g \in PSL_2(\mathbb{R})$, we have $\|v\|_{WP} = \|Ad_g v\|_{WP}$. Thus the WP norm provides a norm defined on the quotient of $\mathbf{Diff}(S^1)$ by the Möbius group. One thinks of this norm as living on the tangent space to $G = \mathbf{Diff}(S^1)/PSL_2(\mathbb{R})$ at the identity, T_eG. One can extend this to a homogeneous metric on all of G by translating vector fields back to the identity.

At this point, we may create a homogeneous metric in two ways. One may choose to translate vector fields back using either right-multiplication

$$R_g h \equiv h \circ g$$

or left-multiplication

$$L_g h = g \circ h$$

From the point of view of putting inner products on tangent vectors, the essential difference is how one interprets a tangent vector to the group. In the setup of left-multiplication, we interpret a tangent vector $v \in T_h G$ as

$$\frac{\partial h}{\partial t} = v$$

and we pull the tangent vector back to the origin through the differential of left-multiplication. In one dimension, this amounts to the map

$$v \mapsto \frac{v \circ h}{h'}$$

Perhaps more naturally, in the setup of right-multiplication we interpret $v \in T_h G$ as

$$\frac{\partial h}{\partial t} = v \circ h$$

That is, we view v as a vector field defined on the space in which h takes values, and the pullback map is

$$v \mapsto v \circ h^{-1}$$

Explicitly, let $\Psi(\theta, t)$ be a smooth path in $\mathbf{Diff}(S^1)$ and let $v(\theta, t) \in \mathbf{Vec}(S^1)$ satisfy $v_t \circ \Psi = \frac{\partial \Psi}{\partial t}$. Then we construct a left-invariant metric on $T_\Psi \mathbf{Diff}(S^1)$ as follows. The pullback of v to the identity under Ψ at time t is

$$\begin{aligned}(v \circ \Psi) \cdot \left(\Psi^{-1}\right)' \circ \Psi &= \frac{v \circ \Psi}{\Psi_\theta} \\ &= \frac{\Psi_t}{\Psi_\theta}\end{aligned}$$

where $\Psi_t = \frac{\partial}{\partial t}\Psi$ and $\Psi_\theta = \frac{\partial}{\partial \theta}\Psi$. If we expand the pullback in series we have

$$\frac{\Psi_t}{\Psi_\theta} = \sum_{-\infty}^{\infty} a_n(t) e^{in\theta}$$

again with

$$\left\|\frac{\Psi_t}{\Psi_\theta}\right\|_{WP}^2 = \sum_{2}^{\infty}(n^3 - n)|a_n(t)|^2$$

And the length of the path $\Psi(\theta, t)$ is, by definition

$$L[\Psi] \equiv \int_0^T \left(\sum_{2}^{\infty}(n^3 - n)|a_n(t)|^2\right)^{\frac{1}{2}}$$

Construction of the right-invariant metric is similar, but using the pullback under right-multiplication we expand

$$\Psi_t \circ \Psi^{-1} = \sum_{-\infty}^{\infty} b_n(t) e^{in\theta}$$

and evaluate the inner product

$$\left\|\Psi_t \circ \Psi^{-1}\right\|_{WP}^2 = \sum_{2}^{\infty}(n^3 - n)|a_n(t)|^2$$

In [**40**], Mumford and Sharon work with left-invariant metrics. In classical Teichmüller theory, the right-invariant version of the WP metric is typically used. We follow the classical theory and adopt the right-invariant form, which is much more convenient for our purposes.

3.3. The WP Inner Product and Beltrami Differentials. Let f_μ and f_λ solve the Beltrami equation for $\mu, \lambda \in L^\infty(\Delta)_1$ and consider the map f_ω defined by

$$f_\omega \circ f_\lambda = f_\mu$$

One may compute that

$$\omega = \left\{ \frac{\mu - \lambda}{1 - \bar{\lambda}\mu} \frac{f_{\lambda,z}}{\bar{f}_{\lambda,\bar{z}}} \right\} \circ (f_\lambda)^{-1}$$

Further, for a bounded measurable function $\nu : \mathbb{C} \to \mathbb{C}$, we have

$$\lim_{t \to 0} \frac{\omega(\lambda + t\nu) - \omega(\lambda)}{t} = \left\{ \frac{\nu}{1 - |\lambda|^2} \frac{f_{\lambda,z}}{\bar{f}_{\lambda,\bar{z}}} \right\} \circ (f_\lambda)^{-1} \equiv L_\nu^\lambda$$

This is the definition of L_ν^λ. L_ν^λ is an element of $L^\infty(\Delta)$. Let $N(\Delta)$ denote the "infinitesimally trivial" Beltrami differentials, i.e. that subset of $L^\infty(\Delta)$ satisfying

$$\iint_\Delta \nu(z)\phi(z)dxdy = 0$$

for all quadratic differentials ϕ defined on Δ. We may identify the space $L^\infty(\Delta)/N(\Delta)$ with the tangent space to **Teich**(Δ) at the origin.

Given two Beltrami differentials $\mu, \nu \in L^\infty(\Delta)/N(\Delta)$, the Weil-Petersson inner product is defined by

$$\langle \mu, \nu \rangle_{WP} \equiv \iint_\Delta \mu\bar{\nu}\rho^2 dxdy$$

where $\rho = \frac{2}{1-|z|^2}$ defines the Poincaré metric on the disk. By right translations one may define an inner product on each tangent space of **Teich**(Δ).

3.4. Distortion of Quasicircles is Bounded Uniformly by Weil-Petersson Norms of Tangent Vectors. Here we show that the infinitesimal deformation of a quasicircle in some direction ν is controlled by the WP norm of the tangent vector. That is, let $[\lambda]$ be a point in **Teich**(Δ). Then given a vector ν tangent to **Teich**(Δ) at $[\lambda]$, we have the following:

Theorem 4.1. *Let* $v = \nu * \frac{1}{\pi z}$ *and set* $\Omega = f^{\lambda}(\Delta)$*. Then for any* $z \in \partial\Omega$*,*

$$|v(z)| \leq \frac{2}{\pi}\sqrt{|\mathrm{Supp}(\nu)|}\|\nu\|_{WP}$$

where $|\mathrm{Supp}(\nu)|$ *is the Euclidean area of the support of* ν*.*

Proof. Let $S = \mathrm{Supp}(\nu)$. By the measurable mapping theorem and normalization of f^{μ}, we know that

$$v = \nu * \frac{1}{\pi z}$$

Thus

$$\begin{aligned}
|v(z)|^2 &= \left|\frac{1}{\pi}\iint_{\mathbb{C}} \frac{\nu(\xi)}{\xi - z} dxdy\right|^2 \\
&= \left|\iint_S \frac{|S|}{\pi}\frac{\nu(\xi)}{\xi - z}\frac{dxdy}{|S|}\right|^2 \\
&\leq \iint_S \left|\frac{|S|}{\pi}\frac{\nu(\xi)}{\xi - z}\right|^2 \frac{dxdy}{|S|} && \text{by Jensen's inequality} \\
&= \frac{|S|}{\pi^2}\iint_S \left|\frac{\nu(\xi)}{\xi - z}\right|^2 dxdy
\end{aligned}$$

Let $\Omega = f^{\lambda}(\Delta)$, with hyperbolic metric defined by some scalar ρ_{Ω}. At any point $\xi \in \Omega$

$$\frac{1}{|\xi - z|} \leq \frac{1}{\mathrm{d}(\xi, \partial\Omega)} \leq 2\rho_{\Omega}(\xi)$$

where the second inequality follows from the fact that $\rho_{\Omega} \geq \frac{1}{2}\rho_D$ on any foliating arc F_t (see lemma 3.1) and the fact that $\rho_D \geq \frac{1}{\mathrm{d}(\xi,\partial\Omega)}$. Combining, we have

$$\begin{aligned}
|v(z)|^2 &\leq \frac{4|S|}{\pi^2}\iint_S |\nu(\xi)|^2 \rho_{\Omega}^2 dxdy \\
&= \frac{4|S|}{\pi^2}\|\nu\|_{WP}^2
\end{aligned}$$

This completes the proof. □

4. Quasisymmetry and Distortion of Quasicircles

While the results of the previous section are useful, they aren't necessarily the most natural; in particular the assumption that a vector field has finite WP norm is much too restrictive. One can still obtain bounds on approximations without requiring the smoothness necessary for a vector field to have finite WP norm. Quasisymmetry, the one-dimensional analog of quasiconformality, is the essential feature a vector field must posess.

4.1. Quasisymmetry and Uniform Approximations to Shapes.

Definition 4.1 (Quasisymmetric map $\mathbb{R} \to \mathbb{R}$). A homeomorphism $h : \mathbb{R} \to \mathbb{R}$ is said to be quasisymmetric if there exists a constant $M \in \mathbb{R}$ such that

$$\frac{1}{M} \leq \left| \frac{h(x+t) - h(x)}{h(x) - h(x-t)} \right| \leq M$$

for all $x, t \in \mathbb{R}$.

There is an analogous definition for circle maps:

Definition 4.2 (Quasisymmetric map $S^1 \to S^1$). A homeomorphism $h : S^1 \to S^1$ is said to be quasisymmetric if there exists a constant $M \in \mathbb{R}$ such that

$$\frac{1}{M} \leq \left| \frac{h(e^{i(x+t)}) - h(e^{ix})}{h(e^{ix}) - h(e^{i(x-t)})} \right| \leq M$$

for all x and all $|t| < \frac{\pi}{2}$.

One says that h satisfies an M*-condition* if it is quasisymmetric with constant M. It is well-known [**3**] that any quasisymmetric map $S^1 \to S^1$ can be extended to a K-quasiconformal map $\Delta \to \Delta$ for a K which depends only on M. As M vanishes, so does the best possible K. The Ahlfors-Beurling extension is a particularly simple means of extending a quasisymmetric map, although it is not invariant under the

Möbius group. Let $h : \mathbb{R} \to \mathbb{R}$ satisfy an M-condition and define

$$u(x,y) = \frac{1}{2y} \int_{x-y}^{x+y} h(t)dt$$
$$v(x,y) = \frac{1}{2y} \int_{0}^{y} \left(h(x+t) - h(x-t)\right) dt$$

Then the map $ex(h)$, defined by $x+iy \mapsto u+iv$, is quasiconformal with K that depends only on M. As stated, this does not extend the identity by the identity, but this is rectified by using the extension $x+iy \mapsto u+2iv$. This map is still quasiconformal and now extends the identity by the identity. The Ahlfors-Beurling extension is also natural for real affine transformations: if $S_1(z) = a_1 z + b_1$ and $S_2(z) = a_2 z + b_2$, then

$$ex(S_1 \circ h \circ S_2) = S_1 \circ ex(h) \circ S_2$$

We can use this to construct quasiconformal extensions of circle maps. If we lift a homeomorphism $g : S^1 \to S^1$ via the universal covering map $x \mapsto e^{2\pi i x}$, we obtain a homeomorphism $h : \mathbb{R} \to \mathbb{R}$. Thus if $H = ex(h)$, we have by affine invariance that

$$H(z+1) = H(z) + 1$$

since $h(x) + 1 = h(x+1)$. Now note that the covering map $x \mapsto e^{2\pi i x}$ extends to the cover $z \mapsto e^{2\pi i z}$ of the punctured unit disk. The Ahlfors-Beurling extension fixes infinity, so via the covering map we may now construct a quasiconformal extension of g to the entire disk, with a fixed point at 0 (the image of infinity under the covering map).

4.2. Quasisymmetric Approximations to Welding Maps. Given a Beltrami coefficient $\mu \in L^\infty(\Delta)$, recall the construction of the maps f^μ and f_μ used in the two models of universal Teichmüller space. f^μ solves the Beltrami equation for the coefficient

$$\mu_0(z) = \begin{cases} \mu & , z \in \Delta \\ 0 & , otherwise \end{cases}$$

with the normalization that $f^{\mu} = z + O(1/z)$ at infinity, and f_{μ} solves the Beltrami equation for the coefficient

$$\mu_S(z) = \begin{cases} \mu & , z \in \Delta \\ \bar{\mu}(\frac{1}{\bar{z}})\frac{z^2}{\bar{z}^2} & , otherwise \end{cases}$$

normalized, say, to fix 0, 1, and ∞. Each quasicircle $Q = f^{\mu}(S^1)$ has an associated welding homeomorphism $h : S^1 \to S^1$ given by $h = f_{\mu}\big|_{S^1}$.

We would like to know how making small perturbations in a welding map will change the corresponding quasicircle. A natural notion of "small", in this setting, is given by composing the perturbed map and the original, and measuring the constant of quasisymmetry associated with the composed mapping. The following lemma is one result along these lines:

Lemma 4.2. *Let $\{h_k : S^1 \to S^1\}$ be a family of quasisymmetric homeomorphisms with $K_{QS}[h_k \circ h^{-1}] \to 0$ as $k \to \infty$ for some homeomorphism $h : S^1 \to S^1$. Then the Hausdorff distance $d_{Haus}(Q_k, Q) \to 0$ as $k \to \infty$.*

Proof. Let $\phi_k = h_k \circ h^{-1}$. Each ϕ_k can be extended to a quasiconformal map $\Delta \to \Delta$. The corresponding Beltrami coefficients μ_k have norm $\|\mu_k\|_\infty$ which depends only on $\|\phi_k\|_{QS}$. In particular, $\|\mu_k\|_\infty \to 0$ as $k \to \infty$. By basic properties of quasiconformal maps, the solutions $\{f^{\mu_k}\}$ are equicontinuous, hence they form a normal family and converge uniformly on compact subsets to a limiting map f. Since $\|\mu_k\|_\infty \to 0$, f is conformal on the extended complex plane. In fact, f must be the identity, since that is the unique map with the correct normalization at infinity. The lemma follows by considering the images of S^1 under the maps f^{μ_k}.

□

In fact, we have a more precise result. The tangent space to $\mathbf{Homeo}_{QS}(S^1)$ is given by the space Z of Zygmund vector fields. A real-valued vector field $V(z)\frac{\partial}{\partial z}$ is in Z if there is a constant B such that

$$\|V\|_Z = \sup_{x,t} \left| \frac{V(e^{i(x+t)}) - 2V(e^{ix}) + V(e^{i(x-t)})}{t} \right| \leq B$$

where the supremum is over all $x \in [0, 2\pi]$ and $|t| < \pi$. This is an infinitesimal version of quasisymmetry. If a vector field V satisfies such a condition, then maps $x \mapsto x + \epsilon v(x) + O(\epsilon^2)$ are, to first order, ϵB-quasisymmetric. We can use this Zygmund condition to show that the differential of the welding isomorphism is, near the identity, a bounded linear map in the Zygmund norm on $T_0\mathbf{Homeo}_{QS}$ and the sup norm on the normal part of vector fields on the circle. Recall that, when properly normalized, the differential at the origin is the map D_0 defined by

$$V(\theta) \mapsto \frac{1}{2}\left(iV(\theta) + HV(\theta)\right) e^{i\theta} \frac{\partial}{\partial z}$$

To obtain uniform bounds in the Hausdorff metric, we must control the normal part of the vector field.

Theorem 4.2. *The map D_0 is a bounded map from the Zygmund space to the space of normalized vector fields on S^1 with the sup norm.*

Proof. Let $V \in Z$. If we take a path of homeomorphisms $h_t : S^1 \to S^1$ with $h_t(z) = z + tV(z) + o(t)$ then

$$K_{QS}(h_t) \leq 1 + t\|V\|_Z + o(t)$$

We can extend h_t to a family of quasiconformal maps $\tilde{h}_t : \hat{\mathbb{C}} \to \hat{\mathbb{C}}$ which are solutions to the Beltrami equation with symmetric coefficients μ_t (i.e. $\mu_t(z) = \bar{\mu}_t(1/\bar{z})\frac{z^2}{\bar{z}^2}$). It follows from the Ahlfors-Beurling extension [**3, 24**] that $|\mu_t| \leq C\|V\|_Z$.

Thus V extends to a vector field $\widetilde{V}\frac{\partial}{\partial z}$ defined on $\hat{\mathbb{C}}$ with

$$\widetilde{V} = \dot{\mu} * \frac{1}{\pi z} = \iint_{\hat{\mathbb{C}}} \frac{\dot{\mu}(\xi)}{\xi - z}$$

where $\dot{\mu} = \frac{\partial \mu_t}{\partial t}\Big|_{t=0}$. The corresponding tangent vector $\widetilde{W}$ acting on the quasicircle is given by convolution with the Beltrami coefficient which agrees with $\dot{\mu}$ on Δ and is 0 on Δ^*:

$$\widetilde{W}(z) = \iint_\Delta \frac{\dot\mu(\xi)}{\xi - z}$$

and $D_0 V = \widetilde{W}\big|_{S^1}$. Further, at any point $z \in S^1$,

$$\begin{aligned}
|(D_0 V)(z)| &= \left| \iint_\Delta \frac{\dot\mu(\xi)}{\xi - z} \right| \\
&\leq \iint_\Delta \left| \frac{\dot\mu(\xi)}{\xi - z} \right| \\
&\leq C \|V\|_Z
\end{aligned}$$

$\square$

The measurable mapping theorem also gives some geometric intuition. Given a Beltrami coefficient μ, we have

$$f^{t\mu}(z) = z + tv(z) + o(t)$$

for $v(z) = \mu * \frac{1}{\pi z}$. If a perturbation of a welding map extends to a quasiconformal map with coefficient μ, and $\|\mu\|_\infty$ is small, we can largely understand the difference between the two maps as convolution of μ with the Cauchy kernel. Given the local nature of both the quasiconformal extensions and convolution with the Cauchy kernel, one sees, for example, that the deformation of Q arising from a locally supported perturbation of h will also be strongest at points nearby in the plane.

CHAPTER 5

Compression of 2D Shapes via Teichmüller Theory

1. Background: ϵ-Entropy and Coding

Our ultimate goal in this chapter is to produce a lossy compressor for 2D shapes. That is, given a point in some metric space of shapes, we wish to produce an ϵ-approximating shape which can be described using as few bits as possible. To evaluate the performance of any such scheme, one needs a notion of optimality for compressors; we appeal to Kolmogorov's ϵ-entropy to determine optimality.

Kolmogorov was aware of Shannon's influential work on coding theory, and introduced the definition of ϵ-entropy as part of his project to understand complexity and information in continuous systems [**27, 14, 15**]. We review the basic definitions and some results, and discuss the connection to coding theory.

1.1. Kolmogorov's ϵ-Entropy. Let $X \subset (M, d)$, where M is a metric space with metric d.

Definition 5.1 (ϵ-cover). A collection of sets $\{U_\alpha\}$ such that $X \subseteq \bigcup U_\alpha$ and $diam(U_\alpha) < 2\epsilon$, is called an ϵ-cover for X.

Definition 5.2 (ϵ-entropy). Let N_ϵ be the cardinality of a minimal ϵ-cover of X. The ϵ-entropy of X is $H_\epsilon = \log_2 N_\epsilon$.

We omit many important technical aspects of the theory. The ϵ-entropy is a way of describing the 'massiveness' of infinite-dimensional spaces. In terms of code lengths, it provides a bound on the cost, in bits, of encoding elements of X with encoding error no greater than ϵ. For Lipschitz functions in the uniform norm, we have a particularly simple way of computing the ϵ-entropy. We will only sketch the main idea in the proof of the following theorem.

Theorem 5.1 (ϵ-entropy of C-Lipschitz functions). *Let* $F = \{f : [a,b] \to \mathbb{R} \mid f(a) = 0, |f(x) - f(y)| \leq C|x-y|\}$ *equipped with metric* $d(f,g) = \|f-g\|_\infty$.

$$H_\epsilon(F,d) = \begin{cases} \frac{(b-a)C}{\epsilon} - 1 & , \frac{(b-a)C}{\epsilon} \in \mathbb{Z}_+ \\ \left\lfloor \frac{(b-a)C}{\epsilon} \right\rfloor & , otherwise \end{cases}$$

The key ingredient in the proof is the observation that C-Lipschitz functions stay within corridors bounded by piecewise linear functions of slope $\pm C$ (see figure 5.1). These corridors form a cover for F, and the corridor boundaries give us an ϵ-approximating set. Thus the proof amounts to counting the number of corridors required to cover the set of C-Lipschitz functions. How many such corridors are there? The basic idea is revealed in the simple case $\epsilon = C = 1$ on the interval $[0, n]$. This computation is identical to counting standard random walks; of course there are 2^n such walks. In the general case, there are $2^{\frac{|b-a|C}{\epsilon}}$ corridors, up to taking integer parts at the end of the interval. Thus

$$H_\epsilon(F, d) \approx \frac{|b-a|C}{\epsilon}$$

and the precise result is as stated in the theorem.

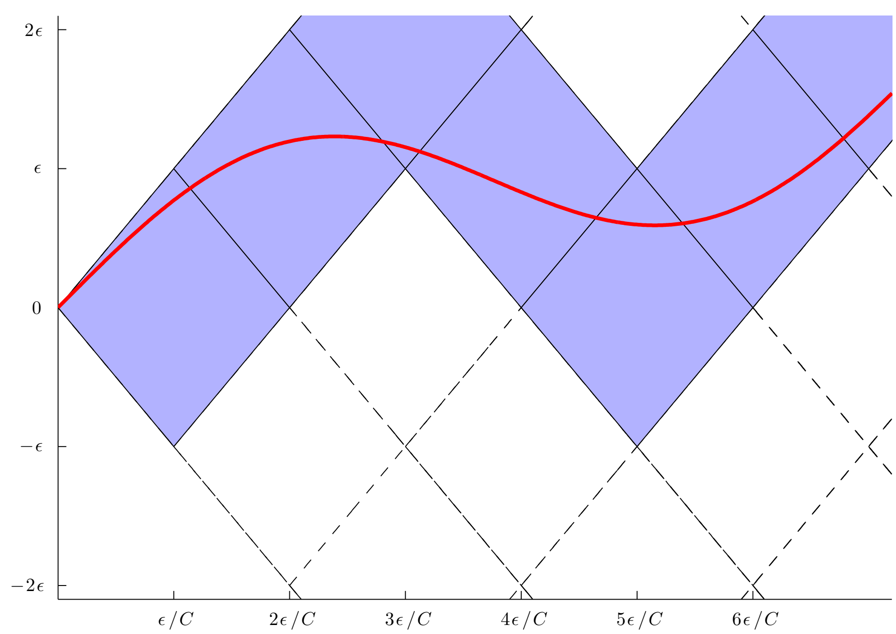

FIGURE 5.1. C-Lipschitz functions stay within ϵ-corridors whose boundaries are piecewise linear with slope $\pm C$.

1.2. Connection with Coding Theory. In lossy coding theory, one asks "given a metric space X, how many bits must I use in order to represent each element in the space with error less than ϵ?" If X is compact, the ϵ-entropy gives an answer.

Suppose one obtains an ϵ-cover with N elements. Then by enumerating their centers, one obtains a family of approximating elements with storage requirement at most $\log N$ bits. In the probabilistic setting, if one places a probability distribution p on X which induces the uniform distribution on an ϵ-cover, then by assigning an integer to each element in the cover one can encode the samples with expected bit length $O\left(H_\epsilon\right)$.

2. Adaptive Uniform Coding of Real-Valued Functions

In the preceeding section, we gave an explicit construction for ϵ-approximants to Lipschitz functions. Our next step is to develop a compressor for a less restrictive class of functions than Lipschitz functions. We'll consider the following setup: $f : [a,b] \to \mathbb{R}$ is a function we wish to approximate with a piecewise linear function g. Given $\{x_k\}_{k=1}^N \subset [a,b]$ with $x_1 = a$, $x_N = b$, we'll set g to be a linear interpolant for f with knots at $\{x_k\}$, which means

$$g(x) = \begin{cases} f(x_k) & x = x_k \\ f(x_k) + \frac{x-x_k}{h_k}\left(f(x_{k+1}) - f(x_k)\right) & x \in (x_k, x_{k+1}) \end{cases}$$

where $h_k = x_{k+1} - x_k$. The first problem is choosing our x_k to minimize the L^∞ approximation error. We then show that our choice of $\{x_k\}$ is an optimal encoding, in the sense that it achieves the ϵ-entropy on a reasonably broad class of processes.

2.1. A First Encoder.

In this section we develop an encoder for functions $f : [a,b] \to \mathbb{R}$ with $\int_a^b |f''| < \infty$. We will prove that if we apply the encoding to C-Lipschitz functions, we achieve the ϵ-entropy up to a constant factor. In later sections, we will relax the too-strict assumption that $\int_a^b |f''| < \infty$.

Lemma 5.1 (L^∞ approximation error). *Let $\phi \in C^1([0,h])$, piecewise C^2, with $\phi(0) = \phi(h) = 0$. Then*

$$\max_{0<x<h} |\phi(x)| \leq \frac{h}{4} \int_0^h |\phi''|$$

PROOF. Set

$$x^* = \arg\max_{0<x<h} |\phi(x)|.$$

and assume without loss of generality that $\phi(x^*) > 0$. We want to know how large $\phi(x^*)$ can be. We claim that it suffices to consider ϕ which are concave and symmetric about $h/2$. Indeed, the "concave hull" of ϕ, i.e. the function

$$\tilde{\phi}(x) = \inf\{L(x) : L \text{ is a line lying above the graph of } \phi \ \}$$

is C^1, piecewise C^2, achieves the same maximum as ϕ, and has $\int |\tilde{\phi}''| \leq \int |\phi''|$. So the conclusion will follow if we show it for concave functions. For concave ϕ,

$$\phi\left(\frac{h}{2}\right) \geq \frac{\phi(x^*)}{2}$$

since concavity implies ϕ lies above the line segments joining its endpoints to its maximum.

Now observe that the function

$$\psi(x) = \frac{1}{2}\left(\phi(x) + \phi(h-x)\right)$$

is concave and symmetric about $h/2$ with $\int |\psi''| = \int |\phi''|$. Thus

$$\psi(h/2) = \frac{1}{2}\left(\phi(h/2) + \phi(h/2)\right) \geq \phi(x*)$$

So assuming ϕ is concave and symmetric about $h/2$, we have

$$\begin{aligned}\phi(x^*) &= \int_{h/2}^{h} |f'(s)|ds \\ &= \int_{h/2}^{h}\int_{h/2}^{s} |f''(\xi)|d\xi \\ &\leq \int_{h/2}^{h}\int_{h/2}^{h} |f''(\xi)|d\xi \\ &= \int_{h/2}^{h}\frac{1}{2}\int_{0}^{h} |f''(\xi)|d\xi \\ &= \frac{h}{4}\int_{0}^{h} |f''(\xi)|d\xi\end{aligned}$$

$\square$

Remark. Lemma 5.1 is sharp. Indeed, fix some $h > 0$ and $k > 0$ and ask for a C^2 function ϕ which achieves the greatest value on $[0, h]$, subject to $\int_0^h |\phi''| = k$ and $\phi(0) = \phi(h) = 0$. The supremizing case has $f'' = -k\delta_{h/2}$, which corresponds to a triangle-shaped function with sides of slope $k/2$ and maximum of $\frac{h}{4}k$ achieved at $h/2$.

Applying lemma 5.1, we see that in order to guarantee that a piecewise linear interpolant g is a uniform ϵ-approximation to f, we must choose the stepsize $h_k = x_{k+1} - x_k$ such that

$$(x_{k+1} - x_k)\int_{x_k}^{x_{k+1}} |f''| \leq \epsilon$$

We now compute the number of points this requires.

Lemma 5.2 (Placing $\{x_k\}$.). *Let g be a linear interpolant for f with knots at $\{x_k\}, k = 1, 2, 3, ..., N + 1$. Let $I_k = [x_k, x_{k+1}]$. If*

$$|I_k|\int_{I_k} |f''| = |I_j|\int_{I_j} |f''|$$

for all $k, j \in 1, 2, 3, ...N$, then

$$\|f - g\|_\infty \leq \frac{b-a}{4N^2}\int_a^b |f''|$$

PROOF. We have

$$
\begin{aligned}
N &= \sum_{k=1}^{N} \sqrt{|I_k|} \cdot \frac{1}{\sqrt{|I_k|}} \\
&\leq \sqrt{\sum_{k=1}^{N} |I_k| \cdot \frac{1}{|I_k|}} \\
\implies N^2 &\leq (b-a) \cdot \sum_{k=1}^{N} \frac{1}{|I_k|}
\end{aligned}
$$

If M is the common value

$$M = |I_k| \int_{I_k} |f''|$$

then

$$\|f-g\|_\infty \leq \frac{M}{4}$$

and

$$\int_a^b |f''| = M \sum_{k=1}^{N} \frac{1}{|I_k|} \geq \frac{MN^2}{b-a}$$

This completes the proof. □

We have just showed that the spacing rule

$$(x_{k+1}-x_k) \int_{x_k}^{x_{k+1}} |f''| = (x_{j+1}-x_j) \int_{x_j}^{x_{j+1}} |f''|$$

implies the error bound

$$\|f-g\|_\infty \leq \frac{b-a}{4N^2} \int_a^b |f''|$$

We now show that this knot spacing asymptotically achieves the ϵ-entropy for Lipschitz functions, up to a constant factor given by the cost of storing N points.

THEOREM 5.2. *Let $f : [a, b] \to \mathbb{R}$ be C-Lipschitz with $\int_a^b |f''| < \infty$. Set*

$$h^* = \inf\{h > 0 : \int_x^{x+h} |f''| \le 4C \text{ for all } x \in [a, b-h]\}$$

Then if $\epsilon \le h^*$, the number of points stored is

$$N \le \left\lceil \frac{(b-a)C}{\epsilon} \right\rceil$$

PROOF. By lemma 5.2 we know that

$$N^2 \le \frac{b-a}{4\epsilon} \int_a^b |f''|$$

We wish to get control of the right-hand side. We first estimate the integral. Divide $[a, b]$ into $\lceil \frac{b-a}{h^*} \rceil$ intervals, each of length less than h^*:

$$\int_a^b |f''| = \sum_1^{\lceil \frac{b-a}{h^*} \rceil} \int_{I_k} |f''| \le \left\lceil \frac{b-a}{h^*} \right\rceil \cdot 4C$$

We also need to relate ϵ and h^*. By lemma 5.1,

$$\epsilon \le \max_{x \in [a, b-h^*]} \frac{h^*}{4} \int_x^{x+h^*} |f''| \le Ch^*$$

Returning to the right-hand side of our estimate for N^2 and applying our estimates, we arrive at

$$\begin{aligned}
\frac{b-a}{4\epsilon} \int_a^b |f''| &\le \frac{b-a}{4\epsilon} \left\lceil \frac{b-a}{h^*} \right\rceil C \\
&\le \frac{(b-a)C}{\epsilon} \left\lceil \frac{(b-a)C}{\epsilon} \right\rceil \\
&\le \left\lceil \frac{(b-a)C}{\epsilon} \right\rceil^2
\end{aligned}$$

Taking square roots completes the proof. □

REMARK. This coding does not achieve the ϵ-entropy exactly. There are two problems.

(1) We achieve $\left\lceil \frac{(b-a)C}{\epsilon} \right\rceil$, whereas the actual value is

$$H_\epsilon = \begin{cases} \frac{(b-a)C}{\epsilon} - 1 & , \frac{(b-a)C}{\epsilon} \in \mathbb{Z}_+ \\ \left\lfloor \frac{(b-a)C}{\epsilon} \right\rfloor & , otherwise \end{cases}$$

This could be remedied if we modified our representation slightly; for example, we currently do not assume that $f(a) = 0$.

(2) Storing each point requires us to store the values $(x_k, f(x_k))$. This takes 64 bits if we store both as 32-bit floating-point values. Thus we only achieve a constant multiple of the ϵ-entropy; the exact constant depends on the representation we use for the numbers.

A partial solution to (2) is presented in section 3.

It may be the case that one can find an ϵ-approximant to a function using far fewer interpolating points than our estimates suggest. For example, the function

$$f(x) = \frac{\sin(100x)}{100}$$

oscillates wildly on $[0, 2\pi]$ and hence $\int |f''|$ is large, but $|f|$ remains bounded by $1/100$. So for $\epsilon > 1/100$, f can be uniformly approximated by a straight line segment, which takes only two points to encode. The issue is one of scale: $\epsilon > 1/100$ is too large compared to the excursions of the function. The preceeding lemma thus addresses both the optimality of the compression, as well as the scale at which the estimates become relevant.

Closer inspection of the proof of lemma 5.2 reveals that the existence of a non-zero h^* defines a point of interest for the function, relative to the epsilon-entropy. At $\epsilon = Ch^*$, the estimate is precise, but in general we have

$$N = O\left(\frac{(b-a)}{2}\sqrt{\frac{C}{\epsilon h^*}}\right)$$

That is, the growth of N for a fixed f and h^* may be viewed as $O\left(\frac{1}{\sqrt{\epsilon}}\right)$, with a constant factor defined by h^*. This does not, of course, imply that this approximation scheme bests the ϵ-entropy. Consider a function with constant $|f''| = K$. Then

$$N^2 \leq \frac{b-a}{4\epsilon}\int_a^b |f''| = \frac{(b-a)^2K}{4\epsilon}$$

So, for example, if we're working with a smooth f and we choose ϵ small enough, we take step sizes small enough that the function, roughly speaking, looks like it has locally constant $|f''|$. Over all C-Lipschitz functions, there is no universal scale at which this happens, so there is no conflict with the ϵ-entropy.

Example 5.1 (Expected coding cost for random walks). *Let F be the set of all symmetric random walks taking jumps of size δ on a mesh $\{0, \frac{\delta}{C}, 2\frac{\delta}{C}, ..., K\frac{\delta}{C}\}$. Let $a = 0, b = K\delta/C$. Each $f \in F$ is differentiable except at the jump points, where we interpret f'' in the sense of distributions. On each interval $[n\delta/C, (n+1)\delta/C]$, we have $f' = \pm C$, with probability $1/2$. Therefore we have for all intervals $I_n = [n\delta/C + \delta/2C, (n+1)\delta/C + \delta/2C]$ that*

$$\int_{I_n} |f''| = \begin{cases} 2C & \text{with probability } 1/2 \\ 0 & \text{with probability } 1/2 \end{cases}$$

If N is the expected number of points stored for a given $\epsilon > 0$, we have the bound

$$\begin{aligned} E\left[N\right] &\leq E\sqrt{\frac{b-a}{4\epsilon}\int_a^b |f''|} \\ &= \sqrt{\frac{b-a}{4\epsilon}}E\left[\sqrt{\int_a^b |f''|}\right] \\ &\leq \sqrt{\frac{b-a}{4\epsilon}E\left[\int_a^b |f''|\right]} \\ &= \sqrt{\frac{b-a}{4\epsilon}KC} \\ &= \frac{(b-a)C}{2\sqrt{\epsilon\delta}} && \text{, since } K = C(b-a)/\delta \end{aligned}$$

If ϵ and δ agree, we see exactly $1/2$ the ϵ-entropy.

2.2. Expanding the Domain. The results in the previous section are stated for the most general case, and hold even in the limit when the second derivative exists as a distribution. However, if we impose some regularity on the functions we wish to encode, we will see that the asymptotic behavior of the encoder is far more forgiving than the worst-case bounds

$$N^2 \leq \frac{b-a}{4\epsilon}\int_a^b |f''|$$

would suggest. In fact, if we control the local behavior of the function we see that there are many more functions which we can approximate with finite N, including, for example, certain functions which are merely Hölder continuous. The sufficient condition is a sort of reverse Jensen's inequality, shown in the next lemma.

LEMMA 5.3. *Let $f : [a,b] \to \mathbb{R}$ be such that for any $C > 1$ there exists δ such that*

$$\sqrt{\frac{1}{h}\int_x^{x+h} |f''|} \leq C\frac{1}{h}\int_x^{x+h} \sqrt{|f''|}$$

for all intervals $[x, x+h]$ of length less than δ. Let g be a linear interpolant for f with knots at $\{x_k\}, k = 1, 2, 3, ..., N+1$. If

$$\int_{x_k}^{x_{k+1}} \sqrt{|f''|} = \int_{x_j}^{x_{j+1}} \sqrt{|f''|}$$

for all $k, j \in 1, 2, 3, ...N$, then

$$\|f-g\|_\infty \leq O\left(\frac{C^2}{N^2}\left(\int_a^b \sqrt{|f''|}\right)^2\right)$$

when $\max\{h_k\} < \delta$.

PROOF. From lemma 5.1 and by our assumptions,

$$
\begin{aligned}
|f-g| &\leq h_k \int_{x_k}^{x_{k+1}} |f''| \\
&= h_k^2 \frac{1}{h_k} \int_{x_k}^{x_{k+1}} |f''| \\
&\leq C^2 \left(\int_{x_k}^{x_{k+1}} \sqrt{|f''|} \right)^2
\end{aligned}
$$

By assumption, we choose our mesh $\{x_k\}$ so that

$$\int_{x_k}^{x_{k+1}} \sqrt{|f''|} = \frac{1}{N} \int_a^b \sqrt{|f''|}$$

for all $1 \leq k \leq N+1$. The lemma follows upon substitution. □

REMARK. This result is reminiscent of a result in Leonard's thesis [**31**], in which an adaptive coding scheme was presented with

$$N \leq \frac{1}{\epsilon} \int |f'|$$

We would achieve the same results in this thesis if we used piecewise constant, rather than piecewise linear, approximations, and followed a similar line of argument to the one above. More generally, this suggests that using piecewise polynomial approximations (splines) of order $(n-1)$, one may be able to achieve

$$N \leq \epsilon^{-\frac{1}{n}} \int |f^{(n)}|^{1/n}$$

A heuristic argument is as follows. Expanding f in series about some point, one has

$$f(x+h) = f(x) + hf'(x) + \frac{1}{2}h^2 f''(x) + ... + \frac{1}{n!}h^n f^{(n)}(x) + O(h^{n+1})$$

So if we make the $(n-1)$ order approximation about x

$$g(x+h) = f(x) + hf'(x) + \frac{1}{2}h^2 f''(x) + ... + \frac{1}{(n-1)!}h^{(n-1)} f^{(n-1)}(x)$$

we have that our error is

$$|f(x+h) - g(x+h)| = \frac{1}{n!} h^n f^{(n)}(x) + O(h^{n+1})$$

If we can justify dropping higher-order terms, choosing step sizes of

$$h_k = O\left(\left(\frac{\epsilon}{f^{(n)}}\right)^{1/n}\right)$$

should guarantee uniform bounds on error. Summing step sizes gives the bound on N. Calculating N stored on random walks suggests that any scheme with these storage requirements will have $N \leq \left\lceil \frac{(b-a)C}{\epsilon} \right\rceil$ on C-Lipschitz functions.

In practice, high-order polynomial approximations are extremely challenging to work with, particularly in extrapolation tasks like we have here. It is not clear that such methods would be practical.

Lemma 5.3 greatly expands the class of functions which we may encode with a finite number of bits. The following two examples illustrate the utility and limitations of this result.

Example 5.2. *Consider the Hölder continuous function* $f(x) = x^\alpha$, $0 < \alpha < 1$, *defined on some interval* $[0, b]$. *The integral* $\int_0^b |f''|$ *diverges, but we have*

$$\begin{aligned} \sqrt{\frac{1}{h}\int_x^{x+h} |f''|} &= \sqrt{\frac{\alpha}{h} \left|(x+h)^{\alpha-1} - x^{\alpha-1}\right|} \\ &= \sqrt{\alpha(\alpha-1)x^{\alpha-2} + O(h)} \end{aligned}$$

and

$$\begin{aligned} \frac{1}{h}\int_x^{x+h} \sqrt{|f''|} &= \frac{2}{h}\sqrt{\frac{\alpha-1}{\alpha}} \left|(x+h)^{\alpha/2} - x^{\alpha/2}\right| \\ &= \sqrt{\alpha(\alpha-1)} \left|x^{\alpha/2-1} + O(h)\right| \end{aligned}$$

We form their ratio and obtain

$$\frac{\sqrt{x^{\alpha-2}+O(h)}}{x^{\alpha/2-1}+O(h)} = \sqrt{\frac{1+O(hx^{2-\alpha})}{1+O(hx^{1-\alpha/2})}}$$

For x in any interval $(0,b)$ this ratio tends uniformly to 1 as h goes to zero. Hence lemma 5.3 applies and we see we can bound the approximation error using a finite number of points:

$$\begin{aligned}
|f-g| &\leq O\left(\frac{C^2}{N^2}\int_0^b |f''|\right) \\
&= O\left(\frac{C^2}{N^2}\int_0^b \sqrt{|\alpha(\alpha-1)x^{\alpha-2}|}\right) \\
&= O\left(2\frac{C^2}{N^2}\sqrt{\frac{\alpha-1}{\alpha}}b^{\alpha/2}\right)
\end{aligned}$$

It is worth making a few further remarks on Hölder continuity. The condition $\int_0^b \sqrt{|f''|} < \infty$ implies Hölder continuity at any point of f. That is,

$$\begin{aligned}
&\int_0^b \sqrt{|f''(x)|}dx < \infty \\
\implies &\sqrt{|f''(x)|} < \frac{k}{x^\beta} \qquad \text{, some } \beta < 1 \\
\implies &|f''(x)| < \frac{k_2}{x^{2\beta}}
\end{aligned}$$

By integrating twice, we deduce a Hölder condition on f. That is,

$$\begin{aligned}
|f'(x)| &= f'(b) + \int_b^x f''(\xi)d\xi \\
&\leq |f'(b)| + k_3\left(b^{-2\beta+1} - x^{-2\beta+1}\right) \\
&\leq k_4 x^{1-2\beta}
\end{aligned}$$

Repeating, we obtain

$$|f(x)| \leq k_5 x^{2-2\beta}$$

Since $0 < 2 - 2\beta < 1$, f is Hölder with exponent $2 - 2\beta$. However, Hölder continuity of f is not a sufficient condition for the lemma; the next example demonstrates a Hölder-continuous function to which the lemma does not apply.

EXAMPLE 5.3. *Consider* $f'' = \delta_{x_0}$. *The lemma fails to apply since the integral of* $\sqrt{\delta}$ *vanishes. Consider a triangle-shaped function supported on an interval containing* 0, *with tip at* $x = 0$ *and sides of slope* ± 1. *The second derivative is given by*

$$f''(x) = \left(\begin{array}{cc} -\frac{4}{\epsilon} & x \in [-\epsilon, \epsilon] \\ 0 & elsewhere \end{array} \right.$$

However,

$$\int \sqrt{|f''|} = \int_{-\epsilon}^{\epsilon} \frac{2}{\sqrt{\epsilon}} = 2\sqrt{\epsilon}$$

In the limit where $f'' = -2\delta_0$, *the integral vanishes. The essential failure is that a delta function changes too rapidly; there is no scale below which the two integrals in the lemma statement are comparable.*

2.3. Computing a Mesh with Specified Spacing. In order to carry out the interpolation we have described, we need a way to choose the mesh points $\{x_k\}$. The proof of lemma 5.3 suggests an algorithm for computing the meshes. Lemma 5.3 requires that the knot points $\{x_k\}$ satisfy

$$\int_{x_k}^{x_{k+1}} \sqrt{|f''|} = \int_{x_j}^{x_{j+1}} \sqrt{|f''|}$$

for all k, j. As h_k shrinks, this means that the stepsize is roughly $O\left(\frac{1}{\sqrt{|f''|}}\right)$. In general, we may wish to choose a mesh so that the mesh spacing is approximately $O(\sigma)$, where $\sigma : [a, b] \to [0, \infty]$ is some function. Indeed, we will need to do this in the next section. We will use the following result, which allows us to compute exactly the spacing from lemma 5.3 and provides a quick method for computing the desired mesh in general.

LEMMA 5.4. *Let $\sigma : [a, b] \to [0, \infty]$ be continuous and satisfy $\int_a^b \sigma = b - a$ and $\int_a^b \frac{1}{\sigma} < \infty$. Choose some integer $N > 0$. Then there is an $O(N)$-time algorithm for computing a mesh $\{x_k\}_{k=0}^N$ with $x_0 = a, x_N = b$ where the mesh size satisfies $x_{k+1} - x_k = C\sigma(x_k^*)$ for some $x_k^* \in (x_k, x_{k+1})$. C is independent of k.*

PROOF. Define the function

$$\Sigma(x) = \int_a^x \frac{1}{\sigma(\xi)} d\xi$$

Choose points $\{y_k\}_{k=0}^N$ by setting

$$y_k = \frac{k}{N}(b - a)$$

We claim that the points $x_k = \Sigma^{-1}(y_k)$ form the desired mesh. Indeed,

$$\int_{x_k}^{x_{k+1}} \frac{1}{\sigma(\xi)} d\xi = \frac{b - a}{N}$$

By the mean value theorem, there exists a point $x_k^* \in (x_k, x_{k+1})$ such that

$$\frac{1}{\sigma(x_k^*)}(x_{k+1} - x_k) = \frac{b - a}{N}$$

The conclusion follows with $C = (b - a)/N$. □

2.4. Examples. The next few figures provide some examples of linear interpolants constructed using the method of the previous section with the spacing function

$$\sigma_U(x) = \frac{1}{\sqrt{|f''(x)|}}$$

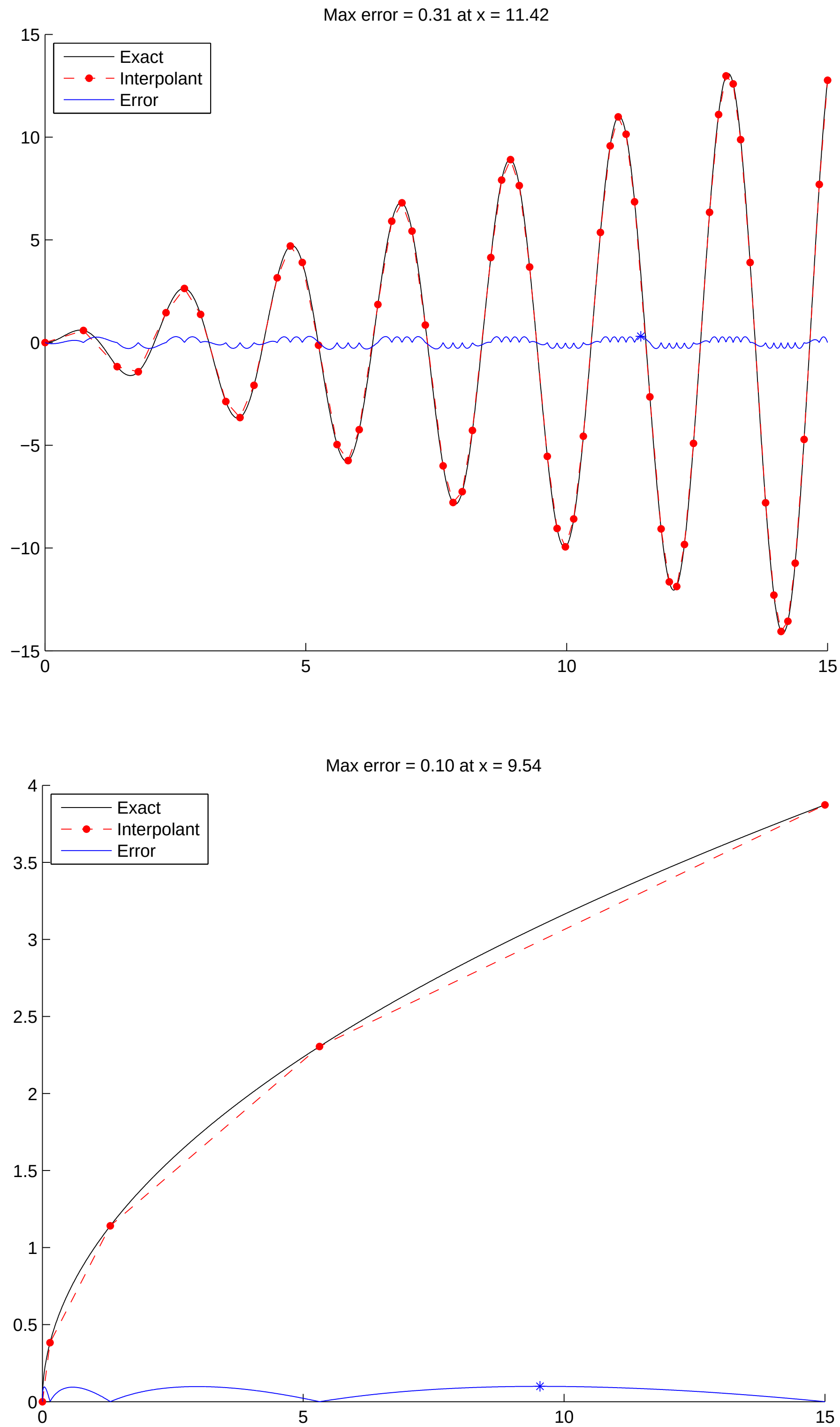

FIGURE 5.2. Above: $x \sin 3x$ and a 60-point interpolant. Below: $\sqrt{x}$ and a 4-point interpolant, computed using the spacing function $\sigma_U(x) = \frac{1}{\sqrt{|f''(x)|}}$ and the method of lemma 5.4

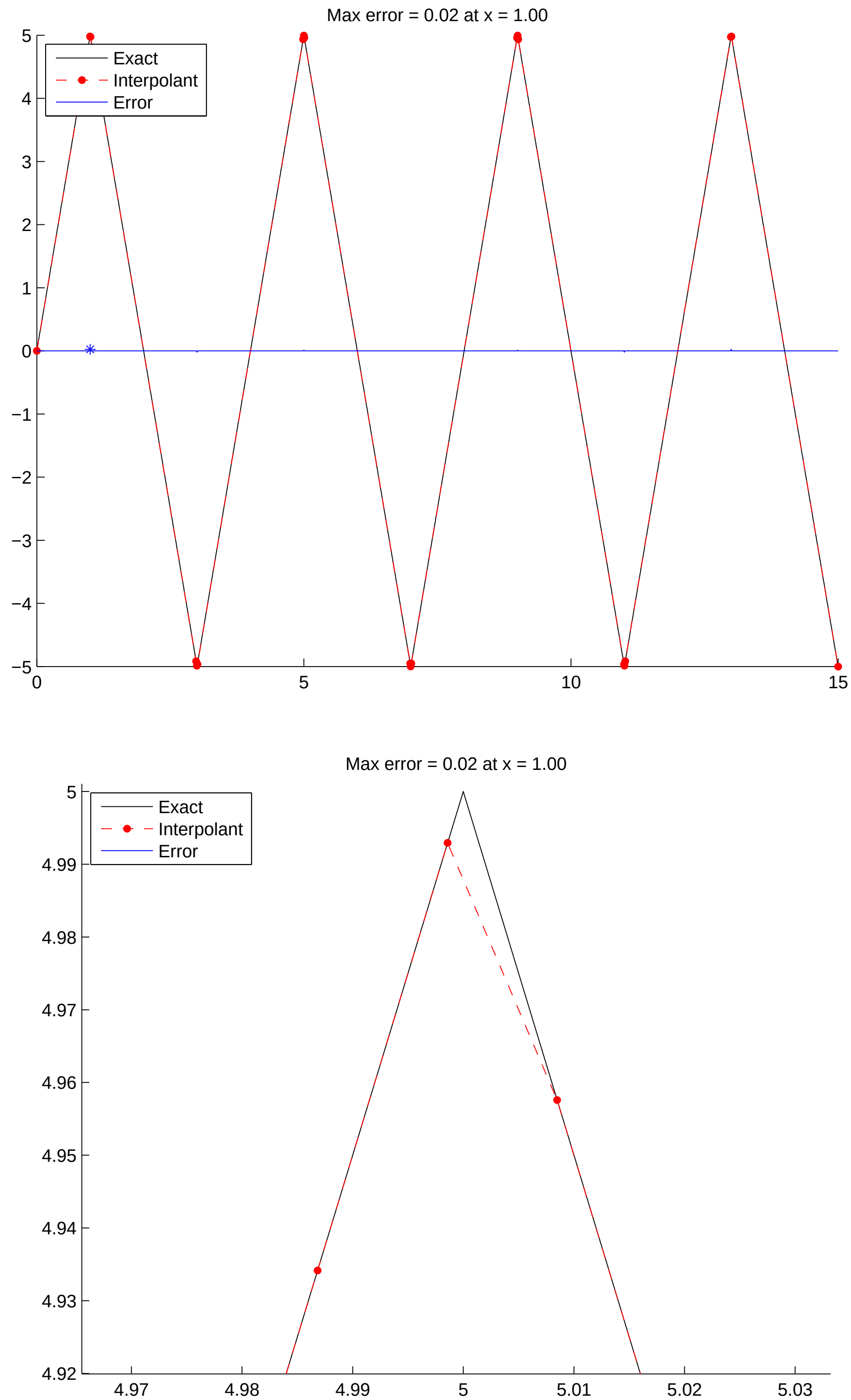

FIGURE 5.3. A 20-point interpolant to a triangle function and a close-up of a tip, both computed using $\sigma_U(x) = \frac{1}{\sqrt{|f''(x)|}}$ and the method of lemma 5.4. The spacing function σ_U gives reasonable results because a δ function is indistinguishable from very large f'' once sampled.

3. Reducing the Bit Cost

So far, we've considered approximating a function f with an interpolant g. However, if we relax two assumptions on g we can save a considerable number of bits. In particular, in this section we'll still consider piecewise linear ϵ-approximants g, but we'll change two assumptions:

(1) At the knot points $\{x_k\}$ we no longer require $g(x_k) = f(x_k)$.
(2) The allowable timesteps h_k are still adaptive, but now take values in some countable set.

Further, we don't choose our spacing as naively as in the previous section, where we paid attention only to the derivatives of the function. Here we operate by extending an approximation as far as we can without exceeding some error threshold ϵ; this is more robust when the function oscillates rapidly but boundedly, for example.

3.1. Discretizing the Values: From Interpolants to Approximations.

We'll now consider the following setup: $f : [a,b] \to \mathbb{R}$ is a function we wish to approximate with a piecewise linear function g. The function g is defined by a finite set of values $g(x_k)$ taken on some mesh $\{x_k\}_{k=1}^{N} \subset [a,b]$ with $x_1 = a$, $x_N = b$.

$$g(x) = \begin{cases} g(x_k) & x = x_k \\ g(x_k) + \frac{x-x_k}{h_k}\left(g(x_{k+1}) - g(x_k)\right) & x \in (x_k, x_{k+1}) \end{cases}$$

where $h_k = x_{k+1} - x_k$. We'll adopt the following notations for the the left-sided derivative and tangent line to g:

$$g'_{-}(x) = \lim_{s \searrow 0} \frac{1}{s}\left(g(x) - g(x-s)\right)$$

$$T_k(x) = g(x_k) + (x - x_k) g'_{-}(x_k)$$

Additionally, we restrict the values $g(x_k)$ and h_k so they have shorter description lengths. We require

$$h_{k+1} = \alpha_{j_k} h_k \qquad , \textit{some } \alpha_{j_k} \in A$$

$$g(x_{k+1}) = h_k T_k + m_k \epsilon \qquad , \textit{some } m_k \in \mathbb{Z}$$

where $A = \{..., \alpha_{-2}, \alpha_{-1}, \alpha_0 = 1, \alpha_1, \alpha_2, ...\}$ is a countable set of $\alpha_i \in \mathbb{R}$, with $\alpha_{i+1} > \alpha_i$ and $\inf\{\alpha_i\} = -\infty$.

If, given some f and a set A, there exists g satisfying these requirements with $\|f - g\|_\infty \leq \epsilon$, we say g is an *ϵ-approximation for f*.

THEOREM 5.3. *Let f be such that $\int_a^b |f''| < \infty$. If for all $\beta \in \mathbb{R}_+$, there exists $\alpha_i \in A$ such that*

$$M\beta \leq \alpha_i \leq \beta$$

then there exists an ϵ-approximation g for f such that N, the number of points stored, satisfies

$$N^2 \leq \frac{3}{8M^2} \cdot \frac{b-a}{\epsilon} \int_a^b |f''|$$

PROOF. We first claim that the number of intervals we need to store to create an ϵ-interpolant does not increase by more than a factor of $1/M$. Let h_k be the current timestep. The largest next timestep h^*_{k+1} we could choose to guarantee an ϵ-interpolant would satisfy

$$\epsilon = \frac{h^*_{k+1}}{4} \int_{x_k}^{x_k + h^*_{k+1}} |f''|$$

Define β_k by

$$h^*_{k+1} = \beta_k h_k$$

However, we cannot choose this timestep. Instead, select α_{j_k} to be the largest element of A such that

$$h_{k+1} \equiv \alpha_{j_k} h_k \leq \beta h_k$$

By assumption on A, we have

$$M \leq \frac{h_{k+1}}{h^*_{k+1}} \leq 1$$

Thus we can take at least M times the maximal distance at each step, and the claim follows. We are halfway there: so far we've assumed g is an interpolant with values $g(x_k) = f(x_k)$. We must now adjust the values $g(x_k)$ to lie at allowable values for an approximation to f, which amounts to shifting the values $g(x_k)$ up or down by an amount less than $\epsilon/2$. Doing this increases error by no more than $\epsilon/2$ over each interval. Since an interpolant satisfies

$$N^2 \leq \frac{b-a}{4\epsilon} \int_a^b |f''|$$

We have shown that for an approximation,

$$(MN)^2 \leq \frac{b-a}{4 \cdot \left(\frac{2}{3}\epsilon\right)} \int_a^b |f''|$$

□

Remark. The condition that for all $\beta \in \mathbb{R}_+$, there exists $\alpha_i \in A$ with

$$M\beta \leq \alpha_i \leq \beta$$

is satisfied, for example, with $M = 1/2$ by the set

$$A = \{..., \frac{1}{8}, \frac{1}{4}, \frac{1}{2}, 1, 2, 4, 8, ...\}$$

In this case we will have

$$N^2 \leq \frac{3}{4} \cdot \frac{b-a}{\epsilon} \int_a^b |f''|$$

While we store more points and make weaker error bounds, we have a win in terms of overall cost of storage. Instead of storing floating-point representations of the numbers $(h_k, f(x_k))$, we need only store a few exact values $x_0, h_0, g(x_0)$ and then everything else is given in terms of the values (α_{j_k}, m_k). These take values in some countable set, and we can create efficient encodings for them. Denote by $K(\alpha_i, m)$ a codeword for the pair (α_i, m). Then the cost of encoding an approximation is

$$Cost(g) = C + \sum_{1}^{N} |K(\alpha_{j_k}, m_k)|$$

If we put some probability distribution on a set F of functions, we can consider optimal encodings for the pairs (α_i, m). Our step sizes h_k and values $g(x_k)$ are now random variables drawn from some distribution. If we make some assumptions, we can obtain estimates for bit lengths of the encodings. We consider timesteps which are Markov

$$p(h_{k+1}|h_k, h_{k-1}, ..., h_1) = p(h_{k+1}|h_k)$$

and we assume further that $p(h_{k+1}|h_k)$ depends only on the ratio $\frac{h_{k+1}}{h_k}$, so we can write

$$p(h_{k+1}|h_k) = f(\alpha_{j_k})$$

and the α_{j_k} are independent random variables. We also would like to assume that the m_k are independent of each other, though m_k is not necessarily independent of α_{j_k}. Under these assumptions, we have

THEOREM 5.4. *The total number of bits required to store g satisfies*

$$E[Cost(g)] = C + E[N] \cdot E|K(\alpha_{j_k}, m_k)|$$

Proof. Apply Wald's equation.

$$\begin{aligned} E[Cost(g)] &= E\left[C + \sum_{1}^{N} |K(\alpha_{j_k}, m_k)|\right] \\ &= C + E\left[\sum_{1}^{N} |K(\alpha_{j_k}, m_k)|\right] \\ &= C + E[N] \cdot E|K(\alpha_{j_k}, m_k)| \end{aligned}$$

□

Remark. More generally, without particular assumptions on the α_{j_k}'s and m_k's, one could use an adaptive encoding scheme along the lines of Lempel-Ziv to store these values. This amounts to learning the empirical distribution and adapting our codewords as we progress.

3.2. Experiments: A Second Algorithm for Encoding Approximations. In this section we show the results of some numerical experiments using two compression algorithms.

The first algorithm is essentially described in the proof of theorem 5.3: given $\{x_j\}_{j=1}^k$, we choose the next values

$$\begin{aligned} h_{k+1} &= \alpha_{j_k} h_k && \text{, some } \alpha_{j_k} \in A \\ g(x_{k+1}) &= h_k T_k + m_k \epsilon && \text{, some } m_k \in \mathbb{Z} \end{aligned}$$

by choosing the largest allowable $h_{k+1} \in A$ and then choosing the $m_k \in \mathbb{Z}$ which minimizes $|g(x_{k+1}) - f(x_{k+1})|$.

The second algorithm is slightly more complicated to explain; we do so now. Let $f : [a, b] \to \mathbb{R}$ be continuous with $\int_a^b |f''| < \infty$. We will construct $g : [a, b] \to \mathbb{R}$, a piecewise linear function s.t. $\|f - g\|_\infty \leq \frac{3}{2}\epsilon$.

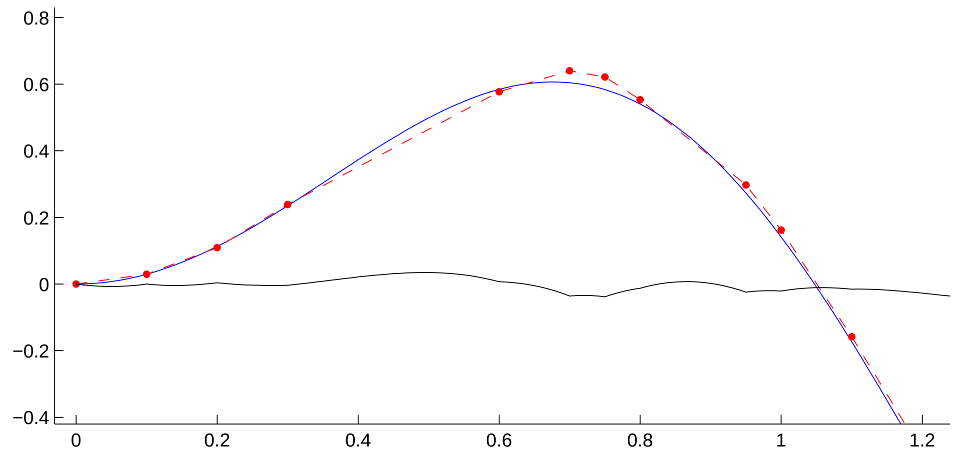

FIGURE 5.4. A piecewise linear approximation to a smooth function.

We will proceed by induction, assuming g is defined by the values $g(x_1), g(x_2), ..., g(x_k)$. Assume that we have chosen points $\{x_j\}$ and values $\{g(x_j)\}$ for $1 \leq j \leq k$ so that

$$|f(x_k) - g_k| < \epsilon/2$$

and

$$\max_{x \in [x_1, x_k]} |f(x) - g(x)| \leq \frac{3}{2}\epsilon$$

We'll continue to use the following notations for the current stepsize and the left-sided derivative:

$$h_j = x_{j+1} - x_j$$

$$g'_{-}(x) = \lim_{s \searrow 0} \frac{1}{s}\left(g(x) - g(x-s)\right)$$

We choose x_{k+1} and g_{k+1} as follows.

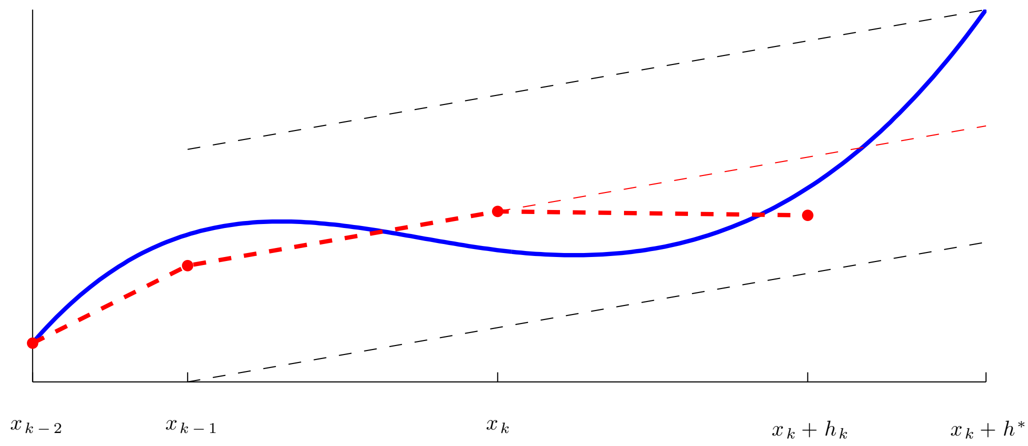

(1) Extend the tangent line:

$$T_k(x) = g(x_k) + (x - x_k)g'_-(x_k)$$

(2) Record the first time the tangent line exits an epsilon corridor about f:

$$h^* = \min\{h > 0 : |f(x_k + h) - T_k(x_k + h)| > \epsilon\}$$

(3) Choose the next timestep $h_k \leq h^*$ as the largest possible value given the set of multipliers A:

$$h_k = \max\{\alpha_k h_{k-1} < h^* : \alpha_k \in A\} \tag{9}$$

(4) Set $x_{k+1} = x_k + h_k$ and choose $g(x_{k+1})$:

$$g(x_{k+1}) = \begin{cases} T_k(x_{k+1}) + \epsilon/2 & , f(x_{k+1}) > T_k(x_{k+1}) \\ T_k(x_{k+1}) - \epsilon/2 & , \text{otherwise} \end{cases} \tag{10}$$

It is easy to verify that we have extended the approximating function in such a way that it satisfies both our requirements:

$$|f(x_{k+1}) - g_{k+1}| < \epsilon/2$$

$$\sup_{x \in [x_k, x_{k+1}]} |f(x) - g(x)| < \frac{3}{2}\epsilon$$

3.3. Storage. The storage costs of the first algorithm are given in theorem 5.4. The second algorithm is more difficult to justify; the problem is obtaining estimates on N. We simply observe that in order to reconstruct a function g produced by the second method, one needs to know:

- $\{x_1, f(a), f'(a), h_1\}$: the initial conditions

  These take finite space depending only on the desired precision.

- $\{s_j\}$, the sign of $\epsilon/2$ in equation 10

  This costs 1 bit per point stored.

- $\{\alpha_j\}$: the amounts by which we modify the step size in equation 9

  This takes variable space. The optimal encoding of α_j depends on the distribution of values assumed by α_j.

So if N is the total number of points stored, we have the cost in bits of encoding f given ϵ

$$Cost(f, \epsilon) = C + N + \sum_{1}^{N} Cost(\alpha_j)$$

And under similar conditions to theorem 5.4,

$$E[Cost(f, \epsilon)] = C + E[N]\,(1 + E[Cost(\alpha_j)])$$

However, in the case of this second algorithm we do not have theoretical justification for our previous estimates on N. Experimental justification will be shown shortly.

3.4. Examples: The Second Algorithm. The next few pages show some examples of the second encoder producing approximations to a variety of functions. In particular we compare the predicted step sizes, which should be given by

$$h = O\left(\frac{\epsilon}{|f''|}\right)$$

with the actual step sizes.

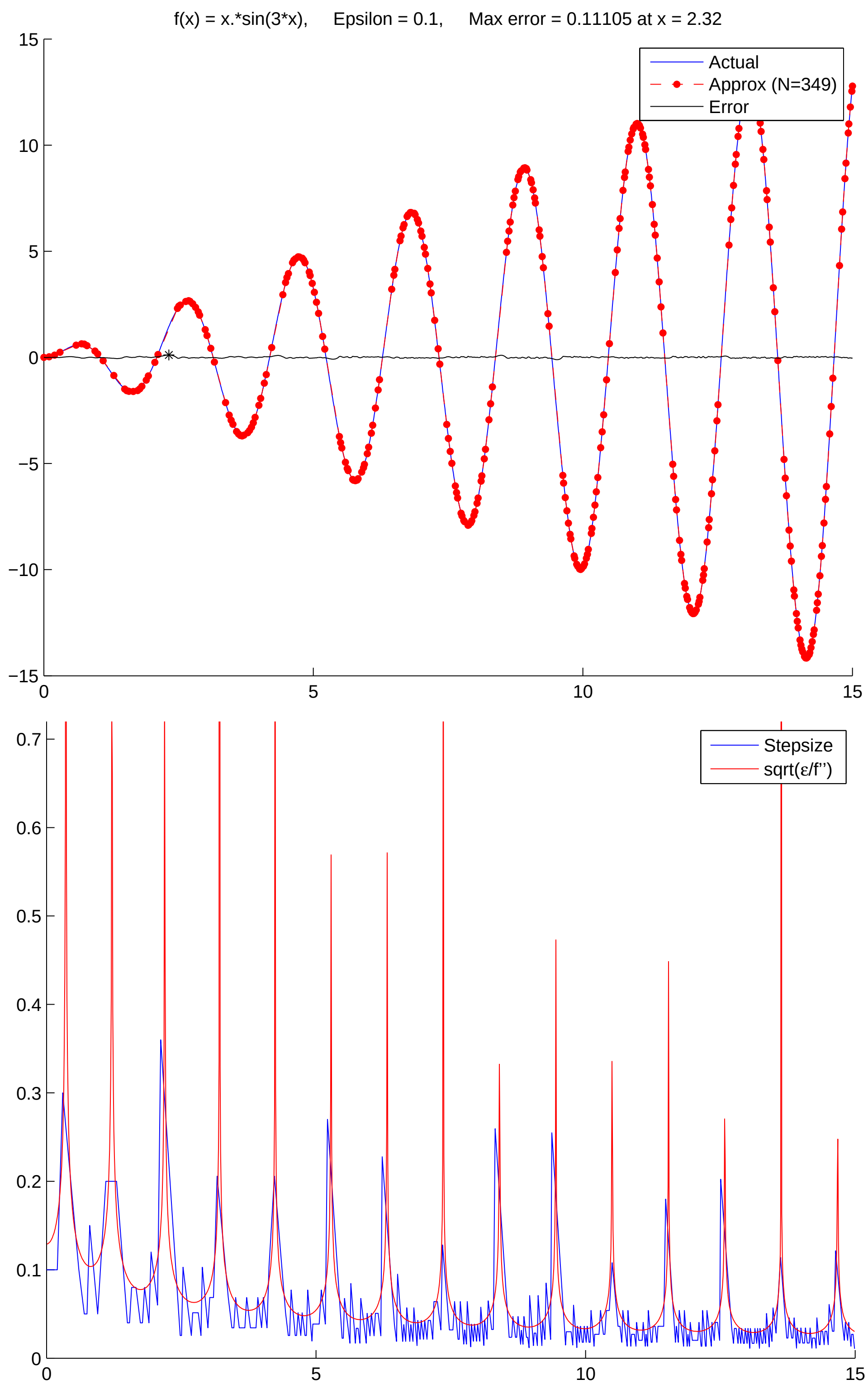

Method two. Above: $x\sin(3x)$, with $\epsilon = .1, N = 349$. Below: Step sizes over the domain. Blue is the actual step size and red is $\sqrt{\epsilon/f''}$.

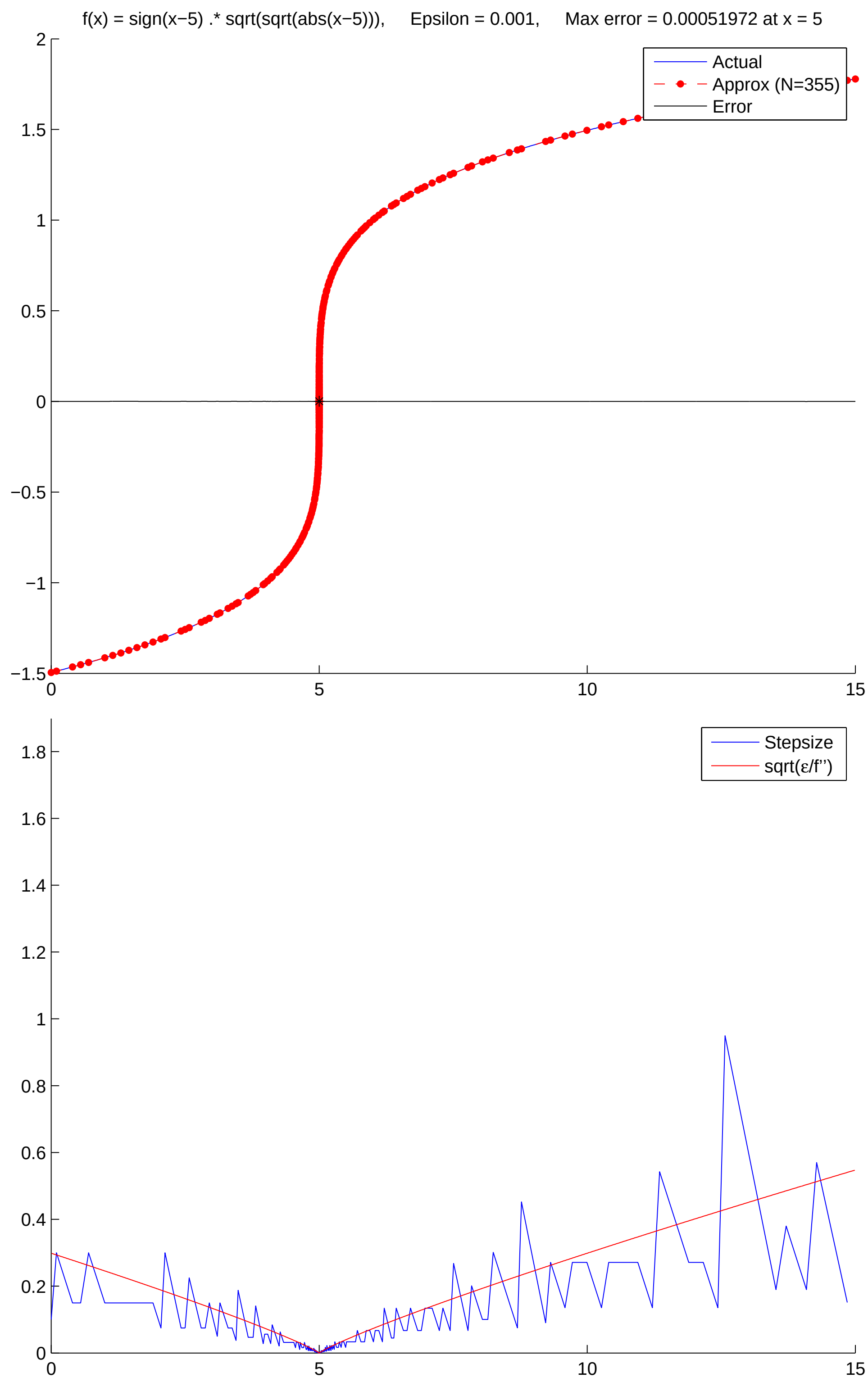

Method two: $f(x) = \text{sign}(x)\sqrt{|x-5|}$. f' is infinite at $x = 5$ but $\sqrt{|f''|}$ is still integrable.

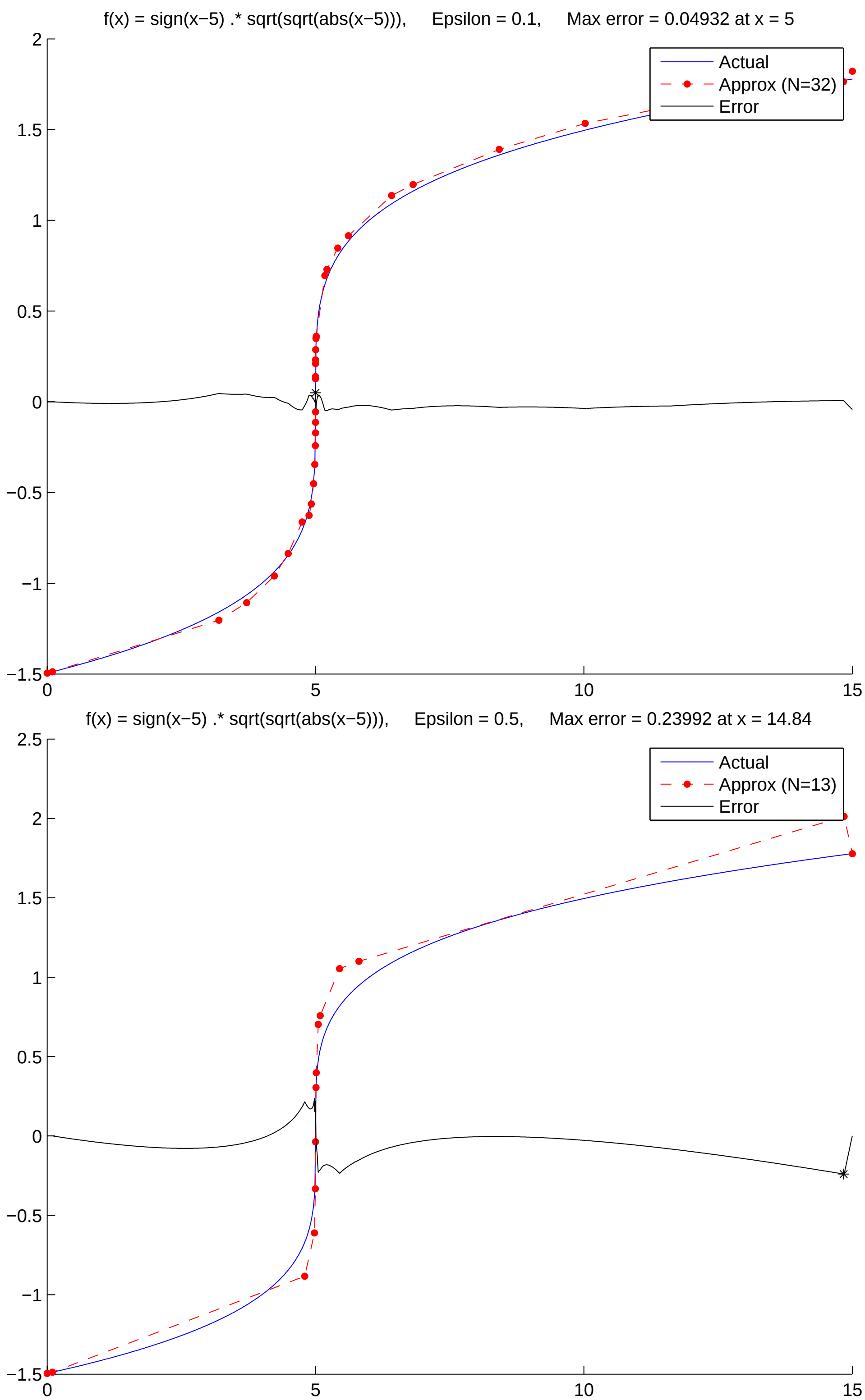

Method two: $f(x) = \text{sign}(x)\sqrt{|x-5|}$. As we relax ϵ, the points still cluster about singularity.

3.5. Examples: Encoding Cost in Bits for Two Algorithms. The next few examples show some comparisons of the resulting cost, in bits, of encoding the approximations. We took the set of legal step increments to be

$$A = \{..., \frac{1}{8}, \frac{1}{4}, \frac{1}{2}, 1, 2, 4, 8, ...\}$$

for both algorithms. Further, we assumed that the distribution on $\alpha \in A$ was such that

$$p(\alpha) \propto 2^{-|\log_2(\alpha)|}$$

Under this distribution, a codeword has length $2 + |\log_2(\alpha)|$ bits. For m_k, we assumed

$$p(m) \propto 2^{-|m|}$$

which implies the code lengths are $2 + |m|$ bits. For the second method, we did not need to store m_k, we only needed to store the sign of $\epsilon/2$.

Neither method is clearly better. The first method stores fewer points, but at higher cost. The second method stores more points, but the bit cost per point is lower. Both seem to have advantages and disadvantages.

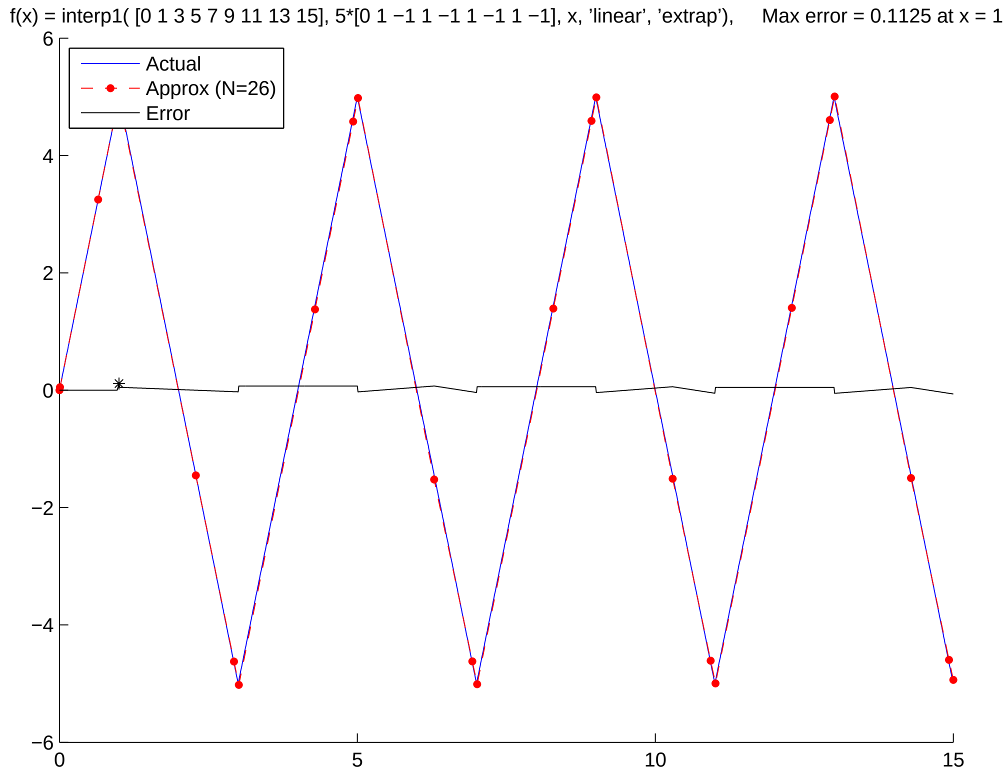

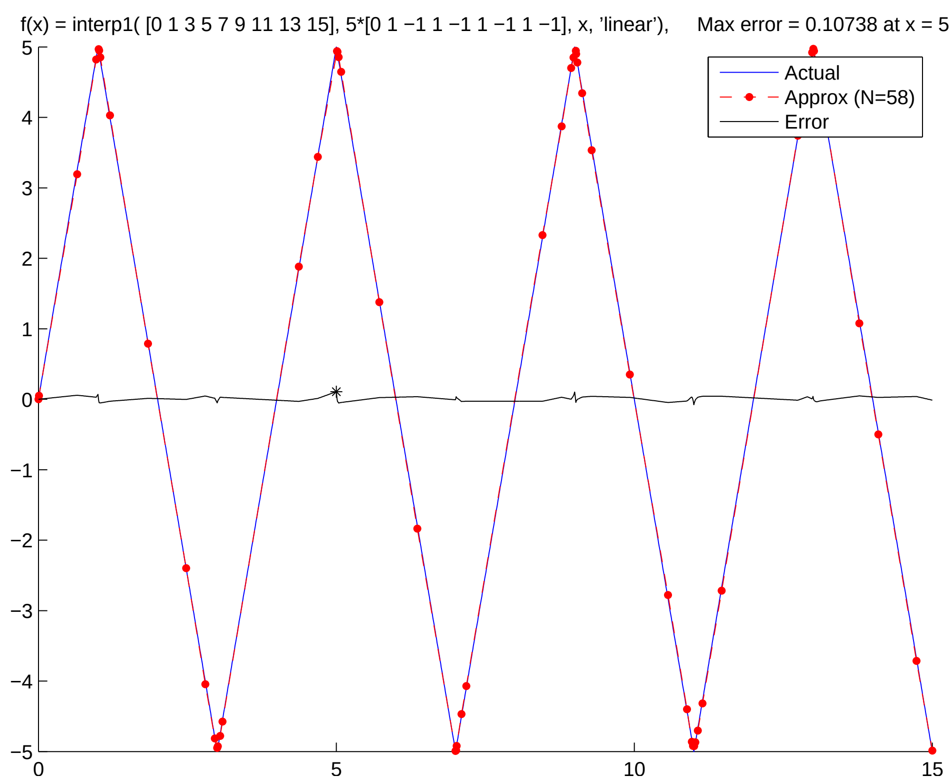

Above: method one, 685 bits. Below: method two, 262 bits.

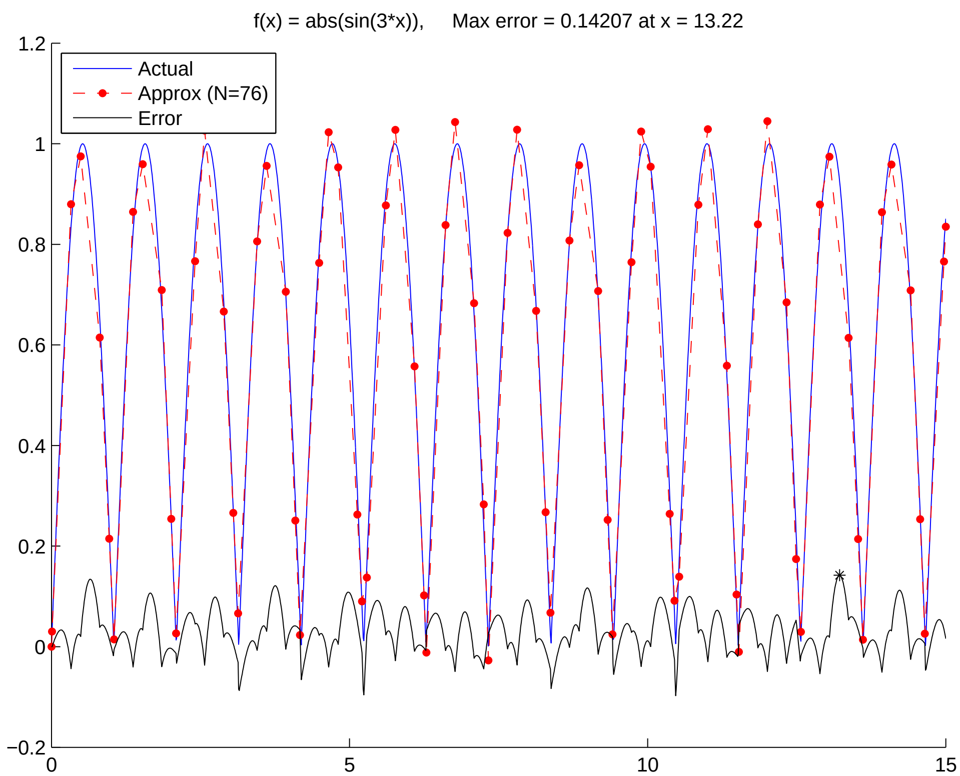

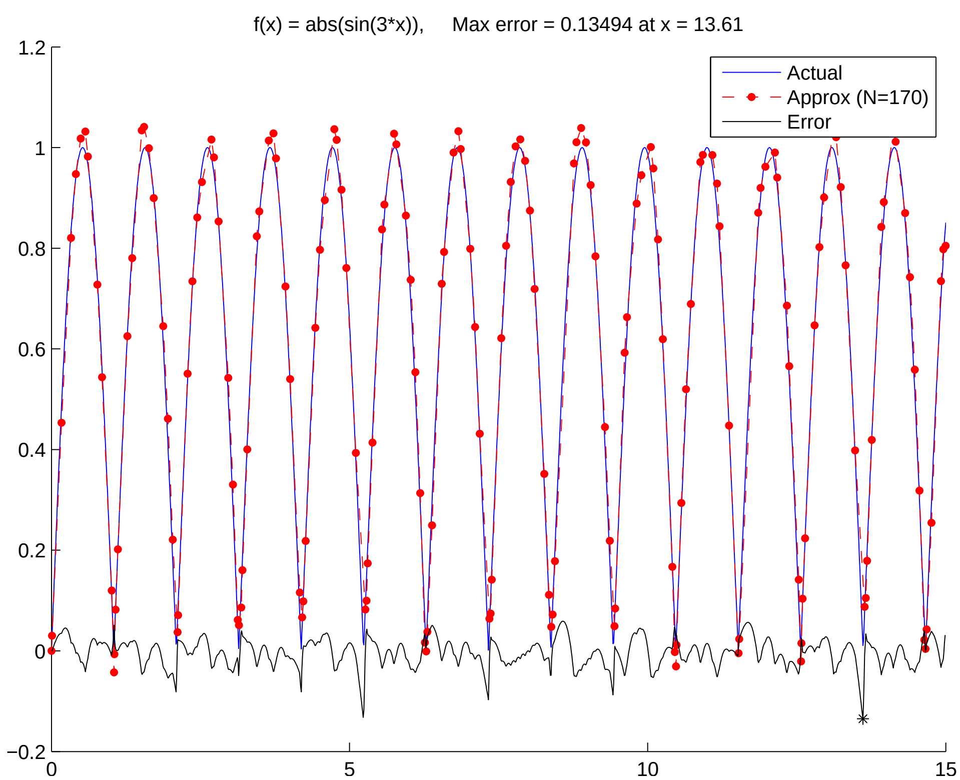

Above: method one, 590 bits. Below: method two, 750 bits.

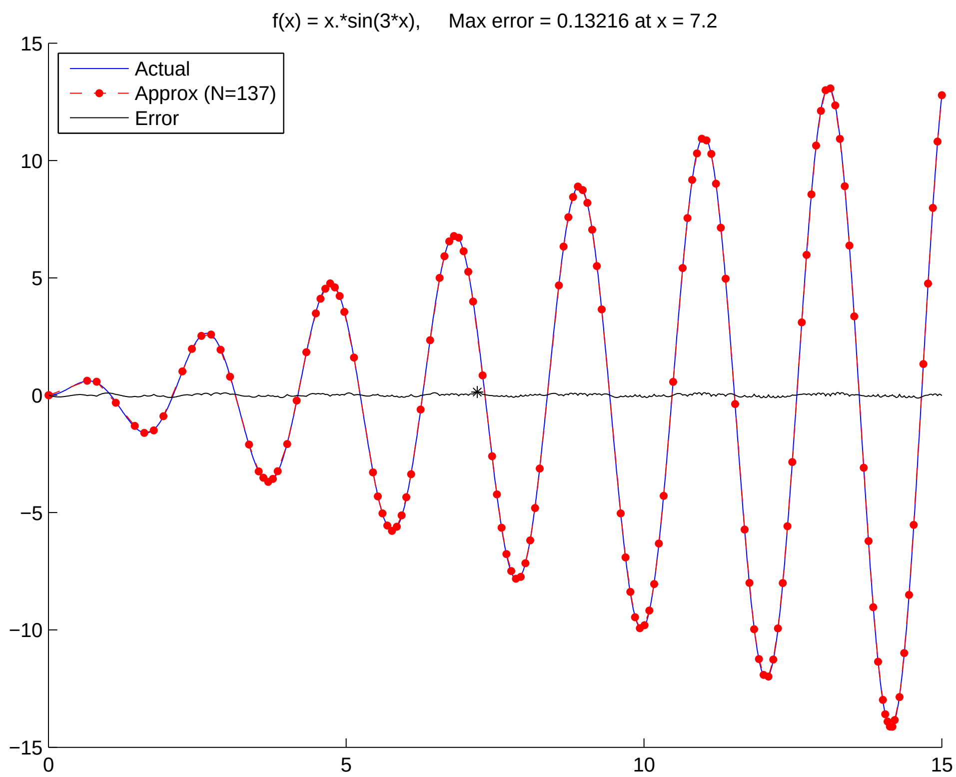

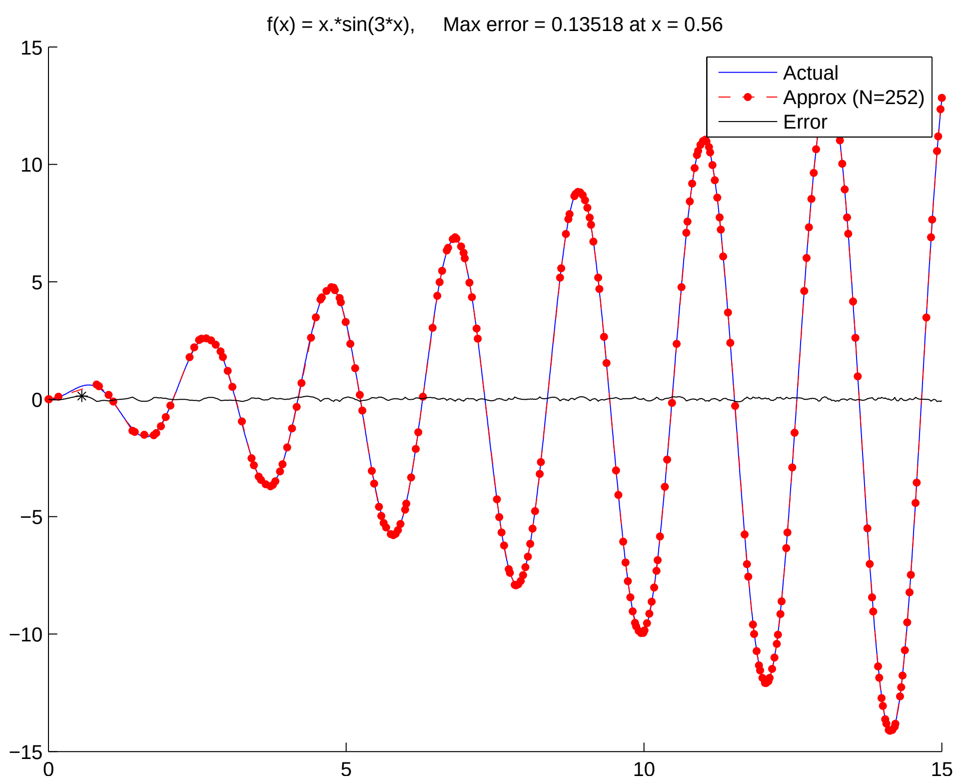

Above: method one, 908 bits. Below: method two, 1063 bits.

4. Adaptive Quasisymmetric Coding of Diff(S^1)

We want to encode shapes by encoding welding maps. As previously discussed, if two welding maps differ only by a quasisymmetric map, then we can obtain uniform bounds on the difference between the corresponding quasicircles. That is, let $f : S^1 \to S^1$ be a welding map for some shape. We wish to find another welding map $g : S^1 \to S^1$ with short description length such that the composition $f \circ g^{-1}$ is quasisymmetric with a small constant of quasisymmetry. This will imply the quasicircles for f and g are uniformly close (see theorem 4.2).

The Ahlfors-Beurling extension is a particularly simple means of extending a quasisymmetric map, although it is not invariant under the Möbius group. Let $h : \mathbb{R} \to \mathbb{R}$ satisfy an M-condition and define

$$u(x, y) = \frac{1}{2y} \int_{x-y}^{x+y} h(t)dt$$
$$v(x, y) = \frac{1}{2y} \int_{0}^{y} (h(x + t) - h(x - t))\, dt$$

Then the map $ex(h)$, defined by $x+iy \mapsto u+iv$, is quasiconformal with K that depends only on M. As stated, this does not extend the identity by the identity, but this is rectified by using the extension $x+iy \mapsto u+2iv$. This map is still quasiconformal and now extends the identity by the identity. It is shown in Ahlfors that the dilitation of the resulting extension satisfies $D < M^2$. In terms of the corresponding Beltrami coefficients, we have $D \geq \frac{1+|\mu|}{1-|\mu|}$ everywhere, or

$$|\mu| \leq \frac{M^2 - 1}{M^2 + 1}$$

Assuming $|\mu|$ is small, we can use the measurable mapping theorem to understand the asymptotic order of approximation. If $f^{t\lambda}$ solves the Beltrami equation $f_{\bar{z}} = \lambda f_z$ for the coefficient λ, then

$$\frac{\partial}{\partial t} f^{t\lambda}\Big|_{t=0} = \frac{1}{\pi z} * \lambda + O(t^2)$$

up to a normalizing quadratic polynomial. So for μ small, our normalized maps satisfy

$$g(z) = f(z) + \mu \circ f^{-1} * \frac{1}{\pi z}$$

to first order. A cheap estimate on the convolution at any point $z \in \partial\Omega$ is as follows:

$$\int \frac{\mu(\xi)}{\xi - z} d\xi \leq |\mu| \int_{\Omega} \frac{d\xi}{|\xi - z|} \leq 2\pi \frac{M^2 - 1}{M^2 + 1} \mathrm{diam}(\Omega)$$

For $M = 1 + \epsilon$ this converges to zero as $O(\epsilon)$.

4.1. Constructing Piecewise Linear Quasisymmetric Approximations to f. We present a heuristic for choosing the mesh spacing. Given some homeomorphism $\phi : [0, 2\pi] \to [0, 2\pi]$, let $k_\phi(x_0)$ denote the constant of quasisymmetry at some point $x_0 \in S^1$; i.e. $k_\phi(x_0)$ is the smallest value of k such that

$$\frac{1}{k} \leq \frac{\phi(x_0 + h) - \phi(x_0)}{\phi(x_0) - \phi(x_0 - h)} \leq k$$

for all $|h| < \pi/2$.

We wish to construct an approximation g to a welding map f. If g is piecewise linear, how far apart can our mesh points for g be before the composition $f \circ g^{-1}$ has a large constant of quasisymmetry? For smooth f, the constant will vanish as the mesh size goes to zero, but this is not a very wise way to choose the mesh points. Consider adding just one segment to a piecewise linear approximation by extending the tangent line to f in both directions. How far can we extend the tangent line at x before $k_{f \circ g^{-1}}(y)$ becomes large at $y = f(x)$?

Lemma 5.5. *Let $g(x+h) = f(x) + hf'(x)$ be the tangent to f at $x \in (0, 2\pi)$. Then*

$$\frac{\phi(y + hf'(x)) - \phi(y)}{\phi(x) - \phi(x - hf'(x))} = \left(1 + \frac{h}{2} \frac{f''(x)}{f'(x)}\right)^2 + O(h^2)$$

where $\phi = f \circ g^{-1}$.

Proof. Define $v : [0, 2\pi] \to \mathbb{R}$ by $f = g + v$, so

$$v(x+h) = f(x+h) - g(x+h) = \frac{h^2}{2} f''(x) + O(h^3)$$

We can then write

$$\phi(y) = f \circ g^{-1}(y) = y + v(g^{-1}(y))$$

Thus if we examine $k_\phi(y)$ at $y = f(x)$,

$$\begin{aligned}
\frac{\phi(y+s) - \phi(y)}{\phi(y) - \phi(y-s)} &= \frac{s + v(g^{-1}(y+s)) - v(g^{-1}(y))}{s + v(g^{-1}(y)) - v(g^{-1}(y-s))} \\
&= \frac{s + v(g^{-1}(y+s))}{s - v(g^{-1}(y-s))} && \text{since } v(g^{-1}(y)) = 0 \\
&= \frac{s + v\left(g^{-1}(y) + \frac{s}{f' \circ f^{-1}(y)}\right)}{s - v\left(g^{-1}(y) - \frac{s}{f' \circ f^{-1}(y)}\right)} \\
&= \frac{s + v\left(x + \frac{s}{f'(x)}\right)}{s - v\left(x - \frac{s}{f'(x)}\right)}
\end{aligned}$$

If we write $s = hf'(x)$, we have

$$\begin{aligned}
&= \frac{hf' + \frac{h^2}{2} f''(x) + O(h^3)}{hf' - \frac{h^2}{2} f''(x) + O(h^3)} \\
&= \frac{1 + \frac{h}{2}\frac{f''(x)}{f'(x)} + O(h^2)}{1 - \frac{h}{2}\frac{f''(x)}{f'(x)} + O(h^2)} \\
&= \left(1 + \frac{h}{2}\frac{f''(x)}{f'(x)}\right)^2 + O(h^2)
\end{aligned}$$

$\square$

So if we take step sizes $h_k = O(f'/f'')$ in our mesh, we obtain uniform bounds on the quasisymmetric constant at any point in the mesh. (In between, we do not have immediate control, although the error will vanish as the mesh becomes finer.) Alternatively, we can use the relation between step size and ϵ in the previous section:

$$h_k = O\left(\sqrt{\frac{\epsilon}{|f''|}}\right)$$

If we want to take steps of $O(f'/f'')$ to control the quasisymmetry, we see that we can achieve this by using an adaptive $\epsilon = (f')^2/f''$.

4.2. Examples. These are some examples and comparisons of the two methods for choosing stepsizes. We ran the algorithm for computing the mesh on a variety of welding maps and then solved for the corresponding quasicircles. The approximating functions g were constructed by choosing N, the number of points to be sampled, and then choosing the mesh spacing using either the 'quasisymmetric' spacing function

$$\sigma_{QS}(x) = \left|\frac{f'(x)}{f''(x)}\right|$$

or the 'uniform' spacing function

$$\sigma_U(x) = \frac{1}{\sqrt{|f''(x)|}}$$

The captions describe the different cases.

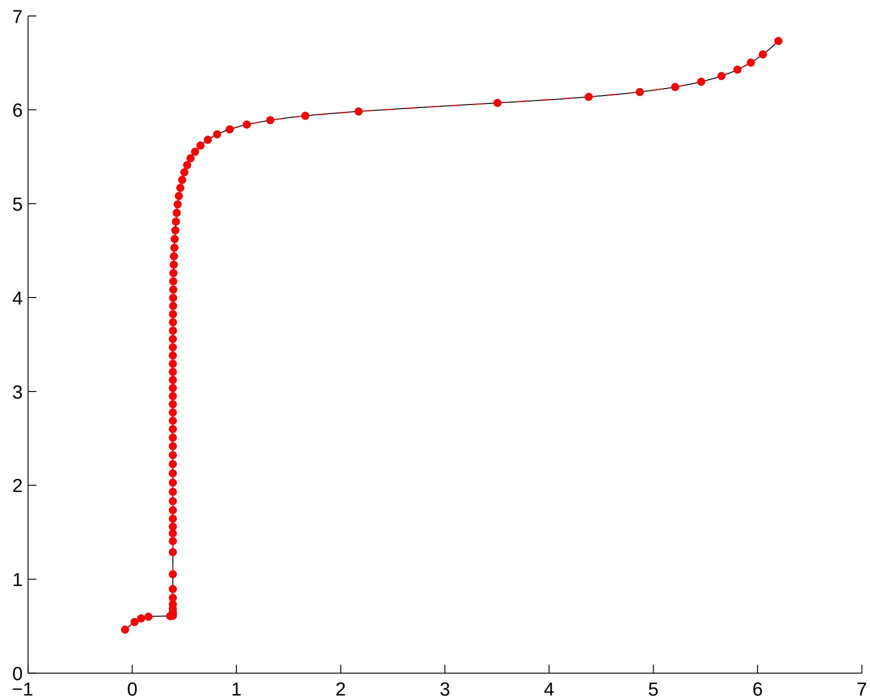

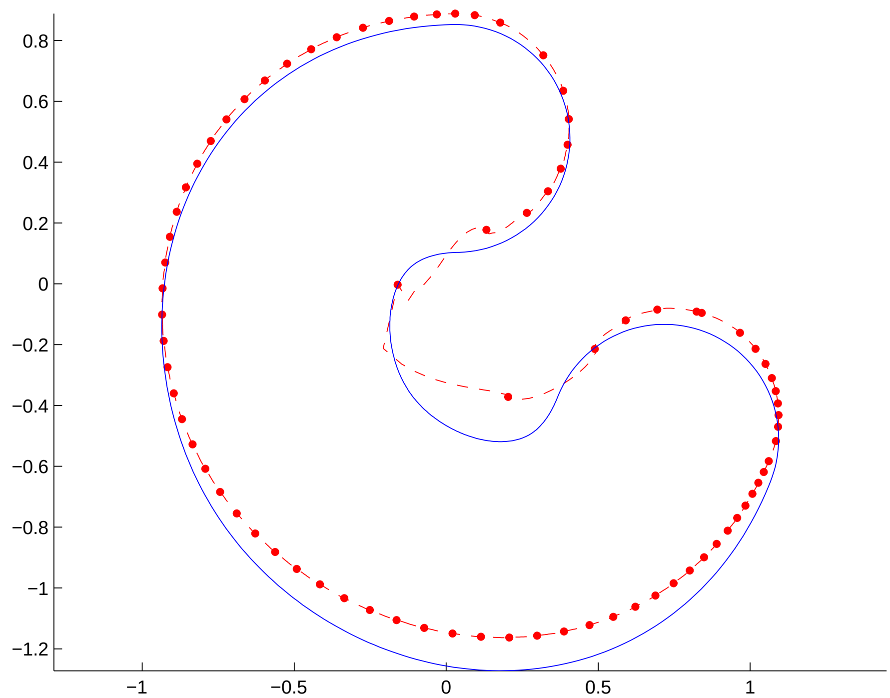

$N = 80$, using just the uniform spacing function. The uniform spacing can't deal properly with the larger negative curvatures.

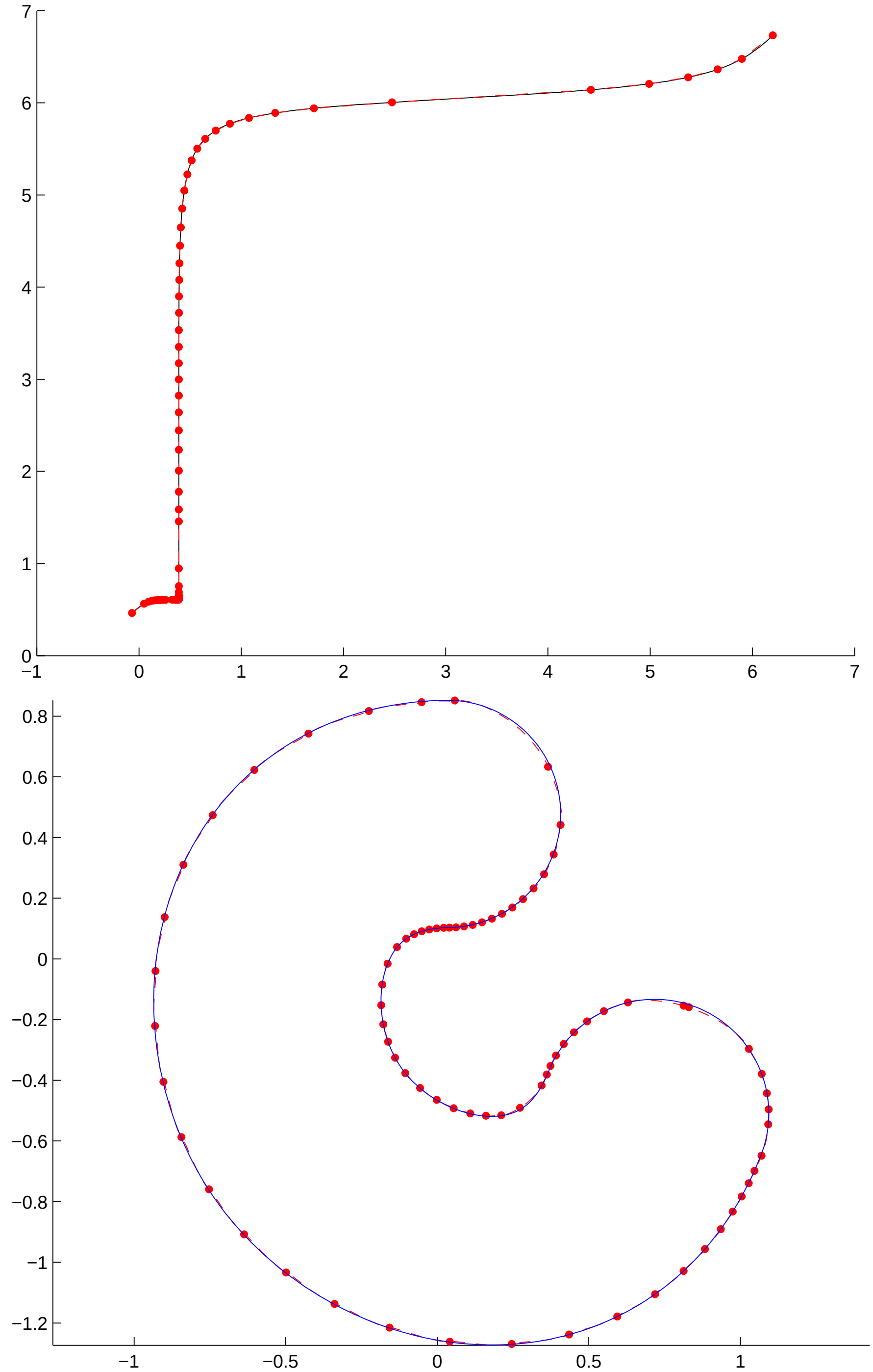

$N = 80$, using the QC spacing function to enforce quasisymmetric approximation.

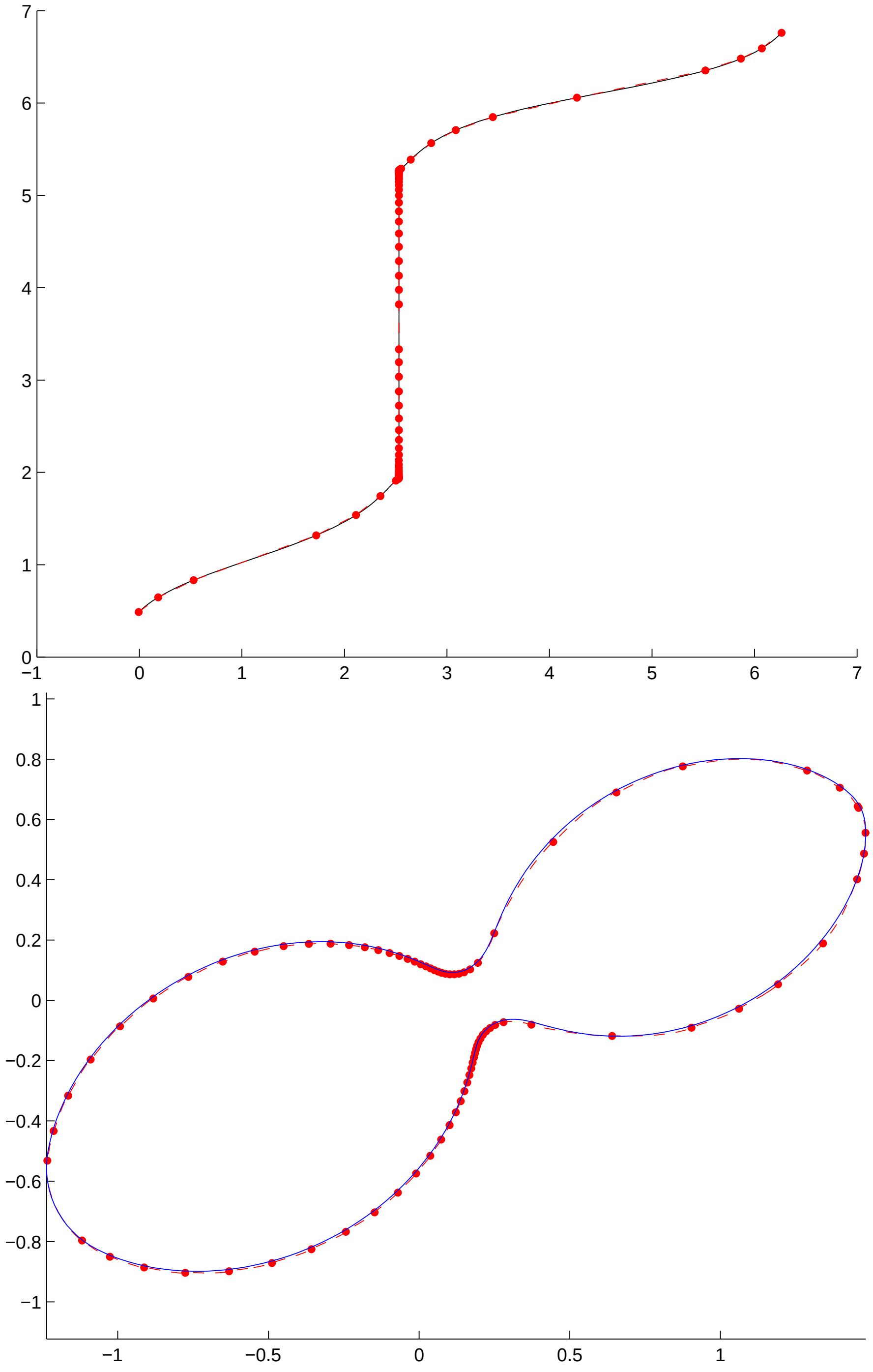

$N = 80$ on a very crowded shape using QC approximation.

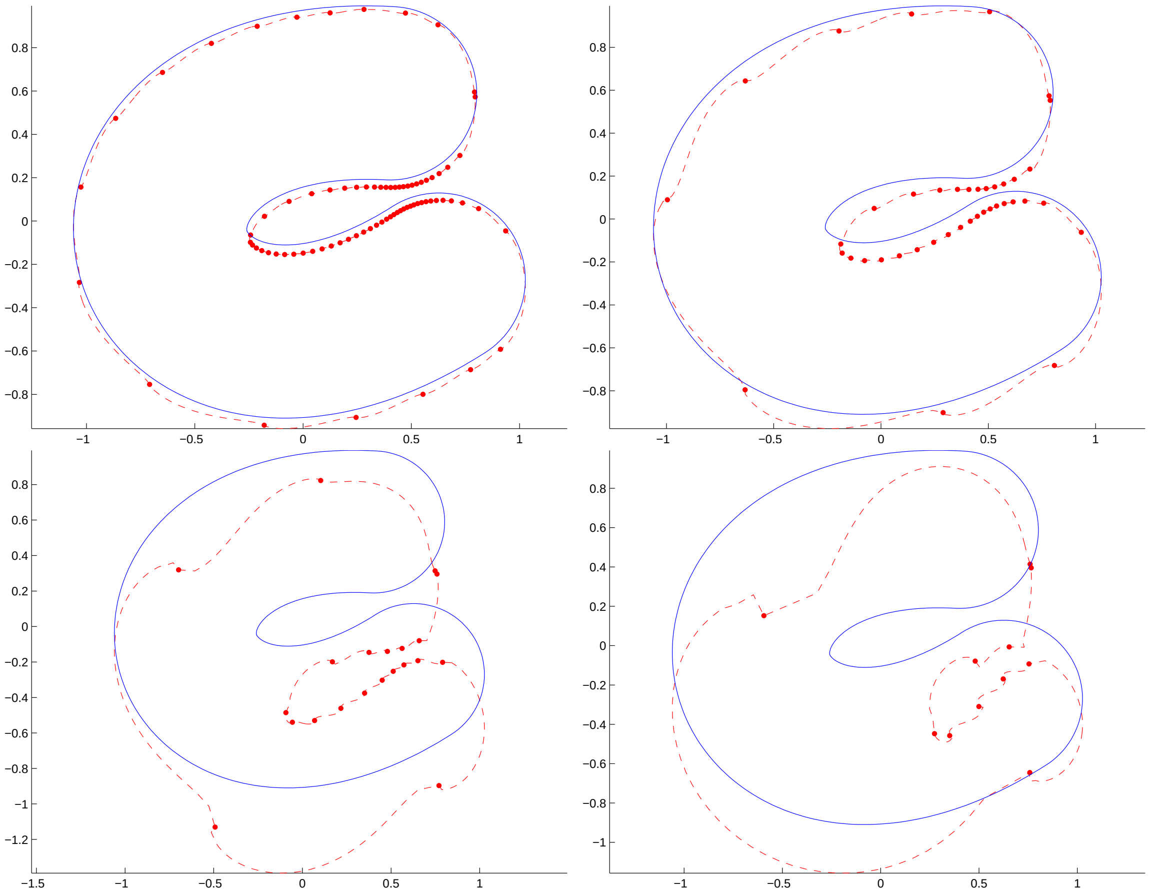

Performance as N decreases, using σ_{QC}. Here we see the same shape approximated by 80, 40, 20, and 10 points on the welding map (linearly interpolated) using quasisymmetric approximation.

APPENDIX A

Stereographic Projection

Let $\hat{\mathbb{C}} \subset \mathbb{R}^3$ be the unit sphere. Stereographic projection $\pi : \hat{\mathbb{C}} \to \mathbb{R}^2$ is a particular conformal map from the sphere to the plane. We will use standard Euclidean coordinates $y = (y_1, y_2, y_3)$ for points on the unit sphere and a single complex coordinate $z = y_1 + iy_2$ for points on the (y_1, y_2) plane. Geometrically, the mapping is as follows (see figure A.1): given a point y on the sphere, consider the straight line

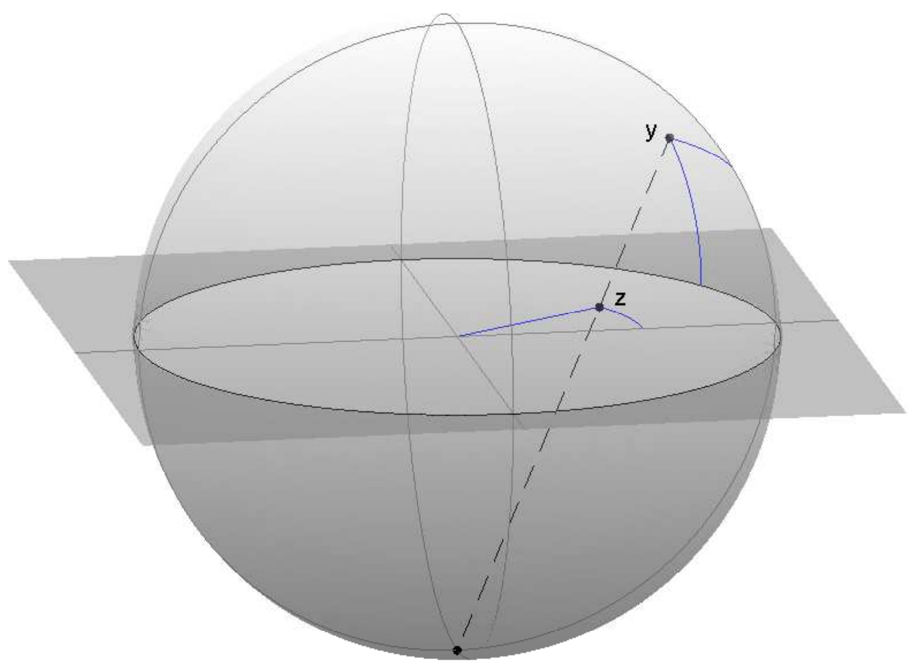

FIGURE A.1. Stereographic projection from the south pole maps the sphere to the plane.

joining y to the south pole $(0, 0, -1)$. Extend the line, if necessary, until it makes contact with the plane at some point z. Define the projection $\pi : \hat{\mathbb{C}} \to \mathbb{R}^2$ by setting $z = \pi(y)$ when $y \neq (-1, 0, 0)$, and extend π to all of $\hat{\mathbb{C}}$ by setting $\infty = \pi((-1, 0, 0))$.

1. Formulas for Stereographic Projection

The mapping $z = \pi(y)$ is defined by the following formulas:

$$
\begin{aligned}
z &= \frac{y_1 + iy_2}{1 - y_3} \\
|z|^2 &= \frac{y_1^2 + y_2^2}{(1 - y_3)^2} = \frac{1 + y_3}{1 - y_3} \\
y_1 &= \frac{z + \bar{z}}{1 + |z|^2} \\
y_2 &= \frac{z - \bar{z}}{i(1 + |z|^2)} \\
y_3 &= \frac{1 - |z|^2}{1 + |z|^2}
\end{aligned}
$$

Or in polar coordinates (r, θ) on the plane and cylindrical coordinates $(r_S, \theta_S, y3)$ on the sphere:

$$
\begin{aligned}
r_S &= \frac{2r}{1 + r^2} \\
\theta_S &= \theta \\
y_3 &= \frac{1 - r^2}{1 + r^2}
\end{aligned}
$$

The Jacobian of the map π^{-1} in any orthonormal coordinates on $\hat{\mathbb{C}}$ and $\mathbb{R}^2$ is

$$
J_{\pi^{-1}}\Big|_z = \begin{bmatrix} \frac{2}{(1+|z|^2)} & 0 \\ 0 & \frac{2}{(1+|z|^2)} \end{bmatrix}
$$

2. Stereographic Projection as a Hyperbolic Isometry

We claim that if we equip the northern hemisphere $\hat{\mathbb{C}} \cap \{y : y_3 > 0\}$ with the metric ρ_{S_Ω} given by $\mathrm{d}s^2 = \frac{\mathrm{d}y_1^2 + \mathrm{d}y_2^2 + \mathrm{d}y_3^2}{y_3^2}$, it becomes a surface of constant curvature -1. Indeed, if we pull this metric back through π^{-1} we obtain the Poincaré metric on the unit disk. That is, in matrix form in orthonormal coordinates we can write ρ_{S_Ω} as

$$
\rho_{S_\Omega} = \begin{bmatrix} \left(\frac{1}{y_3}\right)^2 & 0 \\ 0 & \left(\frac{1}{y_3}\right)^2 \end{bmatrix} = \begin{bmatrix} \left(\frac{1+r^2}{1-r^2}\right)^2 & 0 \\ 0 & \left(\frac{1+r^2}{1-r^2}\right)^2 \end{bmatrix}
$$

So in any orthonormal coordinates on the disk

$$(\pi^{-1})^*\rho_{S_\Omega} = (J_{\pi^{-1}}\big|_z)^2\rho_{S_\Omega} = \begin{bmatrix} \left(\frac{2}{1-r^2}\right)^2 & 0 \\ 0 & \left(\frac{2}{1-r^2}\right)^2 \end{bmatrix}$$

as claimed.

APPENDIX B

The Medial Axis

Definition B.1 (Medial Axis). The medial axis pair $(m(t), R(t))$ of a closed planar region consists of $m(t)$, the curve defined by the locus of centers of maximal circles contained in the region, and $R(t)$, their associated radii.

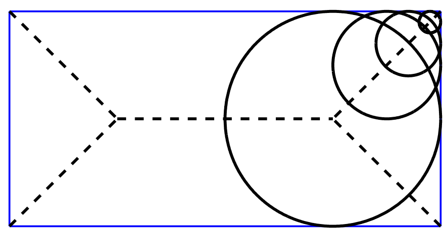

Figure B.1. A rectangle and its medial axis. The branches of the axis are formed by the centers of maximal circles.

The curve $m(t)$ gives a sort of skeleton for a planar region. In general, m can be quite pathological; for example, it may be infinitely branched, and may even have dimension > 1 [1]. However, for a region with real-analytic boundary, m consists of a finite number of smooth branches [**10**] meeting at branch points. In general, the boundaries we consider in this thesis will be real-analytic, and in fact we typically consider behavior only along a single smooth branch.

1. Formulas for the Medial Axis

By a smooth branch of the medial axis, we mean a smooth, arclength-parametrized (unless stated otherwise) pair $(m(t), R(t))$ for a region with smooth boundary.

[1]C. Bishop, personal communication.

Along a smooth branch of the medial axis we adopt the following notation. See figure B.2.

$$m(t) \text{ – an arc-length parametrization of the medial axis.}$$

$$a(t), b(t) \text{ – points of tangency of the medial circle at time } t.$$

$$R(t) \text{ – radius of the medial circle at time } t.$$

$$\kappa_m, \kappa_a, \kappa_b \text{ – Euclidean curvatures of } a(t), b(t), m(t)$$

$$\tau_a, \tau_b, \tau_m \text{ – tangent angle of } a(t), b(t), m(t)$$

$$\nu_a, \nu_b, \nu_m \text{ – angle of normal to } a(t), b(t), m(t)$$

$$\phi \text{ – the angle } \arg(b-m) - \tau_m = \tau_m - \arg(a-m)$$

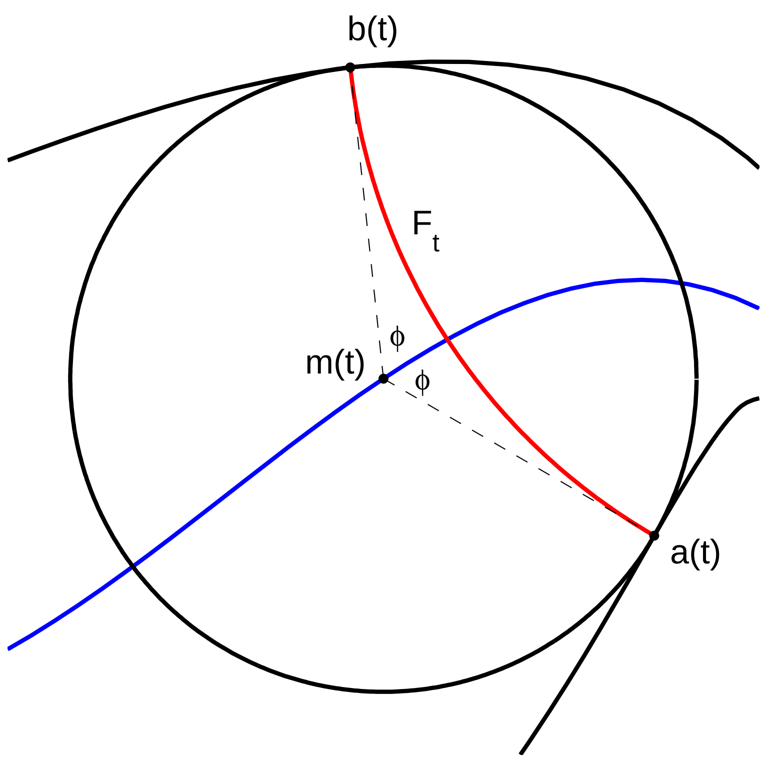

FIGURE B.2. Notation for the medial axis. The axis is shown in blue; $m(t)$ is a parametrization of the medial axis. $a(t), b(t)$ are points of tangency. The red arc $F_t = r^{-1}(B_t)$ is the foliating arc connecting $a(t)$ and $b(t)$. $\phi = \arg(b-m) - \tau_m$ is the angle between one of the dashed lines and the tangent to the medial axis at m.

The following results can be found in [**31**]. We first show how to reconstruct the boundary given the medial axis pair.

THEOREM B.1. *Along a smooth branch of the medial axis*

(1) *The boundary curves corresponding to* $(m(t), R(t))$ *are given by*

$$a(t) = \left(m + R\dot{R}e^{i\tau_m} - R\sqrt{1-\dot{R}^2}e^{i\nu_m}\right)(t)$$
$$b(t) = \left(m + R\dot{R}e^{i\tau_m} + R\sqrt{1-\dot{R}^2}e^{i\nu_m}\right)(t)$$

(2) *Given associated boundary points* $a(s), b(s)$*, the corresponding medial axis pair is given by*

$$R(s) = \frac{|b(s) - a(s)|}{2\sin\phi(s)}$$
$$m(s) = a(s) + R(s)e^{i\nu_a}$$
$$= b(s) + R(s)e^{i\nu_b}$$

Not all pairs $(m(t), R(t))$ are allowable. The following theorem identifies those pairs which are.

THEOREM B.2. *The smooth pair* $(m(t), R(t))$ *is locally the medial axis of a smooth boundary curve if and only if*

(1) $|\dot{R}| < 1$
(2) $|\kappa_m| < \frac{1-\dot{R}^2-R\ddot{R}}{r\sqrt{1-\dot{R}^2}}$

We will frequently need to use the following relationships. See [**31**] for various other relationships which hold along a smooth branch.

Proposition B.1. *Along a smooth branch of the medial axis,*

$$\begin{aligned}
\dot{R} &= -\cos\phi \\
\frac{|b-a|}{2R} &= \sin\phi \\
|\dot{a}| &= \frac{\sqrt{1-\dot{R}^2}}{1-R\kappa_a} \\
|\dot{b}| &= \frac{\sqrt{1-\dot{R}^2}}{1-R\kappa_b} \\
\kappa_m &= \sqrt{1-\dot{R}^2}\left(\frac{\kappa_a-\kappa_b}{(1-R\kappa_a)(1-R\kappa_b)}\right)
\end{aligned}$$

We'll also need a few variations on these formulas; the next proposition gives a short proof of some relations we will use.

Proposition B.2.

$$-\dot{\phi} = \frac{1}{2}(\kappa_a|\dot{a}| + \kappa_b|\dot{b}|) \tag{11}$$

$$\begin{aligned}
\kappa_m &= \frac{1}{2}(\kappa_a|\dot{a}| - \kappa_b|\dot{b}|) \qquad (12) \\
&= \frac{|\dot{a}|-|\dot{b}|}{2R}
\end{aligned}$$

Proof. At any time we have

$$\nu_b = \tau_m + \theta_b + \pi$$

$$\nu_a = \tau_m + \theta_a + \pi = \tau_m - \theta_b + \pi$$

According to our sign convention, $\kappa_b = -\frac{\mathrm{d}\nu_b}{\mathrm{d}t}$ and $\kappa_a = \frac{\mathrm{d}\nu_a}{\mathrm{d}t}$, so implicit differentiation yields

$$\kappa_b|\dot{b}| = -\kappa_m|\dot{m}| - \dot{\theta}_b$$

$$\kappa_a|\dot{a}| = \kappa_m|\dot{m}| - \dot{\theta}_b$$

Formula (11) follows by adding these two equations; (12) follows by subtracting them. We continue computation to obtain the remaining results:

$$
\begin{aligned}
2\kappa_m|\dot{m}| &= \kappa_a|\dot{a}| - \kappa_b|\dot{b}| \\
2\kappa_m|\dot{m}| &= \sqrt{1-\dot{R}^2}\left(\frac{\kappa_a}{1-R\kappa_a} - \frac{\kappa_b}{1-R\kappa_b}\right) \\
&= \sqrt{1-\dot{R}^2}\left(\frac{\kappa_a-\kappa_b}{(1-R\kappa_a)(1-R\kappa_b)}\right) \\
&= \frac{\sqrt{1-\dot{R}^2}}{R}\left(\frac{R\kappa_a-R\kappa_b}{(1-R\kappa_a)(1-R\kappa_b)}\right) \\
&= \frac{\sqrt{1-\dot{R}^2}}{R}\left(\frac{1}{1-R\kappa_a} - \frac{1}{1-R\kappa_b}\right) \\
&= \frac{1}{R}(|\dot{a}| - |\dot{b}|)
\end{aligned}
$$

□

2. Regularity of the Medial Axis

The formulas for reconstructing the boundary curve from the axis seem to indicate a derivative is lost when passing from one to the other. However, this is not the case. The following result appears in [**31**].

THEOREM B.3. *Let s, t and v be arclength parameters for a, b and m respectively.*

(1) *If $(m(v), R(v))$ are a C^p, $p \geq 2$ interior portion of the medial axis pair for boundary curves a, b, with $|\dot{R}| < 1$ and $|\kappa_m| < \frac{1-\dot{R}^2-R\ddot{R}}{r\sqrt{1-\dot{R}^2}}$, then a and b are also C^p.*

(2) *If $a(s), b(t)$ are portions of a C^p curve, $p \geq 2$, corresponding via the medial axis so*

$$1 - \kappa_{ab}\frac{|b-a|}{2\sin\phi} > 0$$

the the associated interior portion of m is C^p.

APPENDIX C

Supporting Calculations for Theorem 3.7

We need to evaluate the area of a sector under the metric $ds^2 = |\nabla \mathrm{Im}\Psi|^2(dx^2 + dy^2)$, that is

$$\int_0^\beta \int_0^\infty |\nabla \mathrm{Im}\Psi|^2 r dr d\theta$$

where

$$\Psi(r,\theta) = \sigma(i(2\arctan r - \pi/2)) + \theta$$

for some conformal self-map σ of the strip. We claim we need only consider σ which are purely elliptic with fixed point 0. We can decompose an arbitrary element $\sigma \in PSL_2(\mathbb{R})$ into a choice of $\sigma(0)$ and an elliptic rotation about $\sigma(0)$. Moving $\sigma(0)$ can be decomposed as a pair of hyperbolics, first with axis equal to the x-axis and the second with axis perpendicular. The first is simply translation and the metric is obviously invariant. In the second case, the action of σ pulls back to a conformal self-map of the sector: it is the restriction to the wedge of a hyperbolic $h : \hat{\mathbb{C}} \to \hat{\mathbb{C}}$ with fixed points at 0 and ∞. In this case

$$\begin{aligned}
\iint_{S_\beta} |\nabla \mathrm{Im}\Psi(r,\theta)|^2 &= \iint_{S_\beta} |\mathrm{Im}\frac{\partial}{\partial r}\sigma(i(2\arctan r - \pi/2))|^2 \\
&= \iint_{S_\beta} |\mathrm{Im}\frac{\partial}{\partial r} i(2\arctan h(r) - \pi/2)|^2 \\
&= \iint_{S_\beta} \left|\frac{dh}{dz}\right|^2 |2\arctan'(h(r))|^2 \\
&= \iint_{h(S_\beta)} |2\arctan'(r)|^2 \\
&= \iint_{S_\beta} |2\arctan'(r)|^2
\end{aligned}$$

as claimed. Hence we need only consider elliptics. An elliptic $\sigma \in PSL_2(\mathbb{R})$ with rotation angle ϕ and fixed point at 0 acts on the strip as

$$\sigma(z) = \log \frac{e^z + 1 + \alpha(e^z - 1)}{e^z + 1 - \alpha(e^z - 1)}$$

for $\alpha = e^{i\phi}$. Further,

$$\frac{d\sigma}{dz} = \frac{4\alpha e^z}{(e^2+1)^2 - \alpha^2(e^{z-1})^2}$$

From this, one may compute

$$\begin{aligned} |\nabla \mathrm{Im}\sigma(z)\big|_{z=iy} &= \frac{d}{dy}\arctan(\cos\phi\tan y) \\ &= \frac{\cos\phi}{\cos^2 y + \cos^2\phi\sin^2 y} \end{aligned}$$

We now compute the area:

$$\begin{aligned} \iint_{S_\beta} |\nabla \mathrm{Im}\Psi(r,\theta)|^2 &= \iint_{S_\beta} |\mathrm{Im}\frac{\partial}{\partial r}\sigma(i\arctan r)|^2 \\ &= \int_0^\beta \int_0^\infty \left(\frac{\cos\phi}{\cos^2 y + \cos^2\phi\sin^2 y}\frac{2}{1+r^2}\right)^2_{y=2\arctan(r)-\frac{\pi}{2}} r dr d\theta \end{aligned}$$

Now let $u = 2\arctan r - \frac{\pi}{2}$ so $du = \frac{2}{1+r^2}dr$; we obtain

$$= \beta \int_{-\pi/2}^{\pi/2} \left(\frac{\cos\phi}{\cos^2 u + \cos^2\phi\sin^2 u}\right)^2 \frac{2r}{1+r^2} du$$

Using the identity

$$r = \frac{1+\tan(u/2)}{1-\tan(u/2)}$$

we eventually find that

$$\frac{2r}{1+r^2} = \cos u$$

So the integral becomes

$$= \beta \int_{-\pi/2}^{\pi/2} \left(\frac{\cos\phi}{\cos^2 u + \cos^2\phi \sin^2 u} \right)^2 \cos u du$$

Now let $v = \sin u$ so $dv = \cos u du$ and we have

$$= \beta \int_{-1}^{1} \left(\frac{\cos\phi}{1 - v^2 + v^2\cos^2\phi} \right)^2 dv$$

$$= \beta \int_{-1}^{1} \left(\frac{\cos\phi}{1 - v^2\sin^2\phi} \right)^2 dv$$

This is in fact a decreasing function of ϕ for $0 \leq \phi \leq \pi/2$. Differentiating under the integral sign, we have

$$\frac{\partial}{\partial\phi} \left(\frac{\cos\phi}{1 - v^2\sin^2\phi} \right)^2 = 2\sin\phi\cos\phi \frac{v^2(2 - \sin^2\phi) - 1}{(1 - v^2\sin^2\phi)^3}$$

Either masochism or Mathematica will lead one to the conclusion that

$$\begin{aligned} (13) \quad & \int_{-1}^{1} 2\sin\phi\cos\phi \frac{v^2(2-\sin^2\phi) - 1}{(1 - v^2\sin^2\phi)^3} dv \\ & \quad = 2\frac{\cos\phi(\sin\phi(\sin^4\phi - 2\sin^2\phi + 1) - (\sin^2\phi + 1)(\sin^2\phi - 1)^2\tanh^{-1}(s))}{\sin^2\phi(\sin^2\phi - 1)^2} \end{aligned}$$

and this function is positive for $-\pi/2 < \phi < 0$, zero at $\phi = 0$, and negative on $0 < \phi < \pi/2$.

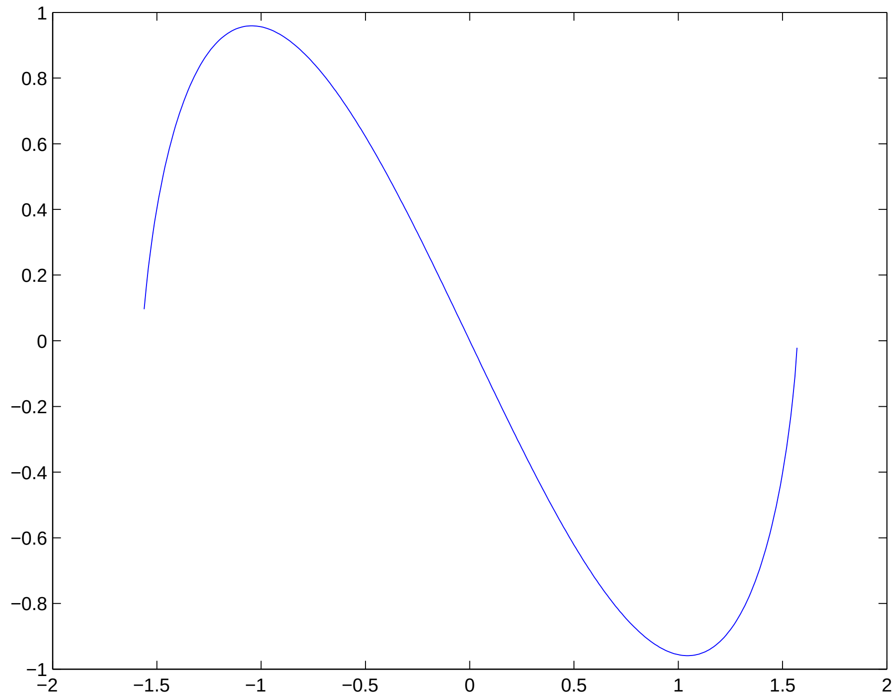

FIGURE C.1. The graph of equation 13: area is maximized at $\phi = 0$.

Bibliography

[1] L. V. Ahlfors. *Conformal invariants: topics in geometric function theory*. McGraw-Hill series in higher mathematics. McGraw-Hill, New York, 1973.

[2] L. V. Ahlfors. *Complex analysis : an introduction to the theory of analytic functions of one complex variable*. International series in pure and applied mathematics. McGraw-Hill, New York, 3d ed edition, 1979.

[3] L. V. Ahlfors and C. J. Earle. *Lectures on quasiconformal mappings*. Wadsworth & Brooks/Cole Advanced Books & Software, Monterey, Calif., 1966.

[4] A. Beurling. Mittag-leffler lectures on complex analysis (1977-1978). In L. Carleson, P. Malliavan, J. Neuberger, and J. Wermer, editors, *The Collected Works of Arne Beurling*. Birkhäuser, 1989.

[5] C. Bishop. An explicit constant for sullivan's convex hull theorem, 1999.

[6] C. J. Bishop. A fast approximation to the riemann map. Preprint, October 2003.

[7] C. J. Bishop. Conformal mapping in linear time. Preprint, January 2007.

[8] H. Blum. Biological shape and visual science. *Journal of Theoretical Biology*, 38:205–287, 1973.

[9] R. D. Canary, A. Marden, D. B. A. Epstein, W. P. Thurston, and S. J. Patterson. *Fundamentals of hyperbolic geometry : selected expositions*, volume 328. Cambridge University Press, Cambridge, UK, 2006.

[10] H. I. Choi, S. W. Choi, and H. P. Moon. Mathematical theory of medial axis transform. *Pacific Journal of Mathematics*, 181(1):57–88, 1997.

[11] T. M. Cover and J. A. Thomas. *Elements of information theory*. Wiley, New York, 1991.

[12] M. P. Do Carmo. *Differential geometry of curves and surfaces*. Prentice-Hall, Englewood Cliffs, N.J., 1976.

[13] M. P. Do Carmo. *Riemannian geometry*. Mathematics. Theory & applications. Birkhäuser, Boston, 1992.

[14] D. L. Donoho. Counting bits with kolmogorov and shannon. Manuscript.

[15] D. L. Donoho, M. Vetterli, R. A. DeVore, and I. Daubechies. Data compression and harmonic analysis. *IEEE transactions on informations theory*, 44(6):2435–2476, 1998.

[16] T. Driscoll. A matlab toolbox for schwarz-christoffel mapping. *ACM Trans. Math. Soft.*, 22:168–186, 1996.

[17] T. Driscoll and L. Trefethen. *Schwarz-Christoffel Mapping*. Cambridge University Press, 2002.

[18] B. A. Dubrovin, A. T. Fomenko, and S. P. Novikov. *Modern geometry–methods and applications*, volume 93- of *Graduate texts in mathematics*. Springer-Verlag, New York, 2nd ed edition, 1992.

[19] P. L. Duren. *Univalent functions*, volume 259. Springer-Verlag, New York, 1983.

[20] D. B. A. Epstein, A. Marden, and V. Markovic. Complex angle scaling. In *Kleinian Groups and Hyperbolic 3-manifolds*, London Math. Soc. Lecture Note Ser., pages 343–362. Cambridge University Press, 2003.

[21] D. B. A. Epstein, A. Marden, and V. Markovic. Quasiconformal homeomorphisms and the convex hull boundary. *Ann. of Math*, 159(1):305–336, 2004.

[22] D. B. A. Epstein and V. Markovic. The logarithmic spiral: A counterexample to the k=2 conjecture. *Annals of Mathematics*, 161(2):925–957, 2005.

[23] O. Forster. *Lectures on Riemann surfaces*, volume 81. Springer-Verlag, New York, 1981.

[24] F. P. Gardiner and N. Lakic. *Quasiconformal Teichmüller theory*, volume v. 76 of *Mathematical surveys and monographs*. American Mathematical Society, Providence, R.I, 2000.

[25] J. B. Garnett and D. E. Marshall. *Harmonic measure*. New math monographs. Cambridge University Press, Cambridge, 2005.

[26] J. H. Hubbard. *Teichmüller theory and applications to geometry, topology, and dynamics*. Matrix Editions, Ithaca, NY, 2006.

[27] A. Kolmogorov and V. Tikhomirov. Epsilon-entropy and epsilon-capacity. In *American Mathematical Society Translations*, volume 17 of *2*, pages 277–364. American Mathematical Society, 1959.

[28] J. M. Lee. *Riemannian manifolds : an introduction to curvature*, volume 176. Springer, New York, 1997.

[29] J. M. Lee. *Introduction to smooth manifolds*, volume 218. Springer, New York, 2003.

[30] O. Lehto. *Univalent functions and Teichmüller spaces*, volume 109. Springer-Verlag, New York, 1987.

[31] K. Leonard. *Measuring Shape Space: Epsilon-entropy, Adaptive Coding and Two-dimensional Shape*. PhD thesis, Brown University, May 2004.

[32] D. E. Marshall and S. Rohde. Convergence of the zipper algorithm for conformal mapping, 2006.

[33] P. W. Michor and D. Mumford. Riemannian geometries on spaces of plane curves. *J.EUR.MATH.SOC*, 8:1, 2006.

[34] D. Mumford. Mathematical theories of shape: Do they model perception? In *Geometric Methods in Computer Vision*, volume 1570, pages 2–10. SPIE, 1991.

[35] S. Nag and A. Verjovsky. Diff(s^1) and the teichmuller spaces. *Communications in Mathematical Physics*, 130:123–138, 1990.

[36] T. Needham. *Visual complex analysis.* Clarendon Press, Oxford, 1997.

[37] C. Pommerenke. *Boundary behaviour of conformal maps*, volume 299. Springer-Verlag, Berlin, 1992.

[38] E. Posner and E. Rodemich. Epsilon-entropy and data compression. *Annals of Mathematical Statistics*, 42(6):2079–2125, 1971.

[39] T. B. Sebastian, P. N. Klein, and B. B. Kimia. Recognition of shapes by editing their shock graphs. *IEEE Transactions on Pattern Analysis and Machine Intelligence*, 26(5):550–571, 2004.

[40] E. Sharon and D. Mumford. 2d-shape analysis using conformal mapping. *International Journal of Computer Vision*, 70(1):55–75, 2006.

[41] K. Siddiqi and B. Kimia. A shock grammar for recognition. In *Proceedings of the Conference on Computer Vision and Pattern Recognition*, pages 507–513, 1996.

[42] K. Siddiqi, A. Shokoufandeh, S. J. Dickinson, and S. W. Zucker. Shock graphs and shape matching. In *ICCV*, pages 222–229, 1998.

[43] K. Stephenson. *Introduction to Circle Packing.* Cambridge University Press, 2005.

[44] D. Sullivan. Travaux de thurston sur les groupes quasi-fuchsiens et les varietes hyperboliques de dimension 3 fibrees sur s^1. In *Bourbaki Seminar*, volume 1979/80, pages 196–214. Springer, Berlin, 1981.

[45] L. A. Takhtajan and L.-P. Teo. *Weil-Petersson metric on the universal Teichmüller space*, volume no. 861. American Mathematical Society, Providence, R.I., 2006.

[46] W. P. Thurston and S. Levy. *Three-dimensional geometry and topology*, volume 35. Princeton University Press, Princeton, N.J., 1997.

[47] R. C. Veltkamp. Shape matching: similarity measures and algorithms. In *Shape Modeling International*, pages 188–199, 2001.

[48] P. Yushkevic, P. Fletcher, S. Joshi, A. Thall, and S. Pizer. Continuous medial representations for geometric object modeling in 2d and 3d, 2002.

[49] S. Zhu and A. Yuille. Forms: A flexible object recognition and modeling system, 1996.